ELECTRON SPIN-LATTICE RELAXATION OF $Cr(CN)_5NO^{3-}$ IN KBr AND KCl

Thesis for the Degree of Ph. D.
MICHIGAN STATE UNIVERSITY
GEORGE T. JOHNSTON III
1967

This is to certify that the

thesis entitled

ELECTRON SPIN-LATTICE RELAXATION
OF $Cr(CN)_5NO^{3-}$ IN KBr AND KCl

presented by

George T. Johnston III

has been accepted towards fulfillment
of the requirements for

Ph.D. degree in Physics

J A Cowen
Major professor

Date 7-18-67

O-169

ABSTRACT

ELECTRON SPIN-LATTICE RELAXATION OF $Cr(CN)_5NO^{3-}$ IN KBr AND KCl

by George T. Johnston III

Electron spin-lattice relaxation times τ_1 of $Cr(CN)_5NO^{3-}$ substitutional in KBr and KCl have been measured for $1 < T < 150°K$. Spin echo techniques employing either picket or single-pulse saturation methods were used. From the temperature dependence of the observed τ_1 values, we conclude that at least three relaxation mechanisms are operative: an anisotropic direct process at $T < 5°K$, an isotropic Raman process at intermediate temperatures, and an anisotropic local mode process at $T > 65°K$. The functional form of the relaxation rate is $\frac{1}{\tau_1} = AT + BT^9 J_8(\theta/T) + C \exp(-\theta_0/T)$, where θ is the Debye temperature and was taken as 170°K for KBr and 230°K for KCl. Empirical values of A, B, C, and θ_0 were determined by least squares computer analysis. Published energy level assignments preclude the possibility of an Orbach process. Therefore, since the parameter θ_0 is 575±30°K for KBr and 610±30°K for KCl, in agreement with published Cr-CN stretch frequencies, we

conclude that the exponential process occurs through the interaction of lattice phonons with vibrational modes localized in the $Cr(CN)_5NO^{3-}$. An anomaly in the T dependence of τ_1 for KBr has been tentatively explained as a driven-mode process, in which relaxation is effected by low frequency (<20 cm^{-1}) bending modes of the complex.

ELECTRON SPIN-LATTICE RELAXATION OF $Cr(CN)_5NO^{3-}$ IN KBr AND KCl

By

George T. Johnston III

A THESIS

Submitted to
Michigan State University
in partial fulfillment of the requirements
for the degree of

DOCTOR OF PHILOSOPHY

Department of Physics

1967

DEDICATION

This thesis is dedicated to my parents and especially to my wife, whose help and understanding helped to make this work possible.

ACKNOWLEDGMENTS

Professor J. A. Cowen, by his encouragement and enthusiasm and patience, has helped to make my undergraduate and graduate study at Michigan State University interesting and exciting. Professor R. D. Spence has provided valuable intuitive insight into many theoretical problems associated with the preparation of this thesis. Mel Olman and many other graduate students of the infrared spectroscopy group have given invaluable aid with computer programming. The good humor and fellowship of Charles Taylor have added immeasurably to the enrichment of my graduate study. Without the able assistance of the personnel of the machine and electronic shops, particularly Ernie Brandt and Nick Rutter, this work would have been impossible. Financial support of the National Science Foundation and the Army Research Office (Durham) was appreciated.

TABLE OF CONTENTS

Page

ACKNOWLEDGMENTS iii

LIST OF TABLES vi

LIST OF FIGURES vii

LIST OF APPENDICES viii

Chapter

I. INTRODUCTION 1

- History 1
- Summary of Theory 2

II. THEORY 8

- Theoretical Background 8
- Direct Process 16
- Raman Process 19
- Orbach Process 24
- Driven-Mode Process 24
- Local Mode Process 26
- Anisotropy of Relaxation Time 32

III. EXPERIMENTAL APPARATUS AND TECHNIQUES . . . 38

- General Description 38
- Spin Echo Techniques 40
- Vacuum Can Cryostat 41
- Crystal Growing 43

IV. SUMMARY AND IMPLICATIONS OF PREVIOUS RESULTS 45

- ESR Spectrium 45
- Infrared and Optical Spectra 46

V. RESULTS AND CONCLUSIONS 49

- General Considerations 49
- Relaxation Results -- KBr 50
- Discussion -- KBr 53
- Results and Discussion -- KCl 62
- Summary 68

Page
REFERENCES 69

APPENDICES 72

LIST OF TABLES

Table Page

I. Effect of lattice on vibrational frequencies of $Cr(CN)_5NO^{3-}$ 48

II. Least squares fit of $\frac{1}{\tau_1} = AT + BT^9J_8(170/T) + C\exp(-575/T)$ to relaxation of $Cr(CN)_5NO^{3-}$ in KBr 52

III. Least squares fit of $\frac{1}{\tau_1} = AT + BT^9J_8(230/T) + C\exp(-610/T)$ to relaxation of $Cr(CN)_5NO^{3-}$ in KCl 65

LIST OF FIGURES

Figure Page

1. Octahedrally-coordinated paramagnetic ion . . . 9
2. The direct process 17
3. Energy level diagram for a Kramers system . . . 18
4. The Raman process 20
5. The local mode process 29
6. Cylindrical cavity 39
7. Vacuum can cryostat 42
8. Temperature dependence of τ_1 for $g_\parallel$ and $g_\perp$ lines in KBr, with fits to $\frac{1}{\tau_1} = AT + BT^9J_8(170/T) + C\exp(-575/T)$ 51
9. Temperature dependence of τ_1 for $g_\perp$ line in KBr, with fit to $\frac{1}{\tau_1} = AT + BT^9J_8(170/T)$ 54
10. Temperature dependence of τ_1 for $g_\parallel$ line in KBr, with fit to $\frac{1}{\tau_1} = AT + BT^9J_8(170/T)$ 55
11. Comparison of thermal paths for the two types of apparatus 61
12. Temperature dependence of τ_1 for $g_\parallel$ and $g_\perp$ lines in KCl, with fits to $\frac{1}{\tau_1} = AT + BT^9J_8(230/T) + C\exp(-610/T)$ 63
13. Temperature dependence of τ_1 for $g_\perp$ line in KCl, with fit to $\frac{1}{\tau_1} = AT + BT^9J_8(230/T)$ 66
14. Temperature dependence of τ_1 for $g_\parallel$ line in KCl, with fit to $\frac{1}{\tau_1} = AT + BT^9J_8(230/T)$ 67

LIST OF APPENDICES

Appendix Page

I. Data for KBr 72

II. Data for KCl 79

III. Fortran Program TOWPLOT Used in Curve Fitting. . 88

IV. Assignment of Weights in Curve Fitting 107

I. INTRODUCTION

History

Electron spin-lattice relaxation phenomena of paramagnetic impurities in crystalline salts has been a subject of both experimental and theoretical interest for more than three decades. Gorter[27] in the 1930's studied relaxation phenomena using susceptibility techniques and Waller,[36] Van Vleck,[32] and Kronig[16] established a theoretical explanation of the results. With the advent of electron paramagnetic resonance the interest in relaxation phenomena was renewed, since resonance provided the possibility of measuring relaxation times in a more direct manner. Experimental resolution limited the results to 4.2°K and below until the late 1950's. Advances in experimental technology, resulting in enhanced sensitivity which allows measurements at higher temperatures, have reopened interest in Van Vleck's theory. Orbach[4] has modified the theory in order to explain a wide range of experimental results, particularly in the rare earth ions. Castle and Feldman[2] have reported results up to 250°K using a saturation-inversion technique, and the experimental technology has reached the point at which measurements above 78°K may be considered routine.

In order to reduce interaction between paramagnetic centers, they are introduced into diamagnetic host crystals in small percentages. Therefore, the paramagnetic centers are at defect sites. Lattice vibrations, which provide the mechanism for relaxation, are modified by a defect, so that one might expect theories formulated for perfect crystals need not apply to real systems. Klemens[3,13] was the first to explicitly consider the consequences of this fact upon the theory of electron spin-lattice relaxation. The work reported in this thesis was undertaken in the hope of being able to more conclusively check the validity of the Klemens theory. We have measured the temperature dependence of τ_1 for the molecular complex $Cr(CN)_5NO^{3-}$ substitutional in KBr and KCl, in the temperature range 1°K to 150°K.

Summary of Theory

In order to understand relaxation time measurements, one must understand the theory of lattice vibrations[38,10] and the theory of paramagnetic resonance.[7,26,29] The overall aim is to calculate the characteristic time (relaxation time) for electron spins that have absorbed energy to relinquish the energy to the thermal bath.

The absorption of energy by a paramagnetic electron is governed by the resonance equation,

$$h\nu = E_1 - E_2 = g\beta H, \qquad (1.1)$$

where ν is the frequency of the applied r.f. signal, h is Planck's constant, E_1 is the final energy of the electron, E_2 is the initial energy, g is a parameter for the paramagnetic system called the spectroscopic splitting factor, β is the Bohr magneton, and H is the applied magnetic field. Assume a certain group of spins with $g = g_1$ have their resonance condition met (1.1). If the r.f. field is turned off, then the spins will be in a non-equilibrium state. There are several interaction paths by which the spin system may return to thermal equilibrium with the lattice. We shall consider two possible paths.

If the coupling of the paramagnetic centers to the lattice is much stronger than the coupling among centers, then the spin system equilibrates with the lattice in a time characterized by τ_1, termed the spin-lattice relaxation time. A spin disposes of its excess energy (via $\vec{L}\cdot\vec{S}$) to the orbital magnetic moment which, in turn, couples the energy to the lattice heat sink by means of the time varying electric field laid down due to modulation of interionic distances by the lattice vibrations. This is the process which we shall study.

If there exists another set of spins with $g_2 \neq g_1$, the spins with g_1 may undergo mutual spin flips with them in a characteristic time denoted τ_{12}, called the cross relaxation time. The energy of the spin flip transitions is not precisely balanced, since $g_1 \neq g_2$, but the dipole-dipole inter-

action may take up or supply the energy necessary for energy conservation.

In the theory of spin-lattice relaxation, one considers the effect of a strain in the immediate vicinity of a paramagnetic ion on the spin Hamiltonian, and uses this perturbation Hamiltonian to calculate the spin relaxation by the usual perturbation techniques.[21,24] It is also usual to express the thermal strain as a superposition of lattice waves in order to describe spin-phonon interaction processes. To lowest order, the component linear in strain gives rise to the direct, or one-phonon process, while the component quadratic in strain gives rise to two-phonon or Raman processes. A Raman process is also obtained by carrying the linear strain term to second order in perturbation theory. An excellent account of the calculations involved is given by R. F. Vieth.[33]

We do not have enough information available to calculate an exact expression for τ_1 in the system under study, but it is still possible to extract the theoretical temperature dependence of τ_1 and compare it with our measured values. By expressing the lattice waves of a crystal in simple classical form, one can obtain several quantum mechanical operators. These operators have the effect of creating or destroying a phonon, a process which occurs when an electron spin absorbs energy from or relinquishes energy to the lattice. Two systems of ions must be con-

sidered:

1) those which have an even number of electrons (non-Kramers systems), and
2) those with an odd number of electrons (Kramers systems).

Waller,[36] Kronig,[16] and Van Vleck[32] originally predicted that two types of relaxation can occur for each system: one which involves one phonon (the direct process) and one which involves two phonons (the Raman process). The direct process occurs at lower temperatures while the Raman process is dominant at higher temperatures. For non-Kramers systems we find $\frac{1}{\tau_1} \propto T$ for the direct process and $\frac{1}{\tau_1} \propto T^7 J_6$, where J_n is a transport integral of order n, for the Raman process. For Kramers systems the situation is a bit more complicated. If zero order wave functions are used in the computation of the necessary matrix elements, the direct process will vanish and the Raman process will have a $T^9 J_8$ dependence. An applied magnetic field may, however, admix excited states with the zero order wave functions to produce a direct process that again is proportional to T and two Raman processes proportional to $T^7 J_6$ and $T^9 J_8$. In addition, if there are energy levels that lie near enough to the ground state, the Raman process may go as $T^5 J_4$. For either type of system, Orbach[24] has shown that if there is an accessible electron energy level with energy Δ above the ground state, and if $\Delta < E_D$, where E_D is the Debye energy of the lattice, then there may be a resonant two phonon process for which $\frac{1}{\tau_1} \propto \exp(-\Delta/kT)$.

The foregoing theories were formulated for a perfect lattice, whereas the paramagnetic ion is at a defect site. Since the lattice vibrations are modified by the defect, one is not justified in using the usual relation between strain and amplitude of a lattice wave, which holds in a perfect crystal. In view of the phenomenological nature of the theory, one would be very hard put to isolate the error introduced from the consequences of an incorrect choice of the strain dependence of the spin Hamiltonian, except when the temperature dependence of the spin-lattice relaxation is modified in some characteristic and unusual manner.

Klemens[3] has shown that relaxation rates (i.e., $\frac{1}{\tau_1}$) proportional to T^3J_2 and $T^{11}J_{10}$ for non-Kramers systems, and T^5J_4 and $T^{13}J_{12}$ for Kramers systems, arise from impurities which have associated with them vibrational frequencies lying within the Debye spectrum of the host lattice.

Montroll and Potts[22] have pointed out that in the case of a substitutional impurity which is lighter than the parent atom, the character of the lattice vibrations is particularly strongly modified, giving rise to a new lattice mode localized near the impurity, and having a frequency ν_0 which lies above the acoustic band. Klemens[13] has predicted $\frac{1}{\tau_1} \propto \exp(-h\nu_0/kT)$ for this case. Relaxation data[2] on the oxygen-divacency (E_1') center in synthetic crystalline quartz have been interpreted in terms of this theory, but the re-

sults are not conclusive.

We surmised that a better test of the theory could be realized from measurement of relaxation in a molecular complex whose localized frequencies ν_o were well defined and amenable to measurement by infrared spectroscopy. An ideal candidate seemed to be $Cr(CN)_5NO^{3-}$ substitutional in alkali halides. The acoustic phonon spectrum of the alkali halides has been studied,[1] so that lattice parameters involved in the "normal" direct and Raman relaxation of paramagnetic impurities are known. Hence we anticipated that any anomalous results should be due to interactions localized in the $Cr(CN)_5NO^{3-}$ complex.

II. THEORY

Theoretical Background

The phenomenological theory of electron spin-lattice relaxation in crystalline solids has been considered by many authors.[13,21,24] According to current hypotheses, the spin-phonon interaction plays the central role in paramagnetic relaxation phenomena.[32,16,21] The process occurs through modulation of the crystalline electric field by the lattice vibrations. This time-varying electric field interacts with the electron's orbital angular momentum, which is coupled to the spin via $\vec{L}\cdot\vec{S}$.

The model we shall initially use is illustrated in Figure 1, which shows a paramagnetic ion surrounded by an octahedron of nearest neighbors that produce an electrostatic field at the ion site. In the unperturbed system these neighbors are assumed stationary. If we allow the neighbors to vibrate (since they are part of the lattice), the crystalline field will be modulated, will perturb the orbital motion of the paramagnetic electrons, and will induce spin transitions by means of spin-orbit interaction. We shall neglect all effects of spin-spin interaction except for energy level broadening. That is, we assume that the spins relax to equilibrium only by giving up energy to the lattice, and not by cross relaxation effects.

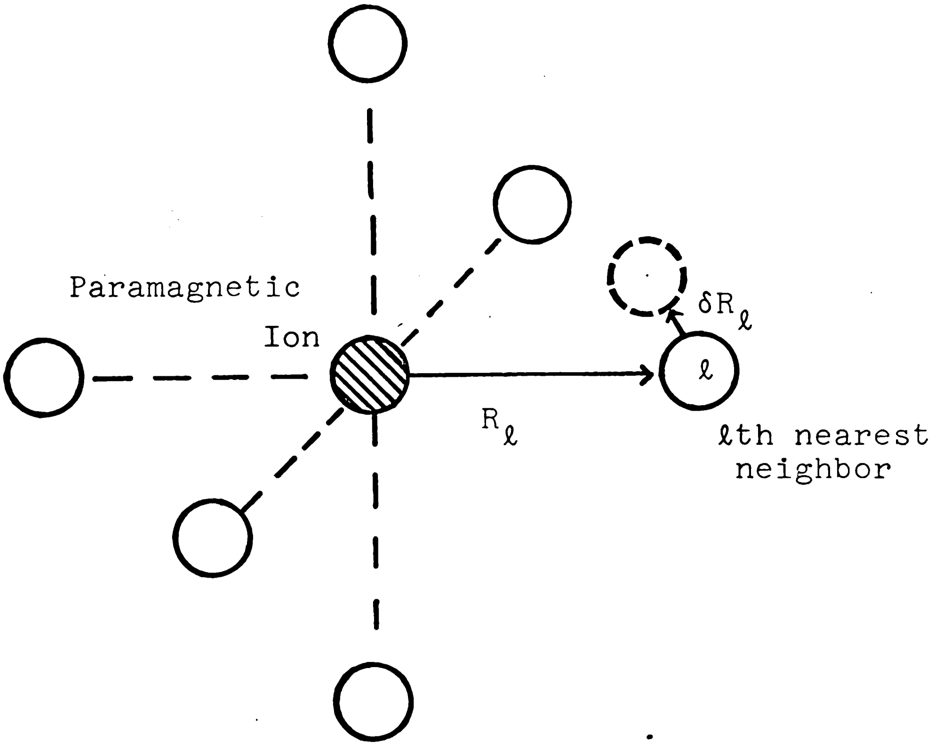

Figure 1. Octahedrally coordinated paramagnetic ion in the crystalline electric field of its nearest neighbors.

Under this assumption we can write the total Hamiltonian in the form[21]

$$\mathcal{H} = \mathcal{H}_L + \mathcal{H}_0 + V + 2\beta\vec{S}\cdot\vec{H} + \lambda\vec{L}\cdot\vec{S} + \beta\vec{L}\cdot\vec{H}. \qquad (2.1)$$

In this equation, β is the Bohr magneton, λ is the spin-orbit coupling parameter, $\vec{S}$ and $\vec{L}$ are the spin and orbital angular momenta of the paramagnetic ion, $\vec{H}$ is the external dc magnetic field, V is the energy of the ion due to the crystalline electric field, $\mathcal{H}_0$ is the energy of the free ion, and $\mathcal{H}_L$ represents the energy stored in the crystal lattice due to lattice vibrations. The lattice Hamiltonian can be written[14]

$$\mathcal{H}_L = \sum_p \hbar\omega_p(\hat{a}_p{}^\dagger \hat{a}_p + \tfrac{1}{2}), \qquad (2.2)$$

where $\hat{a}_p{}^\dagger$, $\hat{a}_p$ are the phonon creation and annihilation operators. They have the properties that

$$\hat{a}_p{}^\dagger|\ldots n_p\ldots> = (n_p+1)^{\frac{1}{2}}|\ldots n_p+1\ldots>$$

$$\hat{a}_p|\ldots n_p\ldots> = (n_p)^{\frac{1}{2}}|\ldots n_p-1\ldots>. \qquad (2.3)$$

The p index represents the phonon mode and branch number, with mode-branch frequency ω_p. If we designate the equilibrium position of an atom in the lattice by $\vec{r}$ and the displacement of this atom from equilibrium by $u_{r\alpha}$ (α = x,y, or z), then $u_{r\alpha}$ can be expanded in normal lattice modes as[14]

$$u_{r\alpha} = \left(\frac{2\hbar}{M}\right)^{\frac{1}{2}} \sum_p (\omega_p)^{-\frac{1}{2}} \phi_{p\alpha}(\hat{a}_p + \hat{a}_p{}^\dagger)\cos(\vec{k}\cdot\vec{r}+\Delta_p), \qquad (2.4)$$

where M is the crystal mass, $\phi_{p\alpha}$ is the αth component of the unit polarization vector for the mode-branch p, $\vec{k}_p$ is the propagation vector for mode-branch p, and Δ_p is an arbitrary phase factor.

In what follows, it shall be assumed for simplicity that the lattice is dispersionless and isotropic, with the result that all phonons have the same velocity, v, and thus we can describe the density of states by the Debye formula[11]

$$\rho(\nu) = \begin{cases} \dfrac{12\pi V\nu^2}{v^3} & \text{if } \nu \leq \left(\dfrac{3N}{4\pi V}\right)^{1/3} v \\ 0 & \text{if } \nu > \left(\dfrac{3N}{4\pi V}\right)^{1/3} v \end{cases} \tag{2.5}$$

Use will also be made of the fact that the average number of phonons in mode p when the crystal is in thermal equilibrium at temperature T is given by

$$N_p = (e^{\hbar\omega_p/kT} - 1)^{-1} \tag{2.6}$$

where $\omega_p = 2\pi\nu_p$.

In order to show the interaction between spin and lattice explicitly, we expand the crystal field potential, V, in a power series in the normal displacements (Q_f) of the nearest neighbor ions:[31]

$$V = V_o + \sum_f \frac{\partial V}{\partial Q_f} Q_f + \tfrac{1}{2} \sum_{ff'} \frac{\partial^2 V}{\partial Q_f \partial Q_{f'}} Q_f Q_{f'} + \ldots, \tag{2.7}$$

where the Q_f's can be related to the ordinary displacements of the neighbors ($\delta R_{\ell\alpha}$) by

$$Q_f = \sum_{\ell\alpha} B_{f\ell\alpha}\delta R_{\ell\alpha} \tag{2.8}$$

and the index ℓ runs over all nearest neighbors. Now $u_{r\alpha}$ is the displacement of any atom, and therefore it includes $\delta R_{\ell\alpha}$ as a special case. Hence $\delta R_{\ell\alpha}$ can be expanded by means of (2.4). In doing this, we make the approximation that the phonon wavelength is considerably greater than the dimensions of the cluster of nearest neighbors, so that $\vec{k}_p \cdot \vec{r} \ll 1$ (assuming, for simplicity that the nucleus of the paramagnetic ion is at the origin). Because the only nearest neighbor displacements effective in modulating the crystalline field are those <u>relative</u> to the spin nucleus, equation (2.4) reduces to

$$\delta R_{\ell\alpha} = \left(\frac{2h}{Mv^2}\right)^{\frac{1}{2}} \sum_p (\omega_p)^{\frac{1}{2}} \phi_{p\alpha}(\hat{a}_p + \hat{a}_p{}^\dagger)\vec{K}_p \cdot \vec{R}_\ell \sin\Delta_k, \tag{2.9}$$

where $\vec{K}_p$ is the unit vector in the $\vec{k}_p$ direction, and we have used $|\vec{k}_p| = \omega_p/v$. Substituting (2.8) and (2.9) into (2.7), we find

$$V = V_0 + \sum_{fp} V^f A^{fp}\Gamma_p + \sum_{ff'pq} V^{ff'} A^{fp} A^{f'q}\Gamma_p\Gamma_q + \ldots. \tag{2.10}$$

where

$$V^f = \frac{\partial V}{\partial Q_f} \;;\; V^{ff'} = \frac{1}{2}\frac{\partial^2 V}{\partial Q_f \partial Q_{f'}} \;;\; \Gamma_p = a_p + a_p{}^\dagger,$$

$$A^{fp} = \left(\frac{2\hbar\omega_p}{Mv^2}\right)^{\frac{1}{2}} \sin\Delta_p \sum_{\ell\alpha} B_{f\ell\alpha}\vec{K}_p \cdot \vec{R}_\ell \;. \tag{2.11}$$

In the foregoing we should distinguish between two different sets of normal modes over which summations have been made. On the one hand, in (2.7) we summed over the relatively small number of modes (Q_f) of the nearest neighbor cluster, and on the other hand in (2.4) we summed over the relatively large number (3N) of traveling wave modes of the lattice. Utilizing (2.1), (2.2), and (2.10), we find for the total Hamiltonian

$$\begin{aligned} \mathcal{H} = {} & \sum_p \hbar\omega_p(\hat{a}_p{}^\dagger \hat{a}_p + \tfrac{1}{2}) + \mathcal{H}_0 + V_0 + 2\beta\vec{S}\cdot\vec{H} \\ & + \lambda\vec{L}\cdot\vec{S} + \beta\vec{L}\cdot\vec{H} + \sum_{fp} V^f A^{fp}\Gamma_p \\ & + \sum_{ff'pq} V^{ff'} A^{fp} A^{f'q} \Gamma_p \Gamma_q \;. \end{aligned} \tag{2.12}$$

We now divide $\mathcal{H}$ into $\mathcal{H}_{\text{lattice}}$, $\mathcal{H}_{\text{spin}}$ and $\mathcal{H}_{\text{interaction}}$. Examining the terms, we find that $\sum_p \hbar\omega_p(\hat{a}_p{}^\dagger \hat{a}_p + \tfrac{1}{2})$ has only lattice coordinates; $\mathcal{H}_0 + V_0 + 2\beta\vec{S}\cdot\vec{H} + \lambda\vec{L}\cdot\vec{S} + \beta\vec{L}\cdot\vec{H}$ involves only paramagnetic electron coordinates; $\sum_{fp} V^f A^{fp}\Gamma_p + \sum_{ff'pq} V^{ff'} A^{fp} A^{f'q}\Gamma_p\Gamma_q$ involves mixed coordinates. The term in electron coordinates is precisely the one that gives rise to the spin Hamiltonian which describes the energy levels that are observed in paramagnetic resonance. In relaxation experiments, we are interested in phonon-induced transitions between these pairs of spin levels. Hence it seems reasonable to set

$$\mathcal{H}_{\text{lattice}} = \sum_{p} \hbar\omega_p(\hat{a}_p{}^{\dagger}\hat{a}_p+\tfrac{1}{2}) \tag{2.13}$$

$$\mathcal{H}_{\text{spin}} = \mathcal{H}_0 + V_0 + 2\beta\vec{S}\cdot\vec{H} + \lambda\vec{L}\cdot\vec{S} + \lambda\vec{L}\cdot\vec{H} \tag{2.14}$$

and to consider

$$\mathcal{H}_{\text{interaction}} = \sum_{fp} V^f A^{fp}\Gamma_p + \sum_{ff'pq} V^{ff'}A^{fp}A^{f'q}\Gamma_p\Gamma_q \tag{2.15}$$

as inducing energy conserving exchanges of quanta between $\mathcal{H}_{\text{spin}}$ and $\mathcal{H}_{\text{lattice}}$. Detailed calculation would involve diagonalizing $\mathcal{H}_{\text{spin}}$ to some appropriate order (the second order would suffice -- this would produce the spin Hamiltonian), finding its energy levels E_n and corresponding state vectors $|\Psi_n>$, and computing the appropriate matrix elements of $\mathcal{H}_{\text{interaction}}$ between simultaneous eigenstates of $\mathcal{H}_{\text{spin}}$ and $\mathcal{H}_{\text{lattice}}$. The rates for the various relaxation processes are then calculated from time-dependent perturbation theory.

Let us rewrite (2.15) as

$$\mathcal{H}_{\text{interaction}} = V_1\hat{\varepsilon} + V_2\hat{\varepsilon}\hat{\varepsilon}' \tag{2.16}$$

where $\hat{\varepsilon}$ and $\hat{\varepsilon}'$ are operators for the average strain due to the lattice vibrations, and are proportional to $\hat{a}$ and $\hat{a}^{\dagger}$, depending on whether a phonon is annihilated or created. Our ignorance of the matrix elements of the V^f for the system under study motivates this simplification. In spite of this ignorance, a number of interesting conclusions about

the various relaxation processes can be drawn.

In evaluating matrix elements of the electron operators V_1 and V_2 of (2.16), we must consider two types of systems:

1) those which have an even number of electrons (non-Kramers systems), and
2) those with an odd number of electrons (Kramers systems).

Kramers' theorem[15] states that each energy level will always be at least twofold degenerate in the presence of purely electric fields, provided the number of electrons is odd. Wigner[37] has shown that this degeneracy is related to the invariance of the system under time reversal, and that a pair of Kramers degenerate states are time conjugates of one another. Kramers' theorem is important to us because it predicts that certain matrix elements of (2.16) vanish if no magnetic field is applied. The presence of a magnetic field will lift the Kramers degeneracy, and give nonzero matrix elements.

The following sections of this chapter summarize the theoretical results for various spin-lattice relaxation mechanisms. Most of these results have been derived elsewhere.[24,33]

Direct Process

Figure 2 depicts a spin initially in state $|b\rangle$ relaxing to state $|a\rangle$ with the consequent emission of one phonon. This method of relaxation is called the direct process. E_s is the energy difference between the spin levels and therefore is also equal to $\hbar\omega_q$, the energy of the emitted phonon. The direct process is usually dominant at low temperatures. If first order time dependent perturbation theory is applied to the linear strain term of the orbit-lattice Hamiltonian (2.16), then for $E_s \ll kT$ we have for the direct process rate

$$\frac{1}{\tau_D} = \frac{3(E_s)^2 kT}{\hbar^2 \pi \rho v^5} \quad |\langle a|V_1|b\rangle|^2 \ , \qquad (2.17)$$

where $\rho = M/V$, the density of the host crystal.

If $|a\rangle$ and $|b\rangle$ are time conjugate states, then the matrix element in (2.17) will be zero by Kramers' theorem. The magnetic dipole-magnetic field interactions can admix excited state Kramers doublets into the wave functions $|a\rangle$ and $|b\rangle$ to produce a nonzero result. To first order, the ground state wave functions in the presence of a magnetic field are

$$|b\rangle' = |b\rangle + \sum_n{}' \frac{\langle n|\vec{\mu}\cdot\vec{H}|b\rangle}{E_b - E_n} \quad |n\rangle \qquad (2.18)$$

$$|a\rangle' = |a\rangle + \sum_n{}' \frac{\langle n|\vec{\mu}\cdot\vec{H}|a\rangle}{E_a - E_n} \quad |n\rangle \qquad (2.19)$$

where $\vec{\mu}$ is the magnetic dipole moment operator and $\vec{H}$ is the

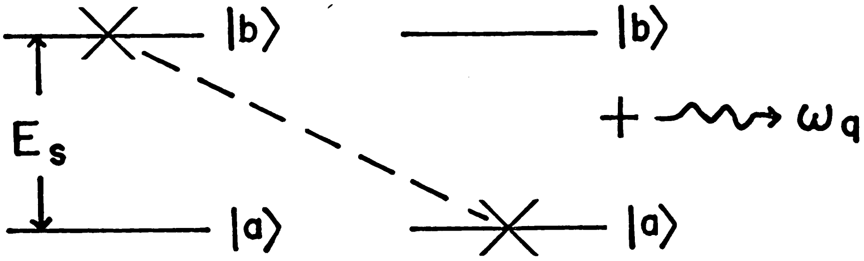

Figure 2. Schematic diagram for the direct process. A single transition is made from |b> to |a> and a phonon of energy E_s is emitted.

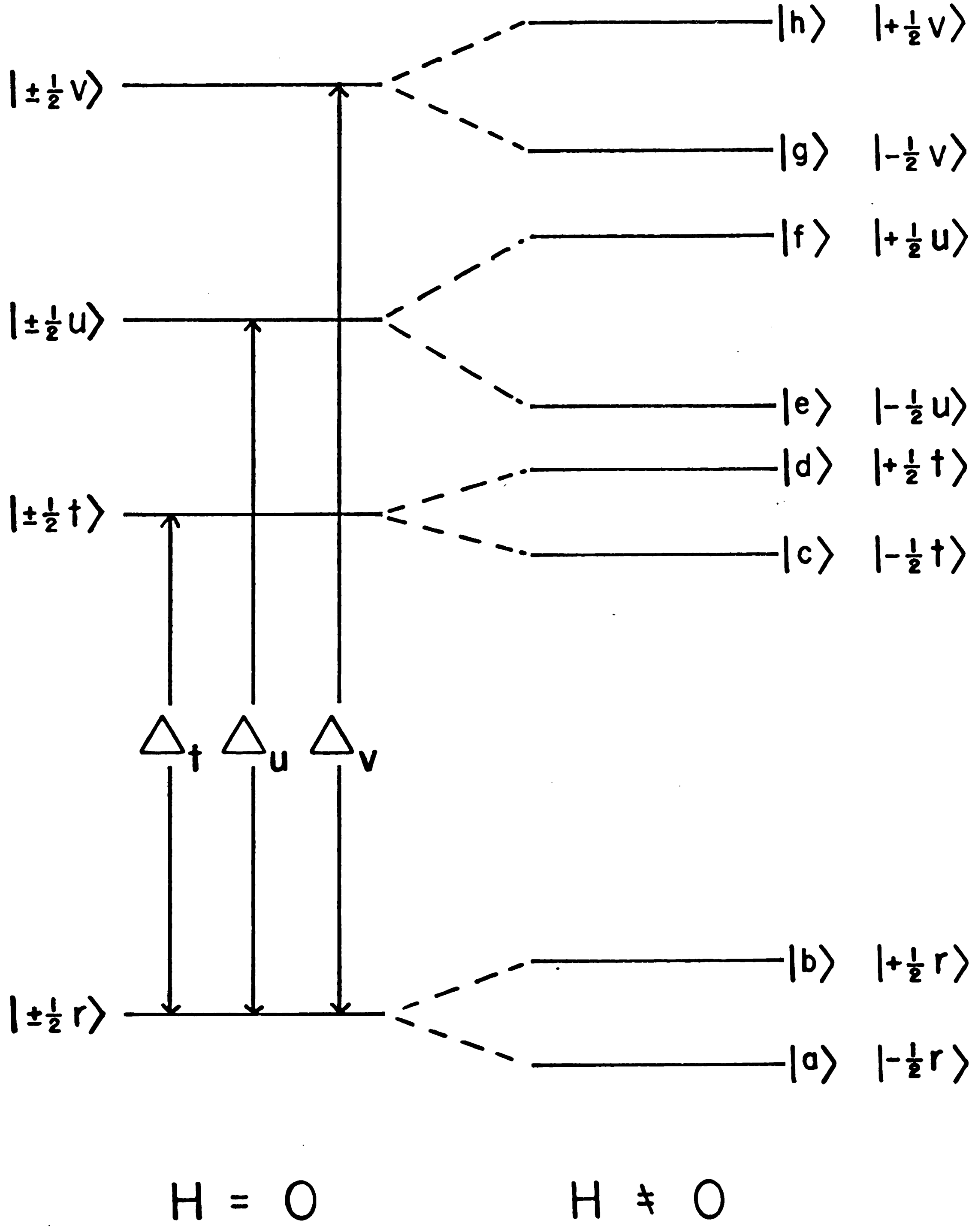

Figure 3. A hypothetical energy level diagram for a Kramers ion in a uniaxial crystal field in the presence of spin-orbit coupling; r, t, u, and v are odd integers.

magnetic field. The only terms that contribute are those which lie near to the ground state (Figure 3). If $|c\rangle$ and $|d\rangle$ are the nearest lying time conjugate states, then by applying time reversal arguments, as well as selection rules on $|\Delta m|$, we are led to the result

$$\frac{1}{\tau_D} = \frac{12E_s{}^2H^2kT}{\hbar^4\pi\rho v^5\Delta_{cd}{}^2} \, |\langle d|\mu|b\rangle\langle a|V_1|d\rangle|^2 \ , \qquad (2.20)$$

where

$$\Delta_{cd} \simeq E_c - E_b \simeq E_a - E_d \qquad (2.21)$$

and μ is the magnetic moment in the direction of H.

Raman Process

In the Raman process lattice phonons are scattered inelastically from the spin system. This results in the creation and destruction of two phonons whose difference in energy equals the splitting of the participating spin states. As outlined in Figure 4 the process we envisage will have an initial state vector specified by a spin being in the state $|b\rangle$ and the phonons (p) and (q) having occupation numbers N_p and N_q, respectively. The final state of the system will find the spin in state $|a\rangle$, a phonon created of type (q), and a phonon of type (p) destroyed. There are several mathematical approaches to such a process. We shall consider two different methods which follow two

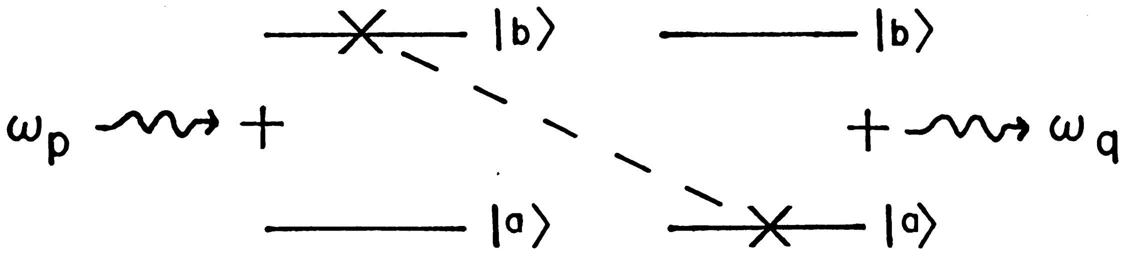

(a) $\frac{1}{\tau_1} \propto \left| \langle a | V_2 | b \rangle \right|^2$

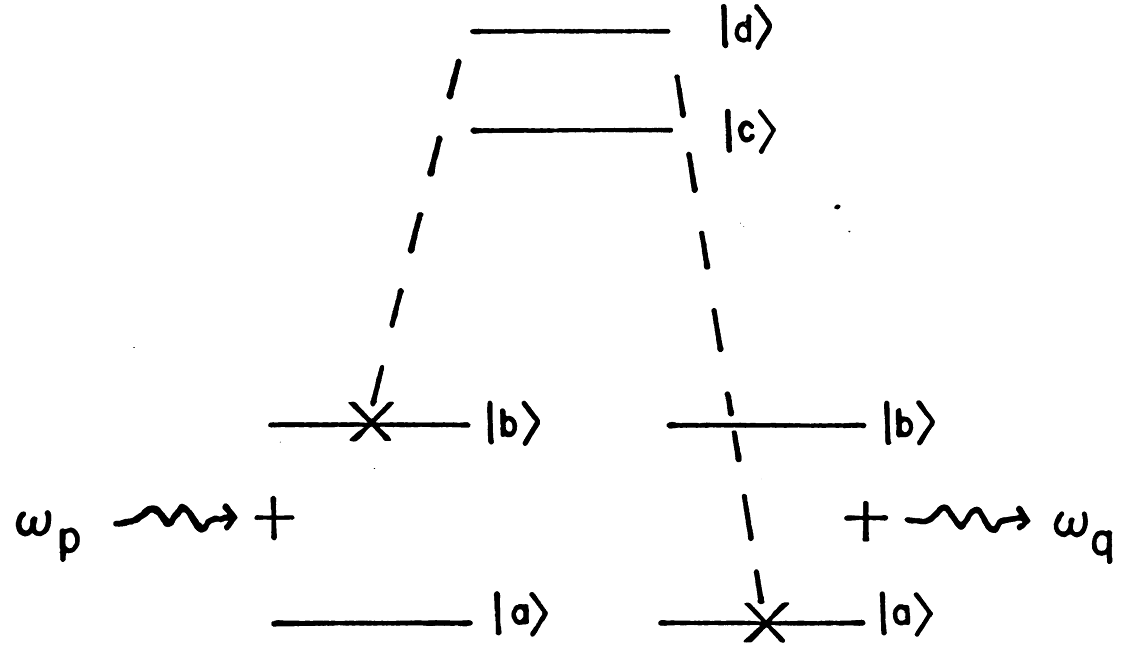

(b) $\frac{1}{\tau_1} \propto \left| \langle a | V_1 | c \rangle \langle c | V_1 | b \rangle \right|^2$

Figure 4. Schematic diagrams for the Raman process. In both cases, $\omega_q - \omega_p = E_b - E_a$.

basically dissimilar physical approaches.

Consider a process in which the quadratic strain term of the interaction Hamiltonian (2.16) is used in first order perturbation theory (Figure 4(a)). The resulting relaxation rate for non-Kramers systems is

$$\frac{1}{\tau_R} = \frac{9k^7}{4\pi^3\rho^2 v^{10}\hbar^7} T^7 J_6\left(\frac{\theta}{T}\right) \quad |\langle a|V_2|b\rangle|^2 \tag{2.22}$$

where

$$J_n(x) \equiv \int_0^x \frac{z^n e^z}{(e^z-1)^2}\, dz \tag{2.23}$$

and θ is the Debye temperature of the lattice.

Here, as in the direct process, the matrix element of V_2 will vanish if $|a\rangle$ and $|b\rangle$ are time-conjugate states, i.e., for a Kramers system. In that case, higher lying electron levels can be admixed by the $\vec{\mu}\cdot\vec{H}$ interaction to give

$$\frac{1}{\tau_R} = \frac{9H^2k^7}{\pi^3\rho^2 v^{10}\hbar^7\Delta_{cd}^2} T^7 J_6\left(\frac{\theta}{T}\right) \quad |\langle d|\mu|b\rangle\langle a|V_2|d\rangle|^2 \tag{2.24}$$

The J_n in (2.22) and (2.24) are called transport integrals and have been tabulated.[23] They are essentially constant for $x>x_n$, where $x_6 = 20$ and $x_8 = 25$, and have the additional property that

$$T^{n+1} J_n\left(\frac{\theta}{T}\right) \rightarrow aT^2 \text{ for } T>\theta/2 \tag{2.25}$$

This follows from the phonon population factor (2.6).

Since

$$e^{x} = 1 + x + \ldots \qquad \text{if } x<<1, \tag{2.26}$$

we have

$$\frac{1}{e^{\hbar\omega/kT}-1} \simeq \frac{kT}{\hbar\omega} \qquad \text{if } kT>>\hbar\omega \ . \tag{2.27}$$

Hence at temperatures high compared to the phonon energies, the phonon occupation numbers are proportional to T. But the transition rates are proportional to phonon occupation numbers. Therefore <u>any</u> two-phonon relaxation process has the asymptotic form $\frac{1}{\tau_1} \propto T^2$ for temperatures comparable to the maximum energy of the phonons involved.

Consider a relaxation process which uses linear strain terms in second order perturbation theory. Here the electron spin in state $|b>$ is considered to undergo virtual (and therefore not energy-conserving) transitions to intermediate states rather than making transition directly to state $|a>$ (Figure 4(b)). For a non-Kramers system this process is describable by

$$\frac{1}{\tau_R} = \frac{9k^7}{4\pi^3\rho^2 v^{10}\hbar^7} T^7 J_6\left(\frac{\theta}{T}\right) \qquad \left| \sum_i{}' \frac{<a|V_1|i><i|V_1'|b>}{\Delta_i} \right|^2 \tag{2.28}$$

$$\text{where } \Delta_i \simeq E_i - E_b \simeq E_i - E_a . \tag{2.29}$$

For a system with an odd number of electrons, the time conjugate nature of the Kramers doublets leads to the "Van Vleck[31] cancellation". The effect of the cancellation is to raise the power of T in the relaxation rate:

$$\frac{1}{\tau_R} = \frac{9k^9}{\pi^3\rho^2 v^{10}\hbar^7} T^9 J_8\left(\frac{\theta}{T}\right) \left|\frac{<a|V_1|c><c|V_1'|b>}{\Delta_{cd}^{\;2}}\right|^2 , \qquad (2.30)$$

where we have considered as intermediate states only the Kramers doublet lying nearest to the ground doublet and have explicitly used the time-conjugate nature of $|c>$ and $|d>$.

We note that in this process it was not necessary to invoke Zeeman admixture of excited states into the ground state in order to achieve a nonvanishing result. The reason is that here we have matrix elements between components of different Kramers doublets rather than between components of the same doublet.

Orbach and Blume[25] have considered the Van Vleck cancellation term further. In the derivation of the T^9J_8 process it is assumed that the states $|c>$ and $|d>$ are split apart from the ground state by a large energy, but for some Kramers systems excited states lie close to the ground doublet. This leads to

$$\frac{1}{\tau_R} = \frac{9k^5}{\pi^3\rho^2 v^{10}\hbar^7} T^5 J_4\left(\frac{\theta}{T}\right) \left|\frac{<a|V_1|c><c|V_1'|b>}{\Delta_{cd}^{\;2}}\right|^2 \qquad (2.31)$$

A rough order of magnitude criterion for this process to dominate in the Raman region is given by Orbach and Blume as

$$\lambda\left(\frac{\lambda}{\Delta}\right) > kT, \qquad (2.32)$$

in addition to $\Delta << k\theta$, where Δ is the appropriate crystal field splitting and λ is the spin-orbit coupling constant.

Orbach Process

Finn, Orbach and Wolf[4] first proposed a two-phonon process which is similar to the Raman process depicted in Figure 4(b), except that the intermediate electron state $|c>$ lies within the lattice phonon spectrum. That is, $E_c < k\theta$. Now the energy denominator of (2.28) displays a resonance. In reality, the denominator does not vanish because of lifetime broadening of the electron energy levels, but the relaxation rate is enhanced considerably over the normal Raman rate. When the resonance denominator is taken into account the predicted relaxation rate for both Kramers and non-Kramers systems contains an exponential term

$$\frac{1}{\tau_{Orb}} \propto \frac{|<a|V_1|c><c|V_1'|b>|^2}{\Delta_{cd}^4} e^{-\Delta/T} \qquad (2.33)$$

where $\Delta(<k\theta)$ is the splitting of the excited state from the ground state. This process is referred to as the Orbach process.

Driven-Mode Process

In the previous discussion we have neglected the effect of the paramagnetic impurity on the lattice vibrations of the host crystal. That is, we have assumed that the strain ε at point $\vec{r}$ due to a lattice wave of wave vector $\vec{p}$ is given by (2.4), even though that expression holds only in a perfect crystal. In order to calculate τ_1 we need to know the strain in the immediate vicinity of the spin site. When the spin is associated with an impurity or defect, this is precisely where expression (2.4) fails. We must, therefore look more closely at the strain at a defect site.

Every defect has associated with it one or more characteristic vibrational frequencies ω_i, which have to be compared to the frequency describing the normal interatomic bond of order $\omega_D (=k\theta/\hbar)$, the Debye frequency. Roughly speaking, we can expect two classes of behavior: (a) cases when ω_i exceeds ω_D sufficiently, so that the vibrations at that frequency are not propagated through the crystal, but are localized at the defect;[22,13] (b) cases when ω_i falls below ω_D so that localized modes in the usual sense are not formed, but the defect system undergoes forced oscillations[3] under the influence of lattice waves. We consider this latter case first, referring to it as the driven-mode process.

Klemens[3] has shown that for an impurity-associated frequency which is less than ω_D, the Raman relaxation rate (2.30) for a Kramers system is modified to the form

$$\frac{1}{\tau_{DM}} \propto T^9 J_8\left(\frac{\theta}{T}\right) + CT^5\left[\left\{J_4\left(\frac{\theta}{T}\right) - J_4\left(\frac{\theta i}{T}\right)\right\} + \left(\frac{T}{\theta_i}\right)^8 J_{12}\left(\frac{\theta i}{T}\right)\right], \qquad (2.34)$$

where $k\theta_i = \hbar\omega_i$ is the energy associated with the defect mode. For a non-Kramers system the analogous term is

$$\frac{1}{\tau_{DM}} \propto T^7 J_6\left(\frac{\theta}{T}\right) + C'T^3\left[\left\{J_2\left(\frac{\theta}{T}\right) - J_2\left(\frac{\theta i}{T}\right)\right\} + \left(\frac{T}{\theta_i}\right)^8 J_{10}\left(\frac{\theta i}{T}\right)\right]. \qquad (2.35)$$

Local Mode Process

We now consider in some detail the case in which frequencies associated with a defect lie above the acoustic band of the host lattice. In such a case the energy of the modes is concentrated in the immediate vicinity of the defect, so that one might expect it to modify very substantially the spin-lattice relaxation of a paramagnetic impurity associated with this defect site.

Since the energy of a local mode greatly exceeds the spin energy, it is not possible to have a direct energy conserving spin-phonon interaction involving a local mode. The only conceivable process is one in which a spin-flip is accompanied by the absorption and subsequent re-emission of a localized phonon. If the local mode frequency were sharp, this process would also violate energy conservation. The local mode frequency is, however, broadened by anharmonic interactions with the phonons of the lattice continuum. The anharmonic effects are expected to be strong, even at $T \ll \theta$, because most of the energy of a localized mode is concentrated near the defect, making the amplitude of the oscillation large. Even at low temperatures a localized phonon can split into two lattice phonons. Klemens[12] has shown that this process broadens the local mode frequency by about 1%. The broadening may therefore be larger than the spin energy (≈ 0.3 cm^{-1} in our experiments), so that energy conservation is relaxed sufficiently to allow this

process to occur.

To take account quantitatively of how the anharmonic broadening and the relaxation of the local mode permit the spin-lattice interaction with absorption and emission of a local phonon, we consider their combined effect to the next order of perturbation theory. A local phonon and the spin combine; in the intermediate state we have the same local phonon, but the spin is inverted, and in the final state the spin stays inverted, and the local phonon has split by anharmonic interaction into two phonons of the Debye continuum. Since there is only one intermediate state, there is a one-to-one correspondence between the overall second order matrix element and the matrix element for the anharmonic interaction between a local phonon and two lattice-wave phonons. Thus the contribution of local phonons to the spin-lattice relaxation is related in magnitude to the anharmonic relaxation time of the local mode.

Let us examine this process in more detail. Consider a two stage process going from state |i> to state |f> via an intermediate state |j>. Such a process is equivalent to going from |i> to |f> with an effective perturbation Hamiltonian

$$\mathcal{H}'_{eff} = \sum_j \frac{\langle f|W|j\rangle\langle j|U|i\rangle}{E_i - E_j} , \qquad (2.36)$$

where U and W are the perturbation Hamiltonians linking |i> and |j>, and |j> and |f>, respectively.

As initial state we take the local mode excited with one phonon, the ion in the higher-lying spin state, and the lattice phonons in equilibrium. (See Figure 5 for more explicit description of the state vectors, including phonon occupation numbers of the relevant modes.) As intermediate state $|j>$ we need to consider only one state, i.e., with one phonon in the local mode and the spin inverted. Hence the sum in (2.36) is reduced to a single term and its denominator is merely the spin energy $E_s \simeq g\beta H$. The interaction represented by $<j|U|i>$ is a Raman process involving only localized phonons, so that we may set $<j|U|i> = <a|V_2|b>\varepsilon_0\varepsilon_0'$ where V_2 is the same as in (2.16) and $\varepsilon_0, \varepsilon_0'$ each represent matrix elements of the strain due to one localized phonon. The final state has the same spin configuration as the intermediate state, but the local phonon is removed and two traveling lattice modes are each excited by an additional phonon. (Figure 5).

The interaction Hamiltonian W connecting states $|j>$ and $|f>$ arises from the cubic anharmonicities (involving three phonons at a time), and is the same as was used by Klemens[12] to describe the relaxation to equilibrium of excess energy in the local mode. We can write $<f|W|j>$ as

$$\xi[N_0(N_1+1)(N_2+1)]^{\frac{1}{2}} \text{ or } \xi[(N_0+1)N_1N_2]^{\frac{1}{2}}, \qquad (2.37)$$

depending on whether a local phonon is annihilated or created, where N_0, N_1, and N_2 are the occupation numbers of the

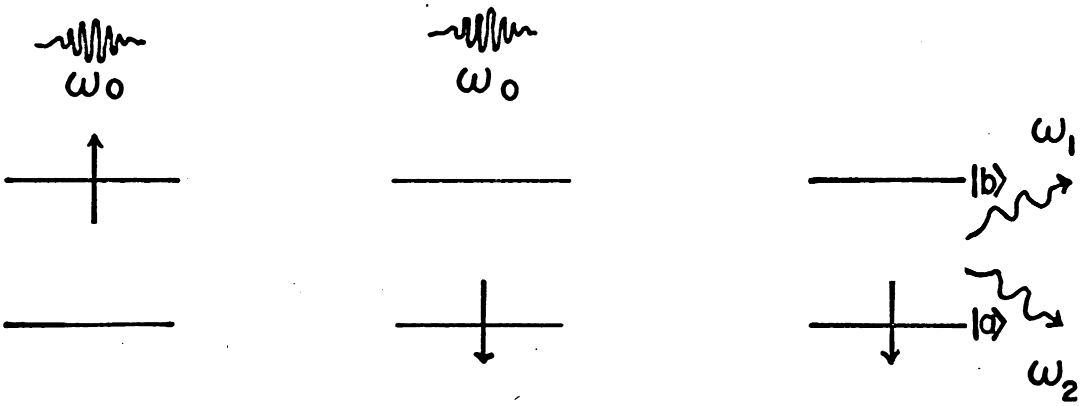

$$\left\langle \begin{matrix} N_0-1 \\ N_1+1 \\ N_2+1 \\ -\frac{1}{2} \end{matrix} \middle| \begin{matrix} a_0 \\ a_1^{\dagger} \\ a_2^{\dagger} \\ \end{matrix} \middle| \begin{matrix} N_0 \\ N_1 \\ N_2 \\ -\frac{1}{2} \end{matrix} \right\rangle \left\langle \begin{matrix} N_0 \\ N_1 \\ N_2 \\ -\frac{1}{2} \end{matrix} \middle| \begin{matrix} a_0^{\dagger} a_0 \\ \\ \\ S_- \end{matrix} \middle| \begin{matrix} N_0 \\ N_1 \\ N_2 \\ +\frac{1}{2} \end{matrix} \right\rangle$$

$$\omega_0 = \omega_1 + \omega_2$$

Figure 5. Schematic diagram of the local mode process, along with the appropriate matrix element. N_0, N_1 and N_2 are the number of phonons in the local mode and traveling modes.

local mode and traveling modes. The perturbation Hamiltonian (2.37) can be used in time dependent perturbation theory to show[12] that the relaxation rate of the local mode is inversely proportional to $\sum_f |<f|W|j>|^2$, i.e.,

$$\frac{1}{\tau_0} \propto \sum_f (N_1 + N_2 + 1), \qquad (2.38)$$

where the sum is over all final states which satisfy the energy condition $\omega_0 = \omega_1 + \omega_2$. For example, consider the case $(\hbar/k)\omega_0 \simeq 600°K$, with the Debye temperature of the host lattice ($\simeq 200°K$). The only lattice phonons which can participate in relaxing the local mode are those out in the "tail" of the phonon distribution, i.e., those for which $(\hbar/k)\omega > \theta_D$. When this restriction is taken into account, (2.38) may be approximated by

$$\frac{1}{\tau_0} \propto e^{-\theta_0/2T} + e^{-\theta_0/2T} + 1 \quad . \qquad (2.39)$$

As a further simplification, we shall neglect the exponentials in (2.39) as they are small compared to unity, since in our measurements $T<150°K$. Then for the temperature range of interest, Klemens[13] obtains

$$\frac{1}{\tau_0} \simeq \frac{\hbar\omega_0{}^2}{Mv^3} \qquad (2.40)$$

which is independent of temperature. At this point it is clear that the Debye approximation (2.5) for the density of phonon states is not valid for the lattice phonons involved in the local mode process, and that for a serious quantitative calculation we should need a more realistic model. We can, however, draw some significant qualitative conclusions using a "smeared" Debye spectrum, i.e., one for which there are a small number of available states above $\hbar\omega_D$.

We view the overall spin-lattice relaxation via localized modes as a two-step process in which the spin relaxes to the local mode, and then the local mode gives up its energy to the lattice. There is a one-to-one correspondence between every final state in the sum (2.38) and the final state in the overall process, since the spin energy is negligible when compared with the phonon energies. The effective matrix element (2.36) is the matrix element (2.38) multiplied by $[\langle j|U|i\rangle/E_s]$. In order to calculate the rate of change of σ, the fraction of spins in state $|b\rangle$, we must consider both the process depicted in Figure 5 and its inverse. Then

$$\frac{d\sigma}{dt} \propto \sigma N_0(N_1 + 1)(N_2 + 1) - N_1N_2(N_0 + 1)(1 - \sigma). \qquad (2.41)$$

This expression vanishes at equilibrium. If σ deviates from equilibrium by $\delta\sigma$, the term $\delta\sigma$ is proportional to

$$N_0(N_1 + N_2 + 1) + N_1N_2. \qquad (2.42)$$

The term in parentheses is approximately equal to unity by the same argument as given for (2.39). Also,

$$N_1N_2 \simeq e^{-\hbar\omega_1/kT}\, e^{-\hbar\omega_2/kT} = e^{-\hbar(\omega_1+\omega_1)/kT}$$

$$= e^{-\hbar\omega_0/kT} \simeq N_0 \ . \qquad (2.43)$$

Hence (2.42) becomes approximately $2N_0$. Thus the relaxation rate for spins via the overall process involving local phonons is of the form

$$\frac{1}{\tau_{LM}} \simeq 2\left(\frac{\hbar\omega_0^2}{Mv^2}\right)\frac{|\varepsilon_0\varepsilon_0'|^2}{E_s^2}\left|\langle a|V_2|b\rangle\right|^2 N_0, \qquad (2.44)$$

or

$$\frac{1}{\tau_{LM}} \simeq \frac{B}{E_s^2}\left|\langle a|V_2|b\rangle\right|^2 e^{-\theta_0/T}, \qquad (2.45)$$

where the coefficient B is temperature independent, and we have used the fact that θ_0/T is sufficiently great in our measurements to permit setting $N_0 \simeq e^{-\theta_0/T}$. As noted previously, for a Kramers system the electron matrix element in (2.45) vanishes for zero-order states $|a\rangle$, $|b\rangle$. If we allow admixture of higher lying states by the magnetic dipole-magnetic field interaction, the result for a Kramers system is

$$\frac{1}{\tau_{LM}} \simeq \omega_0\left(\frac{\hbar\omega_0}{Mv^2}\right)^3\frac{H^2}{E_s^2\Delta_{cd}^2}\left|\langle d|\mu|b\rangle\langle a|V_2|d\rangle\right|^2 e^{-\theta_0/T} \qquad (2.46)$$

Anisotropy of Relaxation Time

We now discuss possible dependence of τ_1 on the orientation of the applied magnetic field $\vec{H}$, for a Kramers ion in a crystal field of uniaxial symmetry. The relevant parts of the theoretical relaxation rates for the direct process,

the various Raman processes, the Orbach process, the driven mode process, and the local mode process are summarized below:

$$\frac{1}{\tau_D} \propto |\langle d|\vec{\mu}\cdot\vec{H}|b\rangle\langle a|V_1|d\rangle|^2 \, (\Delta_{cd})^{-2} \, T \qquad (2.47)$$

$$\frac{1}{\tau_R} \propto |\langle d|\vec{\mu}\cdot\vec{H}|b\rangle\langle a|V_2|d\rangle|^2 \, (\Delta_{cd})^{-2} \, T^7 J_6 \qquad (2.48)$$

$$\frac{1}{\tau_R} \propto |\langle a|V_1|c\rangle\langle c|V_1'|b\rangle|^2 \, (\Delta_{cd})^{-4} \, T^9 J_8 \qquad (2.49)$$

$$\frac{1}{\tau_R} \propto |\langle a|V_1|c\rangle\langle c|V_1'|b\rangle|^2 \, (\Delta_{cd})^{-4} \, T^5 J_4 \qquad (2.50)$$

$$\frac{1}{\tau_{Orb}} \propto |\langle a|V_1|c\rangle\langle c|V_1'|b\rangle|^2 \, (\Delta_{cd})^{-4} \, e^{-\Delta/T} \qquad (2.51)$$

$$\frac{1}{\tau_{DM}} \propto |\langle a|V_1|c\rangle\langle c|V_1'|b\rangle|^2 \, (\Delta_{cd})^{-4} \, \{T \text{ dep.}\} \qquad (2.52)$$

$$\frac{1}{\tau_{LM}} \propto |\langle d|\vec{\mu}\cdot\vec{H}|b\rangle\langle a|V_2|b\rangle|^2 \, (\Delta_{cd})^{-2} \, e^{-\theta_0/T} \qquad (2.53)$$

The only anisotropy considered here is that due to electron matrix elements. That is, all matrix elements of phonon operators are assumed to be isotropic, which is equivalent to assuming the velocity of sound is independent of direction in the lattice.

Anisotropy of τ_1 in Kramers systems may be attributed to the admixture interaction $\vec{\mu}\cdot\vec{H}$ invoked in (2.18) and (2.19) to give nonvanishing matrix elements of the orbit-lattice Hamiltonian (2.16). To facilitate the quantitative derivation of this result we shall employ the alternative notation

in Figure 3. That is, the states formerly referred to as $|a\rangle$, $|b\rangle$, $|c\rangle$, and $|d\rangle$ shall now be called $|-\frac{1}{2}r\rangle$, $|+\frac{1}{2}r\rangle$, $|-\frac{1}{2}t\rangle$ and $|+\frac{1}{2}t\rangle$, respectively. This notation will emphasize the fact that states such as $|\pm\frac{1}{2}r\rangle$ are time conjugates of one another and are composed of states of half-integral quantum numbers. As stated earlier, this leads to $\langle -\frac{1}{2}r|V_1|\frac{1}{2}r\rangle = 0 = \langle -\frac{1}{2}r|V_2|\frac{1}{2}r\rangle$. The $\vec{\mu}\cdot\vec{H}$ interaction is used to admix higher-lying Kramers doublets such as $|\pm\frac{1}{2}t\rangle$ into the ground doublet. The resulting states, expressed in the new notation, are

$$|-\tfrac{1}{2}r\rangle' = |-\tfrac{1}{2}r\rangle + \vec{H}\cdot \frac{\langle \pm\frac{1}{2}t|\vec{\mu}|-\frac{1}{2}r\rangle}{-\Delta_t} |\pm\tfrac{1}{2}t\rangle \qquad (2.54)$$

$$|+\tfrac{1}{2}r\rangle' = |+\tfrac{1}{2}r\rangle + \vec{H}\cdot \frac{\langle \pm\frac{1}{2}t|\vec{\mu}|+\frac{1}{2}r\rangle}{-\Delta_t} |\pm\tfrac{1}{2}t\rangle \qquad (2.55)$$

The magnetic dipole moment operator $\vec{\mu}$ is proportional to an angular momentum operator, so that if $\langle\frac{1}{2}t|\vec{\mu}|\frac{1}{2}r\rangle \neq 0$, then $\langle\frac{1}{2}t|\vec{\mu}|-\frac{1}{2}r\rangle = 0$. This follows because r is an odd integer and $\vec{\mu}$ can at most connect states differing in m value by ±1. Hence if

$$|-\tfrac{1}{2}r\rangle' = |-\tfrac{1}{2}r\rangle - \vec{H}\cdot \frac{\langle -\frac{1}{2}t|\vec{\mu}|-\frac{1}{2}r\rangle}{\Delta_t} |-\tfrac{1}{2}t\rangle, \qquad (2.56)$$

then

$$|+\tfrac{1}{2}r\rangle' = |+\tfrac{1}{2}r\rangle - \vec{H}\cdot \frac{\langle +\frac{1}{2}t|\vec{\mu}|\frac{1}{2}r\rangle}{\Delta_t} |+\tfrac{1}{2}t\rangle . \qquad (2.57)$$

We take the crystallographic axis as the z-direction, and decompose $\vec{\mu}$ into μ_z and $\mu_\perp$. Consider the matrix element

$$\langle -\tfrac{1}{2}t|\vec{\mu}|-\tfrac{1}{2}r\rangle = \langle -\tfrac{1}{2}t|\mu_z|-\tfrac{1}{2}r\rangle\, \hat{e}_z + \langle -\tfrac{1}{2}t|\mu_\perp|-\tfrac{1}{2}r\rangle\, \hat{e}_\perp \;, \tag{2.58}$$

where $\hat{e}_z$ and $\hat{e}_\perp$ are unit vectors parallel and perpendicular to the z axis, respectively. By use of the following identities,

$$\langle -\tfrac{1}{2}t|\mu_z|-\tfrac{1}{2}r\rangle = -\langle \tfrac{1}{2}t|\mu_z|\tfrac{1}{2}r\rangle \tag{2.59}$$

and

$$\langle -\tfrac{1}{2}t|\mu_\perp|-\tfrac{1}{2}r\rangle = \langle \tfrac{1}{2}t|\mu_\perp|\tfrac{1}{2}r\rangle, \tag{2.60}$$

which follow from the properties of angular momentum operators,[18] the admixed wavefunctions (2.56) and (2.57) become

$$|-\tfrac{1}{2}r\rangle' = |-\tfrac{1}{2}r\rangle + \frac{H}{\Delta_t}[\langle \tfrac{1}{2}t|\mu_z|\tfrac{1}{2}r\rangle\cos\phi - \langle \tfrac{1}{2}t|\mu_\perp|\tfrac{1}{2}r\rangle\sin\phi]\,|-\tfrac{1}{2}t\rangle \tag{2.61}$$

$$|+\tfrac{1}{2}r\rangle' = |+\tfrac{1}{2}r\rangle - \frac{H}{\Delta_t}[\langle \tfrac{1}{2}t|\mu_z|\tfrac{1}{2}r\rangle\cos\phi + \langle \tfrac{1}{2}t|\mu_\perp|\tfrac{1}{2}r\rangle\sin\phi]\,|\tfrac{1}{2}t\rangle \tag{2.62}$$

where ϕ is the angle the external field makes with the z axis.

From the properties of angular momentum operators, $\langle \tfrac{1}{2}t|\mu_z|\tfrac{1}{2}r\rangle$ and $\langle \tfrac{1}{2}t|\mu_\perp|\tfrac{1}{2}r\rangle$ cannot both be different from zero. Consider first the case when $\langle \tfrac{1}{2}t|\mu_z|\tfrac{1}{2}r\rangle \neq 0$. Then (2.62) and (2.63) reduce to

$$|-\tfrac{1}{2}r\rangle' = |-\tfrac{1}{2}r\rangle + \frac{H\cos\phi}{\Delta_t}\langle \tfrac{1}{2}t|\mu_z|\tfrac{1}{2}r\rangle\;|-\tfrac{1}{2}t\rangle \tag{2.63}$$

$$|+\tfrac{1}{2}r\rangle' = |+\tfrac{1}{2}r\rangle - \frac{H\cos\phi}{\Delta_t}\langle \tfrac{1}{2}t|\mu_\perp|\tfrac{1}{2}r\rangle\;|\tfrac{1}{2}t\rangle \;. \tag{2.64}$$

The matrix element of the appropriate part of the linear strain term of the orbit-lattice interaction (2.16) between the new states equals, to first order in H,

$$<-\tfrac{1}{2}r|V_1|\tfrac{1}{2}r>' = \frac{H\cos\phi}{\Delta_t}<\tfrac{1}{2}t|\mu_z|\tfrac{1}{2}r>\{<-\tfrac{1}{2}t|V_1|\tfrac{1}{2}r>-<-\tfrac{1}{2}r|V_1|\tfrac{1}{2}t>\}. \quad (2.65)$$

Since the terms in the curly brackets must each be invariant under time reversal, we have

$$<-\tfrac{1}{2}r|V_1|\tfrac{1}{2}t> = (-1)^{\frac{1}{2}r+\frac{1}{2}t}<\tfrac{1}{2}r|V_1^*|-\tfrac{1}{2}t> = (-1)^{\frac{1}{2}t+\frac{1}{2}r}<-\tfrac{1}{2}t|V_1|\tfrac{1}{2}r>. \quad (2.66)$$

But for Kramers systems r is odd and $\frac{1}{2}t = \frac{1}{2}r$ under the assumption $<\frac{1}{2}t|\mu_z|\frac{1}{2}r> \neq 0$. Hence

$$<-\tfrac{1}{2}r|V_1|\tfrac{1}{2}r>' = \frac{2H\cos\phi}{\Delta_t}<\tfrac{1}{2}t|\mu_z|\tfrac{1}{2}r><-\tfrac{1}{2}r|V_1|\tfrac{1}{2}t>. \quad (2.67)$$

The other possibility, $<\frac{1}{2}t|\mu_\perp|\frac{1}{2}r> \neq 0$, by exactly the same sort of reasoning, leads to

$$<-\tfrac{1}{2}r|V_1|\tfrac{1}{2}r>' = \frac{-2H\sin\phi}{\Delta_t}<\tfrac{1}{2}t|\mu_\perp|\tfrac{1}{2}r><-\tfrac{1}{2}r|V_1|\tfrac{1}{2}t>. \quad (2.68)$$

We note that in practice there exist excited Kramers doublets which have only matrix elements of μ_z with the ground doublet $|\pm\frac{1}{2}r>$, and other excited Kramers doublets which have only matrix elements of $\mu_\perp$ with the ground doublet. These matrix elements may be considerably different in magnitude, and, in addition, the splitting Δ of the two doublets may be different. Therefore, from (2.47), (2.67) and (2.68), we see that the direct process relaxation time may be strongly dependent on the orientation of the external magnetic field $\vec{H}$.

Such anisotropy is not confined to the direct process, for the angle dependence arose from the admixture of excited Kramers doublets into the ground state by the magnetic field. Hence this anisotropy is to be expected for any of the processes in which the admixture has been invoked. In particular, we mention the T^7 Raman process for Kramers systems, and the local-mode process, in addition to the direct process.

A second important feature of the anisotropy discussed above is that the <u>form</u> of the angle dependence is determined by matrix elements of the admixture interaction $\vec{\mu}\cdot\vec{H}$, and is independent of the actual type of relaxation process under consideration. For example, if a Kramers system displays both a direct process and a local-mode process, then the ratio $\tau_{1_\parallel}/\tau_{1_\perp}$ is expected to be the same for both processes, where $\tau_{1_\parallel}$ and $\tau_{1_\perp}$ are the relaxation times when $\vec{H} \parallel Z$ and $\vec{H} \perp Z$, respectively.

The processes described by (2.49), (2.50), (2.51), and (2.52) contain matrix elements of the form

$$|\langle a|V_1|c\rangle\langle c|V_1'|b\rangle|^2(\Delta_{cd})^{-4} \quad . \tag{2.69}$$

Such terms will be anisotropic only if the splitting Δ between the ground doublet and excited doublet is itself a function of magnetic field orientation.

III. EXPERIMENTAL APPARATUS AND TECHNIQUES

General Description

Most of the data to be reported herein were obtained with the spin echo apparatus and right circular cylinder microwave cavity configuration described by Vieth.[34] Figure 6 depicts schematically the cylindrical microwave cavity and associated apparatus for maintaining and measuring temperature. The bifilar manganin heater coil was used to regulate temperatures between 4.2°K and 80°K (with liquid helium below the cavity), or above 78°K (with liquid nitrogen below the cavity). The samples were mounted at the center of the cavity in a styrofoam block. A thermocouple made from gold 0.02% iron and chromel passed through the center of the bottom of the cavity and was secured with Apiezon N grease inside a small hole drilled through the sample. The other end of each thermocouple wire was spot-welded to #36 copper wire, both junctions being far enough below the cavity to be in contact with the cryogenic liquid throughout a set of measurements. The thermocouple emf was monitored with a Leeds-Northrop K-3 potentiometer. The temperature was obtained from a calibration,[5] against a platinum resistance thermometer, of sample thermocouples from each end of the spool of gold .02% iron wire. As a

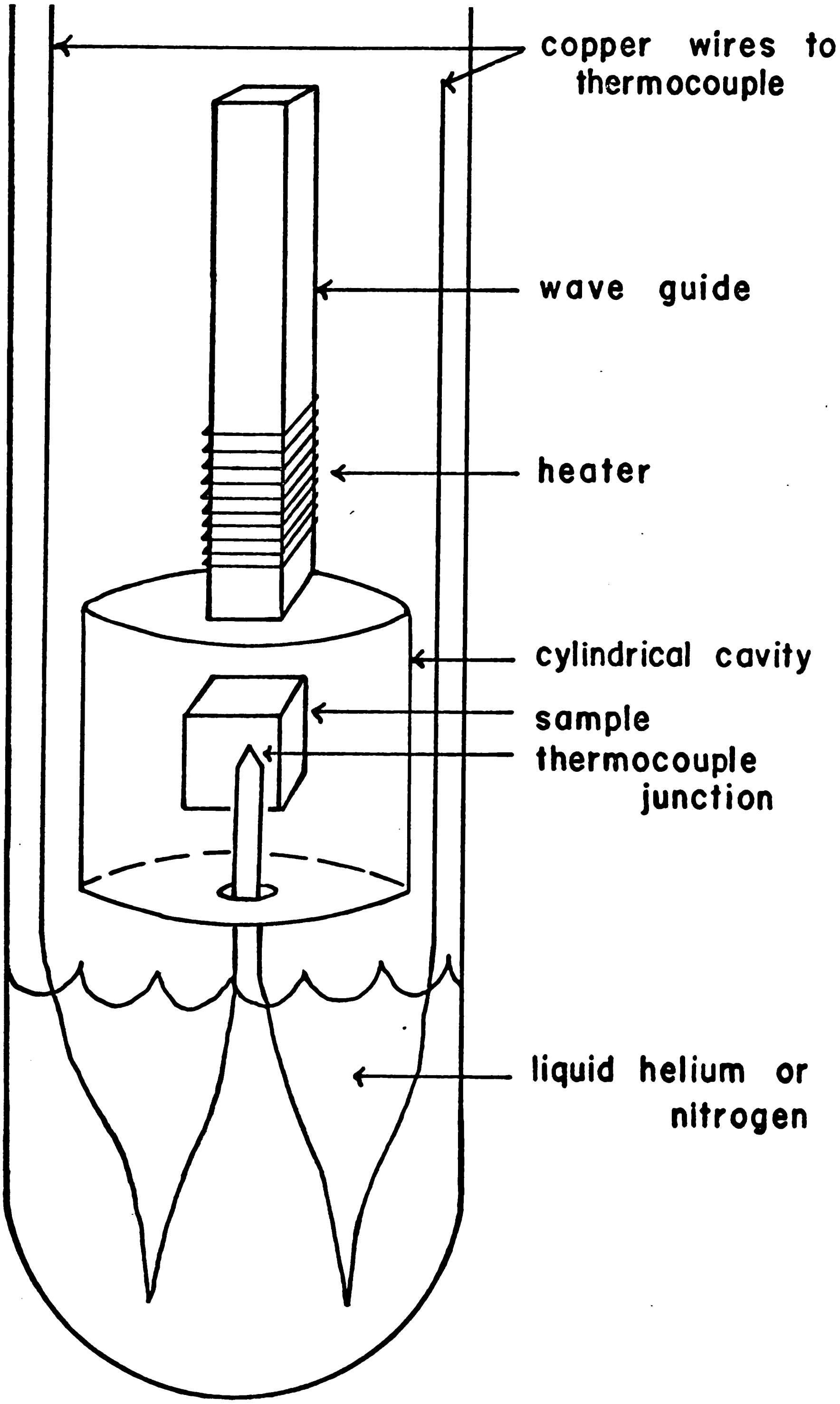

Figure 6. Cylindrical Cavity

further check, we calibrated our particular thermocouple _in situ_ by replacing the sample with a Honeywell germanium resistance thermometer. For T > 10°K the two calibrations are in good agreement, and for T < 10°K the platinum resistance thermometer has very poor temperature resolution compared to the germanium resistor, so we used the calibration based on the latter. Some of the early measurements above 78°K were made with a copper-constantan thermocouple, and results obtained were in good agreement with the subsequent data. Temperatures below 4.2°K were obtained by raising the liquid helium level above the cavity (for better thermal contact between helium and sample), and pumping on the helium with a Kinney vacuum pump at rates up to 230 cu.ft./min. Temperatures down to 1.1°K (as determined by the helium vapor pressure) were obtained in this manner.

Spin Echo Techniques

For temperatures above 20°K we used the conventional $(\pi/2,\pi/2,\pi)$ pulse sequence described by Vieth[34] for production of electron spin echoes.[9,6] At lower temperatures, where τ_1 > 100 msec, we found that cross relaxation effects dominated τ_1 effects to such an extent that this pulse sequence was not usable. Instead, we employed a variation of the "picket" technique[23] in which the initial $\pi/2$ pulse is replaced by a string of pulses. The basic idea of the

picket technique is that the total time during which power is applied to the system is long, so that even if some energy from one pulse is lost by cross relaxation the resonance transition will be pumped many times. The result is that the cross-relaxation transitions are well saturated, so that no more energy is lost by such mechanisms, and the system returns to equilibrium in a time characteristic of the spin-lattice interaction rather than cross relaxation interactions.

Vacuum Can Cryostat

As will be discussed more thoroughly later, some of our low temperature data seemed to imply that the thermocouple junction at the sample in Figure 6 was being cooled by conduction to the helium bath, so that the temperature of the sample was greater than that of the thermocouple junction. A vacuum can cryostat (Figure 7) was constructed to test these ideas. In this apparatus the temperature sensor, a germanium resistance thermometer, was embedded into the wall of a brass TE_{101} rectangular microwave cavity around which a six turn bifilar manganin heater coil was wound. The sample was attached to the inner wall of the cavity with Apiezon N grease and the remainder of the cavity was filled with styrofoam to hold the sample in place.

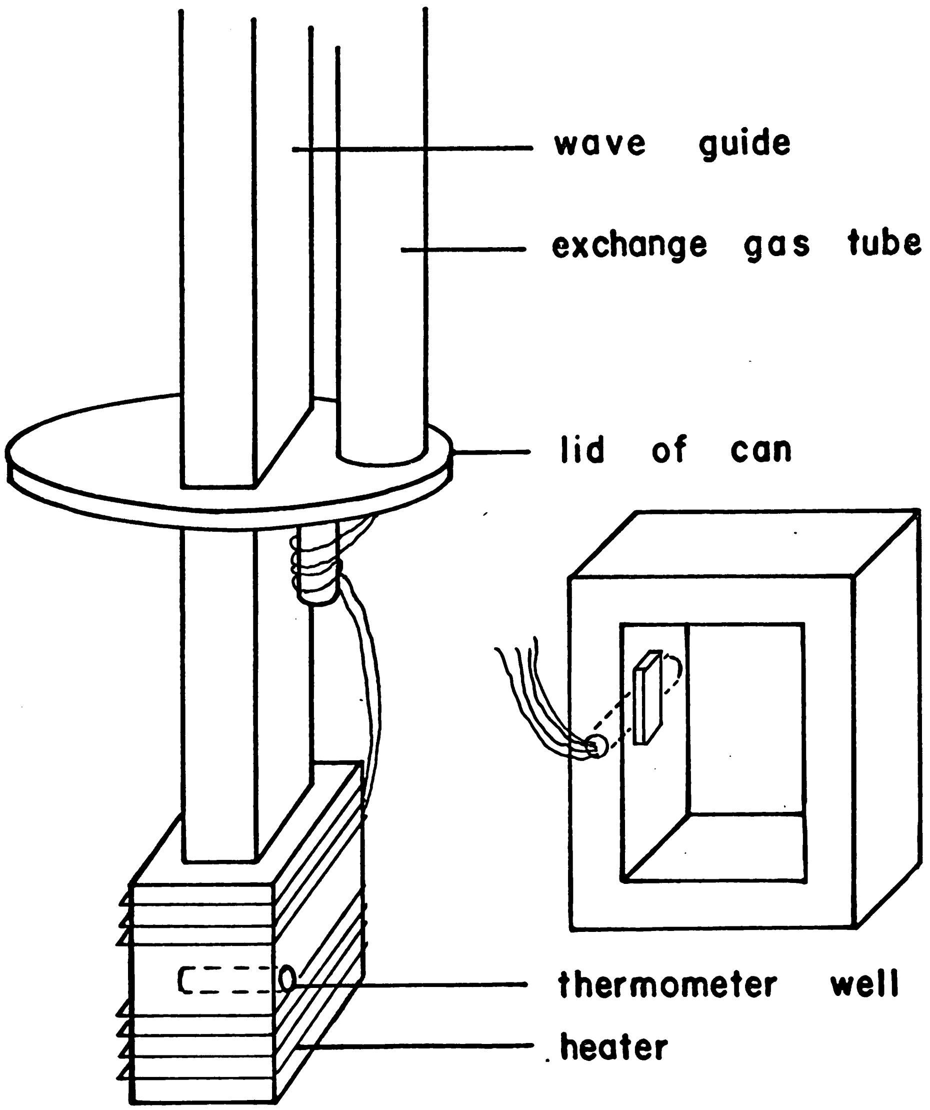

Figure 7. Vacuum can cryostat (left), showing the heater leads wrapped around a brass rod in thermal contact with lid of can. The brass can, normally soft soldered to the lid has been removed. At right is a cutaway view of the rectangular cavity, showing placement of sample with respect to the germanium resistance thermometer.

Operation of the apparatus is as follows:

1) Evacuate the can to a pressure of about 10^{-5} mm Hg.
2) Precool to liquid nitrogen temperature.
3) Introduce helium exchange gas into the can at a pressure of about 2.5 mm Hg.
4) Transfer liquid helium into the dewar.
5) When the germanium resistance thermometer indicates the cavity has cooled to 4.2°K, remove the exchange gas. We were able to pump the exchange gas pressure down below 10μ without observing any temperature change, and therefore we conclude that any heat leak into the cryostat is minimal.

By applying current to the heater we were able to control the temperature very well between 4.2 and 15°K.

Crystal Growing

Alkali halide crystals are normally grown from the melt, but the substitutional $Cr(CN)_5NO^{3-}$ complex used in our experiments was not stable at temperatures above 120°C, so all samples were grown by evaporation of aqueous solutions. Most alkali halides are difficult to grow from water solution. We were able to grow only KBr and KCl crystals large enough for our experiments, since we needed samples approximately 6 mm on a side.

Most crystals used in the measurements were grown at

atmospheric pressure and a temperature of 10±2°C. A few were grown at 21±2°C. Various concentrations of the paramagnetic impurity were used, in order to obtain sufficient signal strength at high temperatures and to reduce cross relaxation at low temperatures. Solutions containing 0.001, 0.01, 0.1, and 1.0 mole percent of $K_3[Cr(CN)_5NO]$ in KBr and KCl were used.

Chemical analysis showed that crystals grown from the 0.001 mole percent KBr solution were about 20 times as concentrated as the solution itself. Because the substitutional complex was yellow, it was possible to get a qualitative idea of the concentration from the shade of yellow of a particular crystal, and nearly every KBr crystal appeared more concentrated than the solution from which it was grown. The coloring of any particular KBr crystal appeared homogeneous, indicating there were no appreciable concentration gradients of the $Cr(CN)_5NO^{3-}$ complex in KBr.

Almost every KCl crystal, on the other hand, had a yellowish spot at the center, and many crystals had visible concentration gradients. We were unable to obtain a satisfactory KCl crystal of intermediate concentration, so our KCl measurements were confined to the highest (>25°K) and lowest (<4.2°K) temperatures.

Optically, the samples were fairly transparent and neither the KBr nor KCl showed visible signs of trapped water.

IV. SUMMARY AND IMPLICATION OF PREVIOUS RESULTS

ESR Spectrum

Single crystals of KBr and KCl with substitutional $K_3[Cr(CN)_5NO]$ were grown from aqueous solution. The complex $Cr(CN)_5NO^{3-}$ goes into the alkali halide lattices as a unit, with the Cr^+ replacing a K^+ and each of the CN^- and NO^+ groups replacing the appropriate halide ion, so that the Cr^+ is octahedrally coordianted (Figure 1), but resides in a crystal field of tetragonal symmetry. That the complex retains its identity in KBr and KCl has been established by ESR and IR measurements.[17]

The ESR spectrum of $CR(CN)_5NO^{3-}$ in KBr and KCl has axial symmetry, with the $g_\parallel$ and $g_\perp$ lines split into triplets by transferred hyperfine interaction with the N^{14} of the NO^+. The symmetry axis is the ON-Cr-CN axis of the complex. The g factor is nearly isotropic with $g_\parallel = 1.9722$ and $g_\perp = 2.0045$ in KBr, and $g_\parallel = 1.9722$ and $g_\perp = 2.0044$ in KCl. N^{14} hyperfine splitting constants (in gauss) are $A_\parallel = 2.89$ and $A_\perp = 7.10$ in KBr, and $A_\parallel = 2.41$ and $A_\perp = 7.10$ in KCl.

During measurement of the ESR spectra, Kuska and Rogers observed that more microwave power was needed to saturate the $g_\perp$ transitions than to saturate the $g_\parallel$ transitions,

suggesting that the relaxation times of the two might be different.

Infrared and Optical Spectra

The Debye temperatures of KBr and KCl shall be taken as 170°K and 230°K, respectively.[1] These values indicate that we should not expect any relaxation process which requires lattice phonons having energies which correspond to temperatures much higher than 300°K.

On the basis of optical and infrared spectra, Manoharan[19] has shown that the splitting Δ_t between the ground state Kramers doublet and the first excited doublet of $Cr(CN)_5NO^{3-}$ is approximately 12,600 cm^{-1}. Now 1 cm^{-1} $\simeq$ 1.44°K, so this corresponds to a temperature of 18,200°K. Therefore, we discard the Orbach process (2.33) and the T^5 Raman process (2.31) of Orbach and Blume, since these processes require that an excited doublet lie close to the ground state.

Far-infrared spectra of $Cr(CN)^5NO^{3-}$ in KBr and KCl yield the results summarized in Table I, where each band is labeled according to its absorption mechanism (e.g., Cr-CN stretch represents the vibration along the Cr-CN band). The presence of strong Cr-CN stretch bands near 400 cm^{-1} makes this complex an ideal candidate for a local mode relaxation process, for the frequency is low enough to

satisfy $\omega_0 = \omega_1 + \omega_2$, and distortion of the Cr-CN bond should be very effective in modulating the crystal field at the Cr^+ site. The IR frequencies of $Cr(CN)_5NO^{3-}$ in KBr and KCl lattices are not markedly different from the corresponding values measured for $K_3Cr(CN)_5NO$ in a Nujol mull (Table I). In addition to the ESR spectrum, this is further evidence that the $Cr(CN)_5NO^{3-}$ complex remains intact in the lattices.

Table I. Effect of lattice on IR frequencies of $Cr(CN)_5NO^{3-}$

	Stretching Frequencies (in cm^{-1})			
Host	N-O	C-N	Cr-NO	Cr-CN
Mull[8]	1630 vs	2120 s 2073 vw	616 m	428 s 397 s 346 s 305 w 291 w
KBr[17]	1656 s 1634 s	2101 s 2123 w		434 401 350
KCl[17]	1707 s 1685 s	2103 s 2112 m		428 397 351 347

Abbreviations: s, strong; m, medium; w, weak; v, very.

V. RESULTS AND CONCLUSIONS

General Considerations

Before a discussion of individual results for the electron spin-lattice relaxation of $Cr(CN)_5NO^{3-}$ in KBr and KCl, some general features common to both cases will be presented. From the fact that our crystals exhibited ESR spectra similar to the published results, we conclude that the complex retained its identity in the lattices. All our relaxation measurements were made with the spin echo spectrometer operating at a microwave frequency of approximately 9.4 GHz. Analysis of the data followed the same procedure as described by Vieth[35] except that instead of measuring the spin echo amplitudes from photographs of oscilloscope traces, we visually determined the amplitudes directly from the oscilloscope by the use of a calibrated grid over the face of the cathode ray tube.

At T = 78°K all three lines of the $g_{\parallel}$ hyperfine triplet had the same relaxation time which was twice that of the τ_1 common to the three $g_{\perp}$ lines. At 4.2°K, any variation of τ_1 among the lines of a particular triplet was attributed to τ_{12} effects, i.e., diffusion of energy from one component of the triplet into the other components. The center line of each triplet was used for determining the temperature

dependence of the relaxation time. Hence, for brevity, we shall refer to "the $g_{\parallel}$ line" or "the $g_{\perp}$ line", meaning the central component of the appropriate triplet.

For $T < 5°K$ and for $T > 60°K$, τ_1 for the $g_{\parallel}$ line is about twice that for the $g_{\perp}$ line. At any particular intermediate temperature both lines have the same relaxation time. The estimated error in the measured values is 10%.

Relaxation Results -- KBr

The results of our measurements of τ_1 as a function of T for the $g_{\parallel}$ and $g_{\perp}$ lines of $Cr(CN)_5NO^{3-}$ in KBr are shown in Figure 8, the data being tabulated in Appendix I. The first striking feature is that τ_1 depends on the orientation of the external magnetic field. That is, the $g_{\perp}$ line relaxes faster than the $g_{\parallel}$ line, except at intermediate temperatures.

As was shown in Chapter II, a variety of functional forms for the temperature dependence of τ_1 may be expected. The curves in Figure 8 represent the best fits (in the least squares sense) of the function

$$\frac{1}{\tau_1} = AT + BT^9 J_8\left(\frac{170}{T}\right) + Ce^{-575/T} \qquad (5.1)$$

to the data for the $g_{\parallel}$ line and the $g_{\perp}$ line, where $J_8(x)$ is as defined in (2.23). The resultant A, B, and C values appear in Table II. These fits were obtained with the

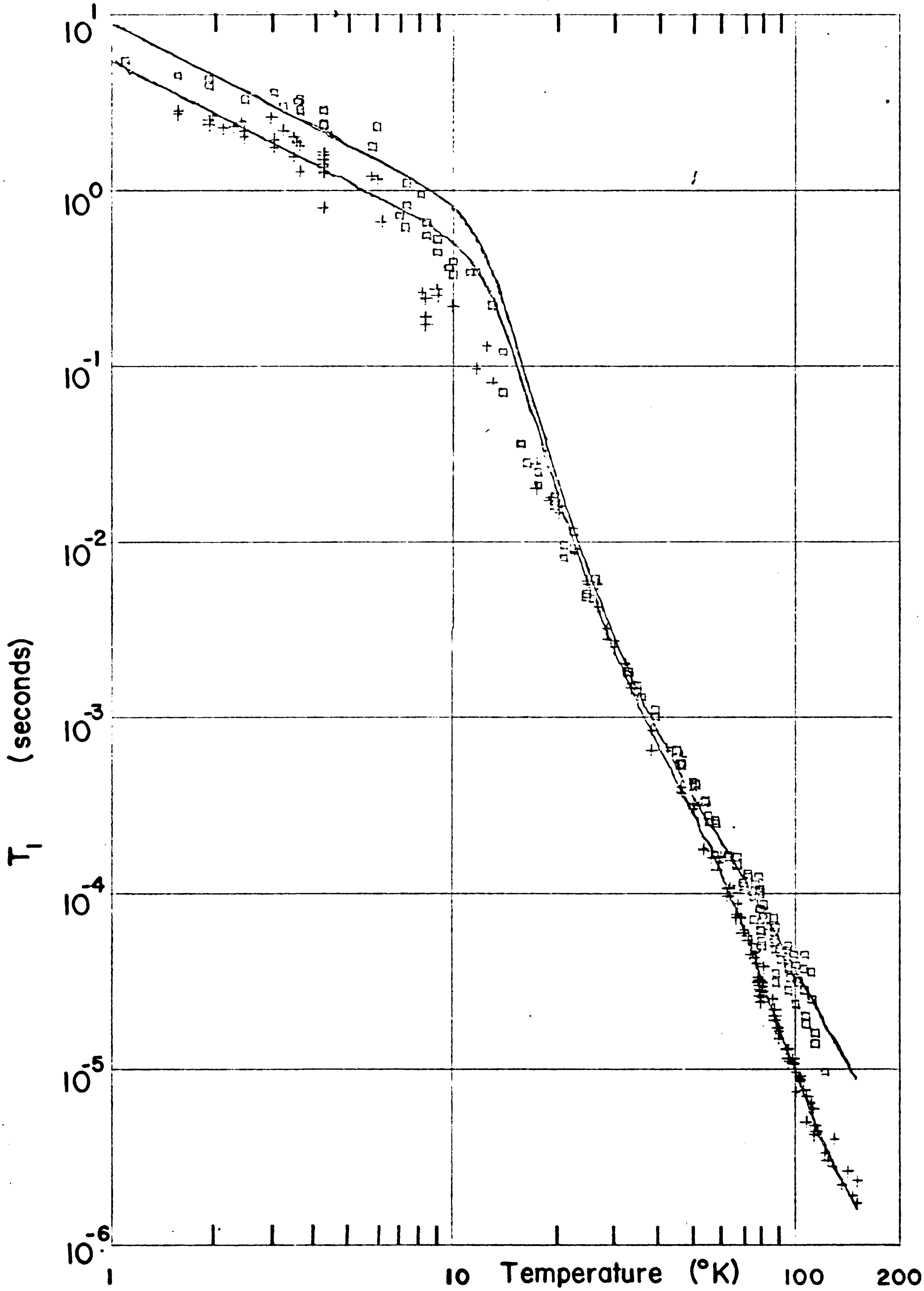

Figure 8. Data for $g_{\parallel}$ (□) and $g_{\perp}$ (+) lines in KBr, with fits to $\frac{1}{\tau_1} = AT + BT^9 J_8(170/T) + C\exp(-575/T)$

Table II. Least squares fit of $\frac{1}{\tau} = AT + BT^9J_8(170/T) + C\exp(-575/T)$ to relaxation of $Cr(CN)_5NO^{3-}$ in KBr

Line	A	B	C
$g_{\parallel}$	0.112±0.006	$(3.67\pm0.16) \times 10^{-15}$	$(3.32\pm0.56) \times 10^{6}$
$g_{\perp}$	0.182±0.007	$(4.23\pm0.16) \times 10^{-15}$	$(2.66\pm0.11) \times 10^{7}$

MSU Control Data 3600 computer, using the 3600 Fortran program TOWPLOT, listed in Appendix III.

Discussion -- KBr

We shall now attempt to justify the particular functional form (5.1) chosen for temperature dependence of τ_1. As was pointed out in Chapter IV, the Orbach process (2.33) and the Orbach and Blume process (2.31) can be discarded on the basis of the energy level assignments of Manoharan.[19]

The direct process (2.20) is dominant at low temperatures (Figure 8). It has been shown in Chapter II that the current theory allows for anisotropy of the direct process relaxation rate, and Figure 8 indicates that in the temperature range $1 < T < 5°K$, the τ_1 values for the $g_{\parallel}$ and $g_{\perp}$ lines differ by a factor of two.

The theory predicts that the Raman relaxation rate should have the form

$$\frac{1}{\tau} \propto T^2, \text{ for } T > \theta/2. \qquad (5.2)$$

But for $T > 90°K$, τ_1 is a much more rapidly varying function of temperature than given by (5.2). The only allowed process which satisfies this criterion is the local mode process. In Figures 9 and 10 we have replotted the data for the $g_{\perp}$ and $g_{\parallel}$ lines, respectively. In addition, each figure has a least squares computer fit to the direct and

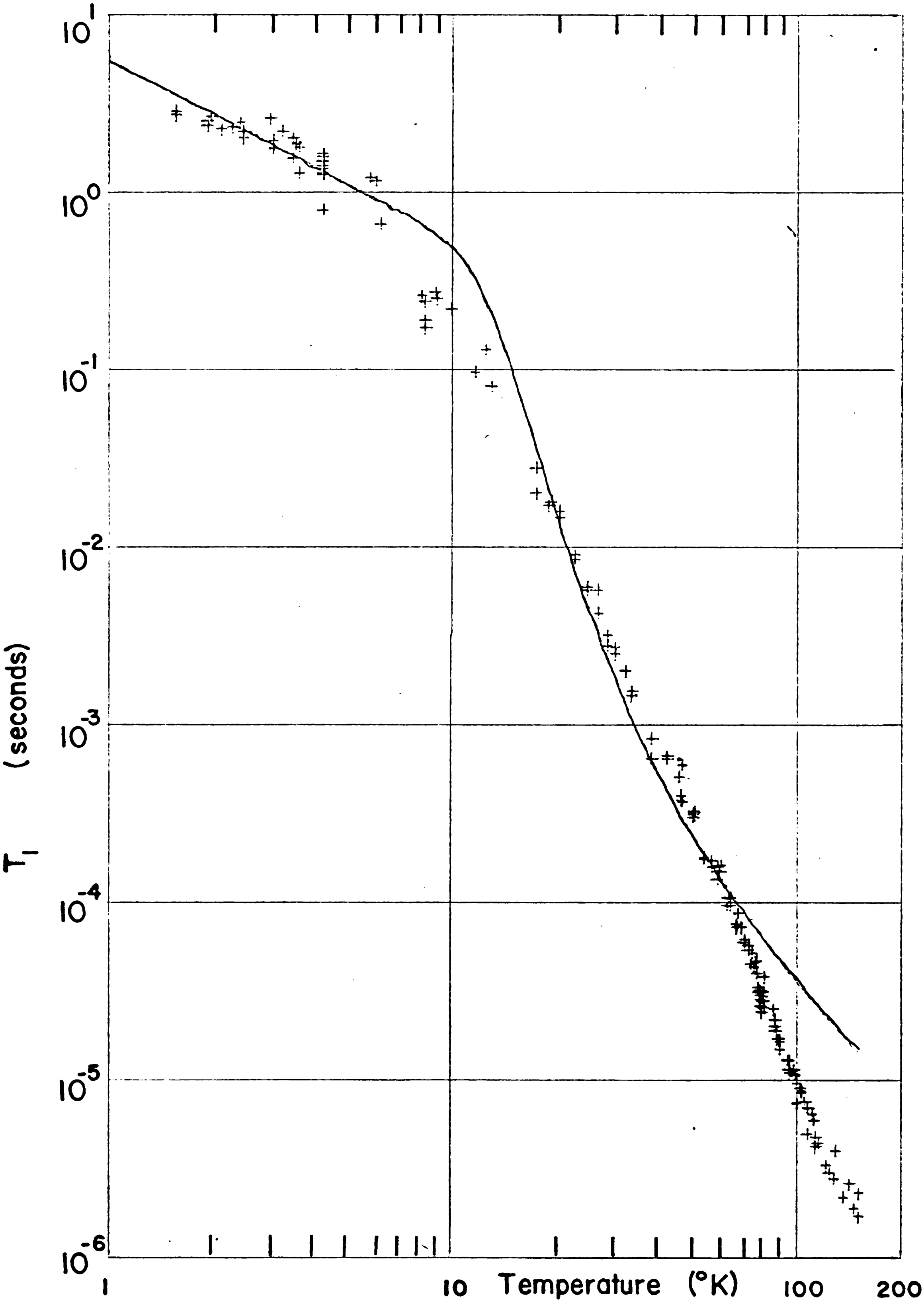

Figure 9. Data for $g_\perp$ line in KBr, with fit to
$\frac{1}{\tau_1} = AT + BT^9 J_8(170/T)$

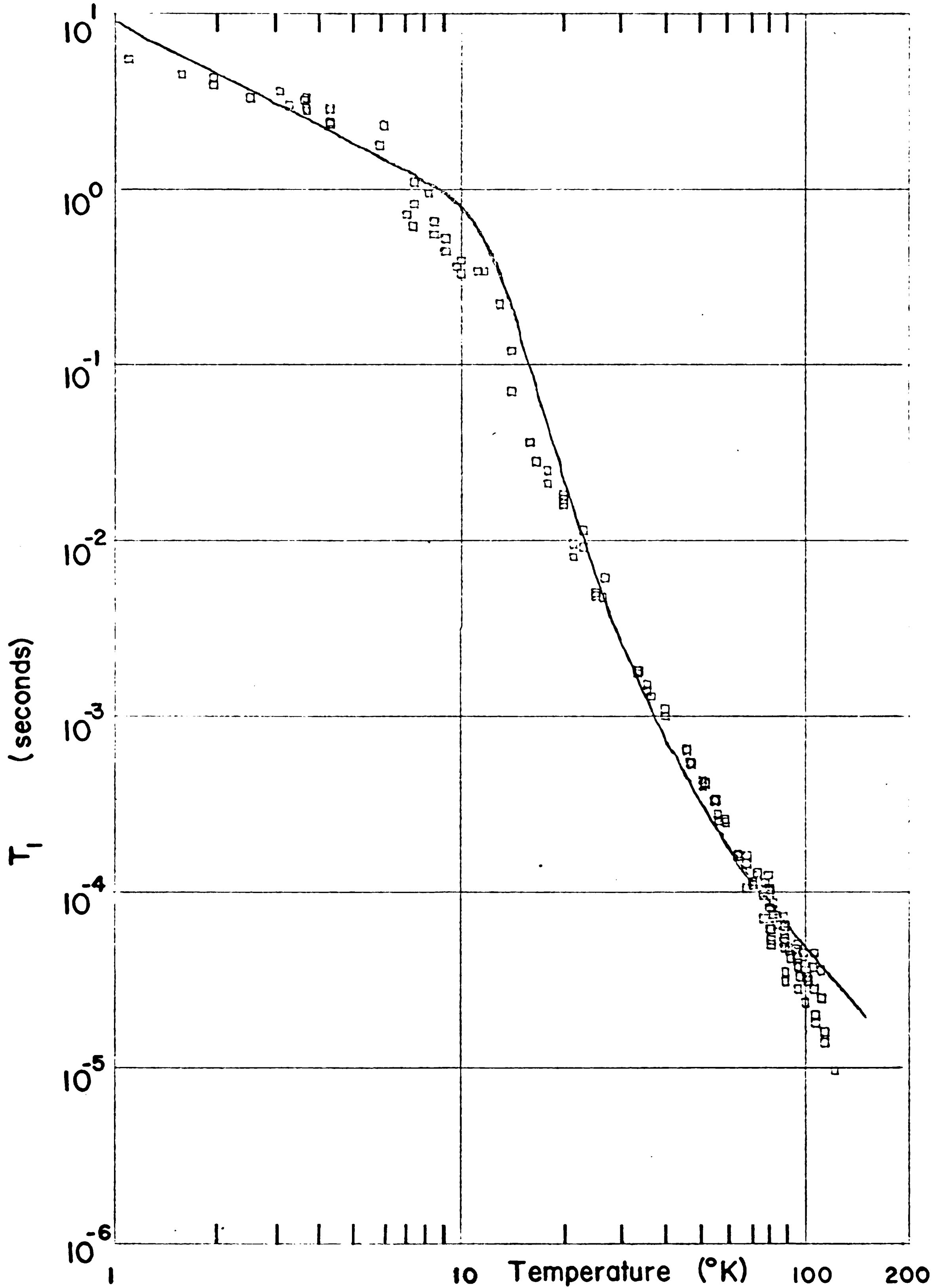

Figure 10. Data for $g_{\parallel}$ line in KBr, with fit to
$\frac{1}{\tau_1} = AT + BT^9 J_8(170/T)$

T^9J_8 Raman processes. That is, the fits have the same form as those used in Figure 8 except that the exponential term (i.e., the local mode process) is deleted. For both the $g_\parallel$ and $g_\perp$ lines the fit is clearly better when the local mode process is included. Anisotropy is observed in the local mode process, as in the direct process. At the very highest temperatures for which we have data on both lines, the ratio of τ_1 values for the $g_\parallel$ and $g_\perp$ lines is slightly greater than the factor of two observed in the direct process, but the qualitative features of the theory discussed in Chapter II are borne out very well.

The empirical value of θ_0 in (5.1) was obtained by fitting

$$\frac{1}{\tau_1} = \alpha T + \beta T^9 J_8\left(\frac{170}{T}\right) + \gamma e^{-\theta_0/T} \qquad (5.3)$$

for various θ_0 values, and observing which value gave the minimum standard error of fit, i.e., the value of θ_0 for which

$$\sum_{i=1}^{N}\left(\frac{1}{\tau_1}_{\mathrm{obs}_i} - \frac{1}{\tau_1}_{\mathrm{calc}_i}\right)^2 w_i \qquad (5.4)$$

was minimum, where w_i is a weighting factor determined as in Appendix IV, and N is the number of data points. For the $g_\perp$ line, $\theta_0 = 550 \pm 25°K$ gave the best fit and for the $g_\parallel$ line the best value of θ_0 was 600±50°K. Neither of these values is exactly equal to one of the reported

infrared frequencies (Table II), but in fact the three IR lines overlap and form a broad band.[20] Therefore, for convenience in comparing the A, B and C values for the $g_\parallel$ and $g_\perp$ lines, we feel justified in using $\Theta_0 = 575°K$ in (5.1).

Now the question of how to account for the data at intermediate temperatures ($10 < T < 50°K$) arises. We discard the driven-mode process temporarily, since there is no spectroscopic evidence for resonant modes of the $Cr(CN)_5NO^{3-}$ which lie within the Debye spectrum of KBr. This point will be discussed more fully later. Neglecting the driven-mode process, we are left with two possible Raman processes, (2.24) and (2.30), which have temperature dependences T^7J_6 and T^9J_8 respectively. We choose the latter for a number of reasons. In the first place, τ_1 is isotropic for $10 < T < 50°K$, whereas the theoretical discussion shows that the T^7J_6 process should exhibit the same form of anisotropy as the direct process. Also, if the local mode process (2.46) is written in the form

$$\frac{1}{\tau_L} \simeq \omega_0 \left(\frac{\hbar\omega_0}{Mv^2}\right)^3 (E_s)^{-2}\Omega^2 \, e^{-\Theta_0/T} \quad , \qquad (5.5)$$

where

$$\Omega \equiv \left| \frac{\langle d|\vec{\mu}\cdot\vec{H}|b\rangle\langle a|V_2|d\rangle}{\Delta_{cd}} \right| , \qquad (5.6)$$

then the Raman process (2.24) becomes

$$\frac{1}{\tau_R} = \frac{9}{\pi^3\rho^2v^{10}}\left(\frac{kT}{\hbar}\right)^7 J_6\left(\frac{\theta}{T}\right)\Omega^2 . \qquad (5.7)$$

From the computer fit (Table II) we have for the $g_\perp$ line,

$$\frac{1}{\tau_L} \simeq 2.66 \times 10^7 \, e^{-\theta_0/T} \quad . \tag{5.8}$$

Comparing (5.5) and (5.8) leads to

$$\Omega^2 \simeq 2.21 \times 10^{-33} \, , \tag{5.9}$$

where we have used $v = 3.56 \times 10^5$cm/sec,[10] $\rho = 2.75$gm/cm^3, $M = \frac{1}{2}(M_{Br} + M_K) \simeq 10^{-22}$gm, and $\omega_0 = 400$cm^{-1}. Substituting (5.9) into (5.7), we obtain

$$\frac{1}{\tau_R} \simeq 2.50 \times 10^{-90} \left(\frac{kT}{\hbar}\right)^7 J_6\left(\frac{\theta}{T}\right) \quad . \tag{5.10}$$

Throughout the temperature range $10 < T < 50°$K, the relaxation rates predicted by (5.10) are 100 to 1000 times greater than the observed values. Hence we conclude again that the $T^7 J_6$ Raman process is not operative in the system under study, for if it were present the relaxation rates should be much greater than they are observed to be at intermediate temperatures.

As pointed out in Chapter II, the $T^9 J_8$ Raman process is not expected to exhibit any anisotropy unless the splittings Δ between the ground doublet and excited doublets are dependent on the orientation of $\vec{H}$. Since the splittings Δ are thousands of cm^{-1} for all levels, the effect of $\vec{H}$ upon them is expected to be negligible. This is verified by the observed isotropy of τ_1 for $10 < T < 50°$K.

In the temperature range $7 < T < 20°K$, the theoretical relaxation rate (5.1) does not fit the data nearly so well as at other temperatures. When this anomaly was first observed it was tentatively explained in terms of poor thermal contact between the sample and thermocouple, the idea being that the thermocouple junction (at the sample) was cooled by conduction along the thermocouple wires running to the helium bath (Figure 6). If this were the case, then the sample temperature would be greater than that indicated by the thermocouple. This, indeed, is consistent with the data obtained (Figure 8).

Such an effect might also be due to thermal gradients in the crystal. The slow relaxation rates of the $Cr(CN)_5NO^{3-}$ at low temperatures require crystals having low concentrations of the paramagnetic impurity in order to reduce τ_{12} effects. Hence crystals of relatively large volume are necessary in order to obtain sufficient signal amplitude at the lower temperatures. The right circular cylinder cavity required a crystal which was ≈6 mm on a side. Such a large crystal was deemed likely to contain thermal gradients. In particular, the surface of the crystal would be hotter than the interior since heat was applied to the cavity by the manganin heater above the cavity (Figure 6).

The vacuum can cryostat (Figure 7), was constructed to test these ideas. The thermal path from heater to sample

for this configuration is compared in Figure 11 with that for the thermocouple and cylindrical cavity. The sample is suspended at the center of the cylindrical cavity by a block of styrofoam, whereas in the rectangular one the sample and thermometer are heat sunk to the relatively massive brass cavity. The most important point is that from the geometry we can conclude that the sample temperature is never likely to be greater than the thermometer temperature whenever power is being applied to the heater on the rectangular cavity. Hence the only type of anomaly we can envision from such apparatus is a shift opposite to that for the cylindrical cavity, i.e., the measured temperature for a given τ_1 might appear higher than the actual temperature, but is not likely to appear lower. But the results obtained from the two different configurations agree, within experimental error. This leads to the conclusion that the anomalous T dependence of τ_1 for $7 < T < 20$°K is a property of the sample and not merely a thermal effect in either piece of apparatus, since the considerations outlined above indicate that the results should be very different in the two cases if the effect were only a thermal one.

At present we do not feel that a satisfactory explanation of the temperature dependence of τ_1 in the range $7 < T < 20$°K can be given. The only speculation we can offer is that the $Cr(CN)_5NO^{3-}$ complex may have some very

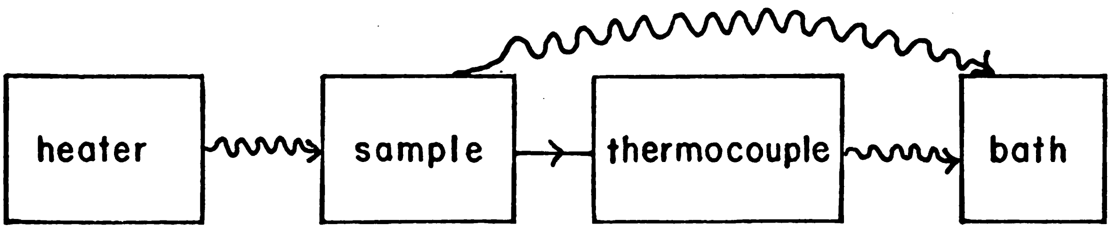

(a) Thermal path for cylindrical cavity

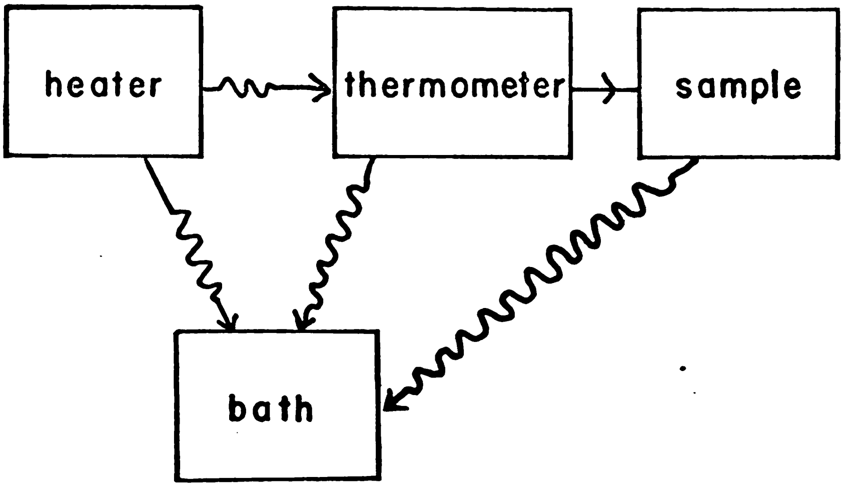

(b) Thermal path for rectangular cavity

Figure 11. Comparison of the thermal paths for the two types of apparatus used. The wavy lines represent weak thermal contact, the length being inversely proportional to the estimated conductance. The straight lines represent paths of good thermal contact.

low frequency bending modes. If so, then we might have the driven-mode process (2.35). Explicit test of this requires knowledge of ω_i, the frequency of the appropriate mode of the complex. Addition of a driven-mode process did not improve the computer fit unless $\hbar\omega_i$ was less than 20 cm^{-1}. For $Cr(CN)_5NO^{3-}$ in alkali halides, infrared measurements[17] have been made down to energies only as low as 250 cm^{-1}. However, Gans[8] et al report a series of IR spectra of $K_3Cr(CN)_5NO$ and $[(CH_3)_4N_3]$ $[Cr(CN)_5NO]$ down to 80 cm^{-1}. The lowest energy absorption bands they observed were 126 cm^{-1} in the latter. When compared with the Debye energies of 118 cm^{-1} and 160 cm^{-1} for KBr and KCl, respectively, these bending mode energies are too high for the driven-mode process to fit the data significantly better than does equation (5.1). Therefore, until more IR data are available, the applicability of the driven-mode process to the case at hand must remain an open question.

Results and Discussion -- KCl

The qualitative results for the relaxation of $Cr(CN)_5NO^{3-}$ in KCl are similar to those in KBr. Data for the $g_{\parallel}$ and $g_{\perp}$ lines are tabulated in Appendix II and are plotted in Figure 12 along with least squares fits of

$$\frac{1}{\tau_1} = AT + BT^9J_8\left(\frac{230}{T}\right) + Ce^{-610/T} \qquad (5.11)$$

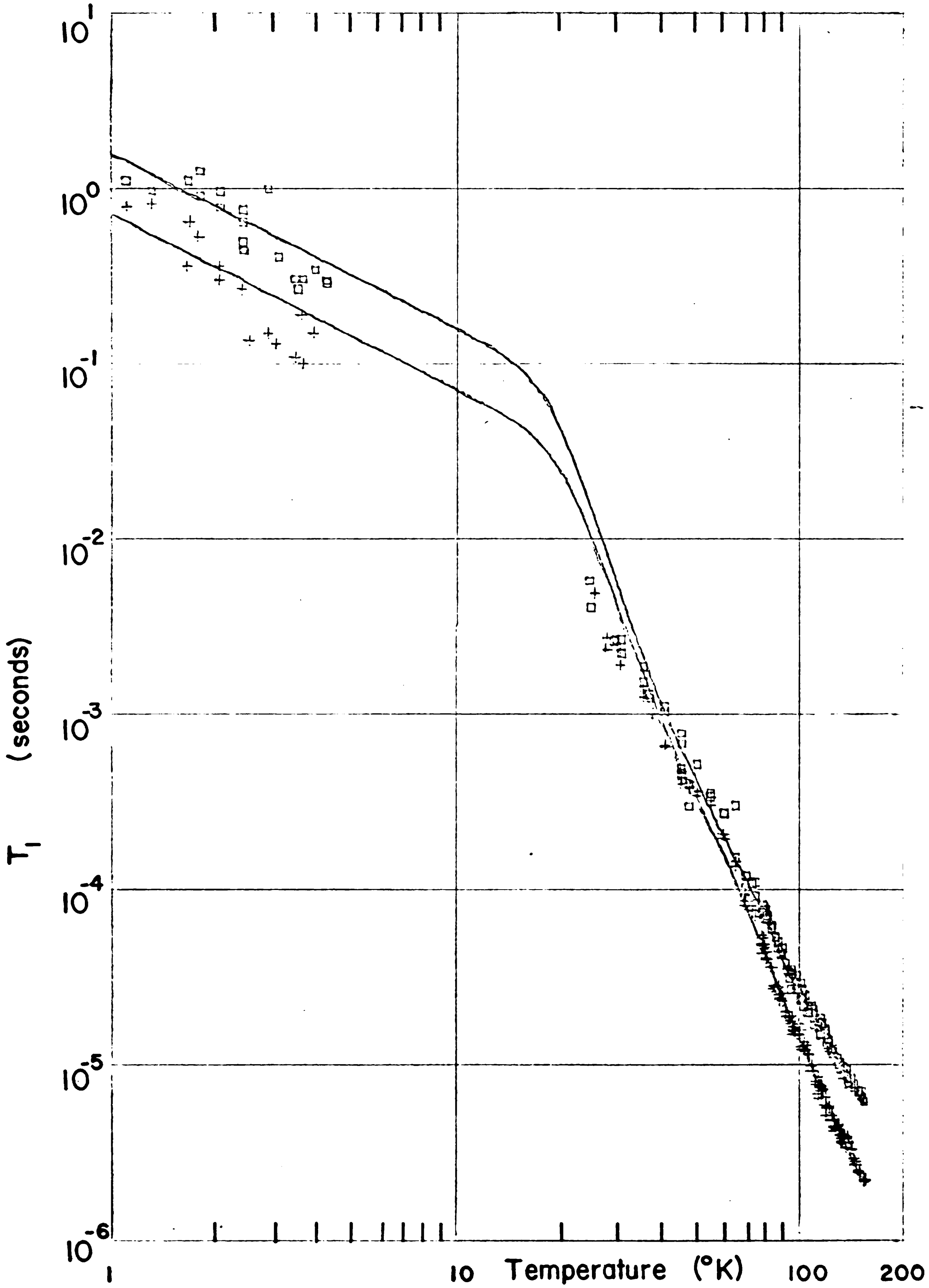

Figure 12. Data for $g_{\parallel}$ (□) and $g_{\perp}$ (+) lines in KCl, with fits to $\frac{1}{\tau_1} = AT + BT^9 J_8(230/T) + C\exp(-610/T)$

to each set of data. The resultant A, B and C values appear in Table III. The quantity θ_0 = 610°K in (5.11) is a compromise between θ_0 = 630±25°K for the $g_\perp$ line and θ_0 = 590±50°K for the $g_\parallel$ line. Our chosen value of θ_0 = 610°K in (5.11) falls within the Cr-CN stretching band (Table I).

There is considerable scatter in the low temperature data, due to the small sizes of samples available, but anisotropy of the direct process was observed. Our inability to grow sufficiently large low-concentration KCl crystals prevented our obtaining data in the range $4.2 < T < 25$°K. This precluded looking for the anomaly of the T dependence, observed in KBr. An isotropic Raman process is observed in KCl, as in KBr. From Figures 13 and 14 we see that the direct and Raman processes alone do not adequately describe the data for $T > 65$°K, whereas Figure 12 indicates that the local mode process fits the high temperature data very well.

Table III. Least squares fit of $\frac{1}{\tau_1} = AT + BT^9 J_8(230/T) + Ce^{-610/T}$ to relaxation of $Cr(CN)_5NO^{3-}$ in KCl.

Line	A	B	C
$g_{\parallel}$	.635±.030	$(6.29\pm.21)\times10^{-17}$	$(6.12\pm.34)\times10^{6}$
$g_{\perp}$	1.39±.07	$(7.54\pm.28)\times10^{-17}$	$(2.01\pm.62)\times10^{7}$

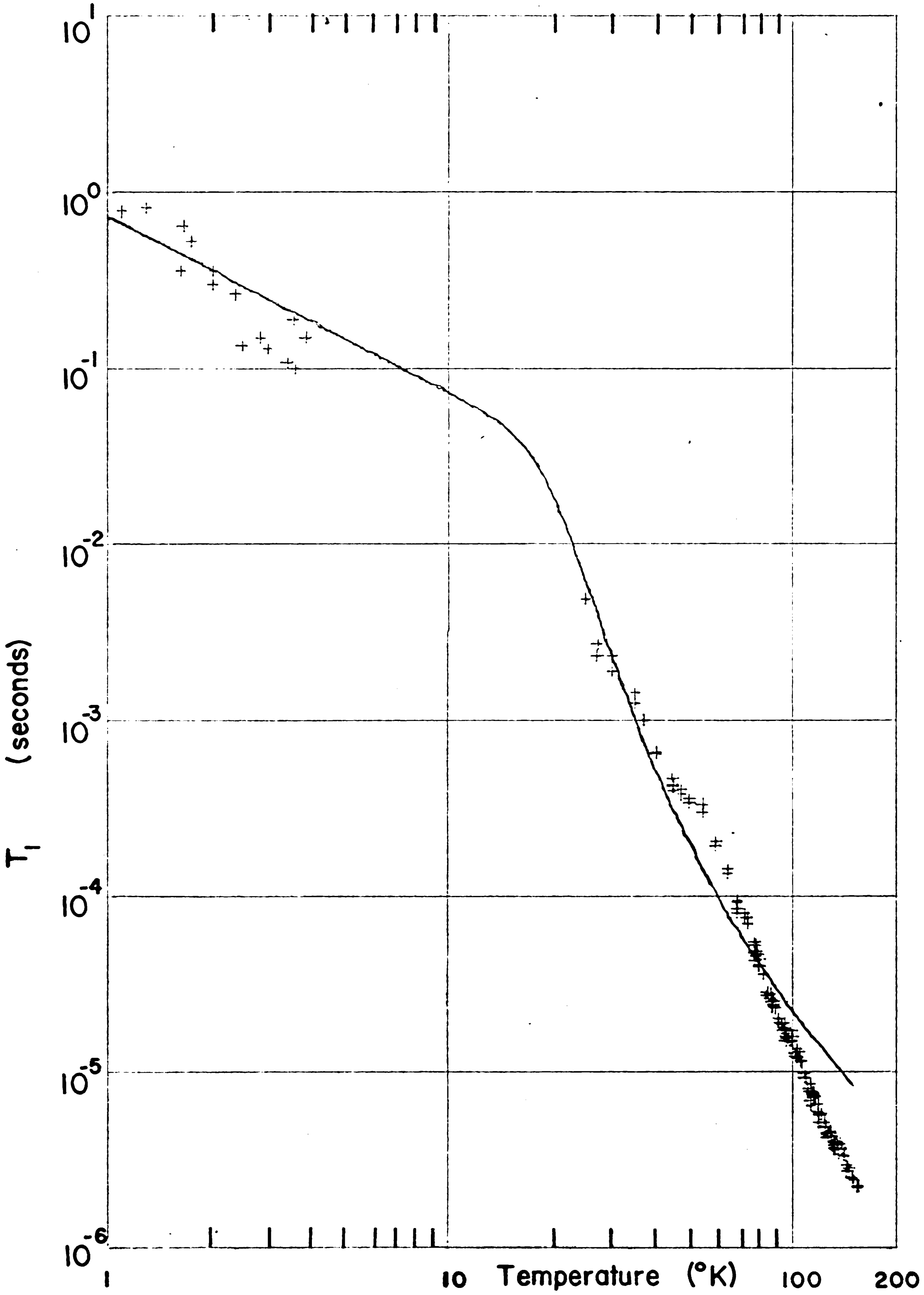

Figure 13. Data for $g_\perp$ line in KCl, with fit to $\frac{1}{\tau_1} = AT + BT^9 J_8(230/T)$

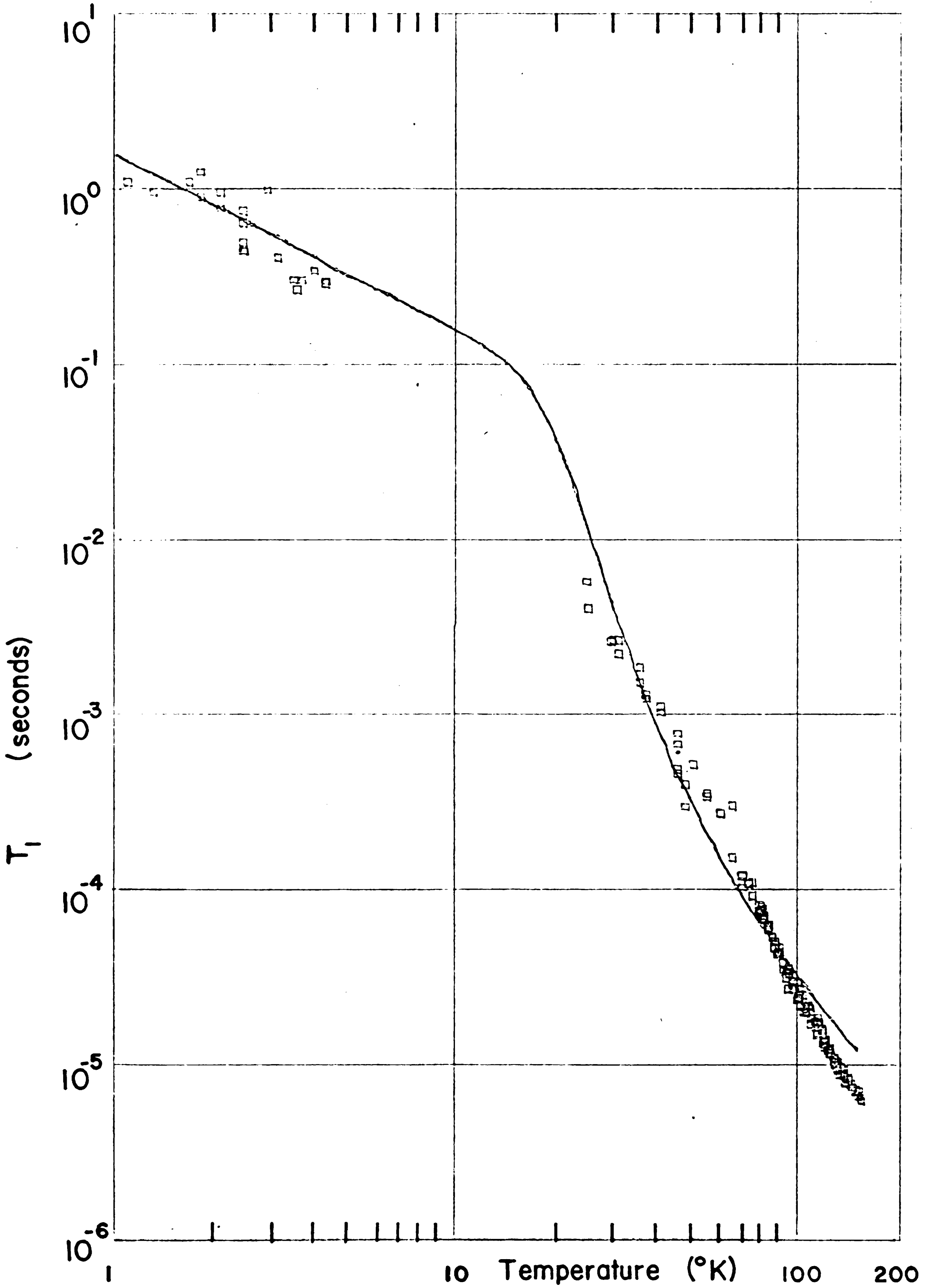

Figure 14. Data for $g_{\parallel}$ line in KCl, with fit to

$$\frac{1}{\tau_1} = AT + BT^9 J_8(230/T)$$

Summary

Electron spin-lattice relaxation times τ_1 of $Cr(CN)_5NO^{3-}$ substitutional in KBr and KCl have been measured for $1 < T < 150°K$. Spin echo techniques employing either picket or single-pulse saturation methods were used. From the temperature dependence of the observed τ_1 values, we conclude that at least three relaxation mechanisms are operative: an anisotropic direct process at $T < 5°K$, an isotropic Raman process at intermediate temperatures, and an anisotropic local mode process at $T > 65°K$. The functional form of the relaxation rate is $\frac{1}{\tau_1} = AT + BT^9J_8(\theta/T) + C\exp(-\theta_0/T)$, where θ is the Debye temperature and was taken as 170°K for KBr and 230°K for KCl. Empirical values of A, B, C, and θ_0 were determined by least squares computer analysis. Published energy level assignments preclude the possibility of an Orbach process. Therefore, since the parameter θ_0 is 575±30°K for KBr and 610±30°K for KCl, in agreement with published Cr-CN stretch frequencies, we conclude that the exponential process occurs through the interaction of lattice phonons with vibrational modes localized in the $Cr(CN)_5NO^{3-}$. An anomaly in the T dependence of τ_1 for KBr has been tentatively explained as a driven-mode process, in which relaxation is effected by low frequency ($<20\ cm^{-1}$) bending modes of the complex.

REFERENCES

1. M. Blackman, Handbuch der Physik 7 (part 1), 325 (1955).

2. J. G. Castle, Jr. and D. W. Feldman, Phys. Rev. 137, A671 (1965).

3. J. G. Castle, Jr., D. W. Feldman, P. G. Klemens, and R. A. Weeks, Phys. Rev. 130, 577 (1963).

4. B. P. Finn, R. Orbach, and W. D. Wolf, Proc. Phys. Soc. 77, 261 (1961).

5. C. L. Foiles (private communication).

6. E. L. Hahn, Phys. Rev. 76, 461 (1949).

7. D. J. E. Ingram, Spectroscopy at Radio and Microwave Frequencies (Philosophical Library, Inc., New York, 1956).

8. P. Gans, A. Sabatini, and L. Sacconi, Inorg. Chem. 5, 1877 (1966).

9. D. E. Kaplan, M. E. Browne, and J. A. Cowen, Rev. Sci. Instr. 27, 1028 (1956).

10. C. Kittel, Introduction to Solid State Physics (John Wiley and Sons, Inc., New York, 1956), p. 93.

11. Ibid., p. 125.

12. P. G. Klemens, Phys. Rev. 122, 433 (1961).

13. P. G. Klemens, Phys. Rev. 125, 1795 (1962).

14. P. G. Klemens, Solid State Physics (Academic Press, Inc., New York, 1958), Vol. 7, p. 1.

15. H. A. Kramers, Proc. Amsterdam Acad. Sci. 33, 959 (1930).

16. R. de L. Kronig, Physica 6, 33 (1939).

17. H. A. Kuska and M. T. Rogers, J. Chem. Phys. 42, 3034 (1965).

18. L. D. Landau and E. M. Lifshitz, Quantum Mechanics (Addison-Wesley Publishing Company, Inc., Reading, Mass.), p. 88.

19. P. T. Manoharan and H. B. Gray, Inorg. Chem. 5, 823 (1966).

20. P. T. Manoharan (private communication).

21. R. D. Mattuck and M. W. P. Strandberg, Phys. Rev. 119, 1204 (1960).

22. E. W. Montroll and R. B. Potts, Phys. Rev. 100, 525 (1955).

23. A. Narath, in Hyperfine Interactions, edited by A. J. Freeman and R. B. Frankel (Academic Press, New York, 1967), p. 287.

24. R. Orbach, Proc. Roy. Soc. A 264, 458 (1961).

25. R. Orbach and M. Blume, Phys. Rev. Letters 8, 478 (1962).

26. George E. Pake, Paramagnetic Resonance (W. A. Benjamin, New York, 1962), p. 84.

27. Ibid., p. 112.

28. W. M. Rogers and R. L. Powell, Tables of Transport Integrals, National Bureau of Standards Circular No. 595 (U. S. Governmental Printing Office, Washington, D. C., 1958).

29. Charles P. Slichter, Principles of Magnetic Resonance (Harper and Row, New York, 1962), p. 165.

30. R. G. D. Steel and J. H. Torrie, Principles and Procedures of Statistics (McGraw-Hill Book Company, New York, 1960), p. 181.

31. J. H. Van Vleck, J. Chem. Phys. 7, 72 (1939).

32. J. H. Van Vleck, Phys. Rev. 57, 426 (1940).

33. R. F. Vieth, Thesis, Michigan State University (1963), Chapter 2.

34. Ibid., Chapter 3.

35. Ibid., p. 112.

36. I. Wallter, Z. Physik 79, 370 (1932).

37. E. Wigner, Nachr. Akad. Wiss. Gottingen Math.-physik. Kl. IIa, 546 (1932).

38. J. M. Ziman, Electrons and Phonons (University Press, Oxford, 1960), p. 21.

APPENDICES

APPENDIX I.

DATA FOR KBr

GPERPENDICULAR LINE IN KBR

EXPERIMENTAL VALUES OF T1 VS T, ALONG WITH T1 VALUES CALCULATED FROM LEAST SQUARES FIT TO EQUATION (5.1).

T	T1(OBS)	T1(CALC)	REL WT	DATE
78.00	3.200-005	3.575-005	0.0000000014	02/08/66
86.50	2.200-005	2.036-005	0.0000000007	02/08/66
86.50	2.000-005	2.036-005	0.0000000005	02/08/66
89.00	1.650-005	1.746-005	0.0000000004	02/08/66
89.00	1.500-005	1.746-005	0.0000000003	02/08/66
94.00	1.300-005	1.306-005	0.0000000002	02/08/66
94.00	1.300-005	1.306-005	0.0000000002	02/08/66
97.70	1.150-005	1.069-005	0.0000000002	02/08/66
97.70	1.150-005	1.069-005	0.0000000002	02/08/66
78.00	3.000-005	3.575-005	0.0000000012	12/08/65
78.00	3.100-005	3.575-005	0.0000000013	12/08/65
78.00	3.200-005	3.575-005	0.0000000014	12/08/65
78.00	3.200-005	3.575-005	0.0000000014	12/08/65
86.70	1.900-005	2.011-005	0.0000000005	12/08/65
94.30	1.150-005	1.285-005	0.0000000002	12/08/65
94.50	1.150-005	1.270-005	0.0000000002	12/08/65
99.30	9.600-006	9.832-006	0.0000000001	12/08/65
102.50	8.600-006	8.374-006	0.0000000001	12/08/65
98.50	1.060-005	1.025-005	0.0000000002	12/08/65
4.20	1.500+000	1.309+000	3.0327513338	11/05/65
4.20	1.400+000	1.309+000	2.6418633841	11/05/65
3.51	1.850+000	1.567+000	4.6131517511	11/05/65
3.51	1.900+000	1.567+000	4.8658810288	11/05/65
2.46	2.200+000	2.236+000	6.5237850915	11/05/65
2.13	2.250+000	2.582+000	6.8236905010	11/05/65
4.20	1.500+000	1.309+000	3.0327513338	11/05/65
6.20	6.600-001	8.852-001	0.5871406582	11/05/65
8.20	2.600-001	6.581-001	0.0911173290	11/05/65
8.40	1.900-001	6.398-001	0.0486588103	11/05/65
12.60	1.300-001	2.814-001	0.0227793322	11/05/65
4.20	1.650+000	1.309+000	3.6696291139	11/03/65
4.20	1.570+000	1.309+000	3.3224127835	11/03/65
3.58	1.800+000	1.536+000	4.3671619205	11/03/65
3.21	2.200+000	1.713+000	6.5237850915	11/03/65
3.44	2.000+000	1.599+000	5.3915579268	11/02/65
3.44	1.550+000	1.599+000	3.2363044797	11/02/65
2.95	2.600+000	1.864+000	9.1117328960	11/02/65
2.29	2.300+000	2.402+000	7.1303353582	11/02/65
1.98	2.650+000	2.778+000	9.4655538853	11/02/65
45.80	5.100-004	4.121-004	0.0000003506	10/15/65
46.10	3.750-004	4.020-004	0.0000001895	10/15/65
50.40	3.100-004	2.851-004	0.0000001295	10/15/65
50.40	3.250-004	2.851-004	0.0000001424	10/15/65
53.80	1.800-004	2.193-004	0.0000000437	10/15/65
54.00	1.750-004	2.160-004	0.0000000413	10/15/65
59.20	1.600-004	1.452-004	0.0000000345	10/15/65
58.80	1.350-004	1.497-004	0.0000000246	10/15/65

```
63,20     1.060-004     1.070-004     0,0000000151     10/15/65
63.00     9.700-005     1.086-004     0,0000000127     10/15/65
72,20     5.400-005     5,424-005     0,0000000039     10/15/65
72,20     5,700-005     5.424-005     0,0000000044     10/15/65
75,60     4.600-005     4.236-005     0,0000000029     10/15/65
76,40     4,700-005     4,001-005     0.0000000030     10/15/65
76,50     4.000-005     3,973-005     0,0000000022     10/15/65
79,90     2,550-005     3,136-005     0,0000000009     10/15/65
79,80     2,750-005     3.157-005     0,0000000010     10/15/65
77,50     3,100-005     3,702-005     0,0000000013     10/15/65
77,30     3,300-005     3,755-005     0,0000000015     10/15/65
73,80     5,200-005     4,824-005     0,0000000036     10/15/65
73,50     4,500-005     4,931-005     0,0000000027     10/15/65
70,30     6,200-005     6,245-005     0,0000000052     10/15/65
 4,20     7,900-001     1,309+000     0,8412178255     10/13/65
17,60     2,800-002     4,843-002     0,0010567454     10/13/65
17,60     2.000-002     4,843-002     0,0005391558     10/13/65
19,20     1.700-002     2,819-002     0,0003895401     10/13/65
19,50     1,800-002     2,561-002     0,0004367162     10/13/65
20,60     1,450-002     1,831-002     0,0002833938     10/13/65
20,60     1,600-002     1,831-002     0,0003450597     10/13/65
22,80     9,000-003     1,005-002     0,0001091790     10/13/65
22,80     8,500-003     1,005-002     0,0000973850     10/13/65
24,80     6,000-003     6,274-003     0,0000485240     10/13/65
24,80     5,700-003     6,274-003     0,0000437929     10/13/65
26,60     4,250-003     4,322-003     0,0000243463     10/13/65
26,60     5,750-003     4,322-003     0,0000445646     10/13/65
28,20     3,200-003     3,213-003     0,0000138024     10/13/65
28,20     2,800-003     3,213-003     0,0000105675     10/13/65
29,70     2,500-003     2,496-003     0.0000084243     10/13/65
29,70     2.700-003     2,496-003     0,0000098261     10/13/65
31,80     2.000-003     1.815-003     0,0000053916     10/13/65
32.00     2.000-003     1.764-003     0,0000053916     10/13/65
33,40     1,450-003     1,458-003     0,0000028339     10/13/65
33,40     1,550-003     1,458-003     0,0000032383     10/13/65
38,20     6,500-004     8,315-004     0,0000005695     10/13/65
38,20     8,400-004     8,315-004     0,0000009511     10/13/65
42,30     6,500-004     5,579-004     0,0000005695     10/13/65
42,30     6,700-004     5,579-004     0,0000006051     10/13/65
46,60     3,700-004     3,858-004     0,0000001845     10/13/65
46,60     6,000-004     3,858-004     0,0000004852     10/13/65
46,20     4,000-004     3,987-004     0,0000002157     10/13/65
50,30     3.000-004     2,873-004     0,0000001213     10/13/65
50,30     3,200-004     2,873-004     0,0000001380     10/13/65
56,60     1,600-004     1,771-004     0,0000000345     10/13/65
56,60     1,700-004     1,771-004     0,0000000390     10/13/65
60,10     1,620-004     1,356-004     0,0000000354     10/13/65
59,90     1,500-004     1,377-004     0,0000000303     10/13/65
64.00     9,700-005     1,006-004     0,0000000127     10/13/65
63,60     1,070-004     1,022-004     0,0000000154     10/13/65
68,60     7,200-005     7,094-005     0,0000000070     10/13/65
68,60     7.200-005     7,094-005     0,0000000070     10/13/65
78,00     2,850-005     3,575-005     0,0000000011     07/23/64
78,00     2,600-005     3,575-005     0,0000000009     07/23/64
```

```
  80.00     3.800-005     3.114-005     0.0000000019     07/24/64
  85.50     2.500-005     2.168-005     0.0000000008     07/24/64
  89.00     1.700-005     1.746-005     0.0000000004     07/24/64
  94.10     1.300-005     1.299-005     0.0000000002     07/24/64
  98.20     1.080-005     1.041-005     0.0000000002     07/24/64
 102.00     9.000-006     8.583-006     0.0000000001     07/24/64
 102.80     8.750-006     8.253-006     0.0000000001     07/24/64
 105.00     7.500-006     7.429-006     0.0000000001     07/24/64
 107.30     7.000-006     6.681-006     0.0000000001     07/24/64
 110.00     6.500-006     5.926-006     0.0000000001     07/24/64
 111.60     6.000-006     5.533-006     0.0000000000     07/24/64
 114.30     4.400-006     4.946-006     0.0000000000     07/24/64
 123.00     3.000-006     3.551-006     0.0000000000     07/24/64
 128.50     4.000-006     2.941-006     0.0000000000     07/24/64
 135.00     2.200-006     2.397-006     0.0000000000     07/24/64
 141.20     2.600-006     2.005-006     0.0000000000     07/24/64
 145.00     1.900-006     1.810-006     0.0000000000     07/24/64
 150.00     1.700-006     1.593-006     0.0000000000     07/24/64
 150.00     2.300-006     1.593-006     0.0000000000     07/24/64
  79.50     2.950-005     3.223-005     0.0000000012     07/27/64
  79.50     3.100-005     3.223-005     0.0000000013     07/27/64
  70.00     6.000-005     6.387-005     0.0000000049     07/30/64
  75.00     4.300-005     4.423-005     0.0000000025     07/30/64
  79.00     2.400-005     3.335-005     0.0000000008     09/30/64
  79.00     2.800-005     3.335-005     0.0000000011     09/30/64
  87.00     1.700-005     1.974-005     0.0000000004     09/30/64
  94.50     1.100-005     1.270-005     0.0000000002     09/30/64
  99.50     7.400-006     9.731-006     0.0000000001     09/30/64
 106.50     5.000-006     6.929-006     0.0000000000     09/30/64
 113.00     4.800-006     5.218-006     0.0000000000     09/30/64
 113.00     4.200-006     5.218-006     0.0000000000     09/30/64
 121.00     3.300-006     3.818-006     0.0000000000     09/30/64
 127.00     2.800-006     3.092-006     0.0000000000     09/30/64
   4.20     1.270+000     1.309+000     2.1740109450     03/21/66
   4.20     1.250+000     1.309+000     2.1060773151     03/21/66
   4.20     1.360+000     1.309+000     2.4930563853     03/21/66
   3.57     1.280+000     1.541+000     2.2083821268     03/21/66
   3.01     1.760+000     1.827+000     4.1752224586     03/21/66
   3.01     1.950+000     1.827+000     5.1253497542     03/21/66
   2.45     2.000+000     2.245+000     5.3915579268     03/21/66
   2.41     2.450+000     2.282+000     8.0907066138     03/21/66
   1.93     2.520+000     2.850+000     8.5596373647     03/21/66
   1.93     2.350+000     2.850+000     7.4437196626     03/21/66
   1.56     2.700+000     3.525+000     9.8261143216     03/21/66
   1.56     2.850+000     3.525+000    10.9482323148     03/21/66
   6.00     1.150+000     9.152-001     1.7825838396     03/21/66
   5.80     1.200+000     9.471-001     1.9409608537     03/21/66
   8.40     2.400-001     6.398-001     0.0776384341     03/21/66
   8.40     1.700-001     6.398-001     0.0389540060     03/21/66
   8.95     2.700-001     5.916-001     0.0982611432     03/21/66
   9.05     2.500-001     5.831-001     0.0842430926     03/21/66
  10.00     2.200-001     5.032-001     0.0652378509     03/21/66
  11.70     9.700-002     3.575-001     0.0126822921     03/21/66
  13.05     8.000-002     2.458-001     0.0086264927     03/21/66
```

GPARALLEL LINE IN KBR

EXPERIMENTAL VALUES OF T1 VS T, ALONG WITH T1 VALUES CALCULATED FROM LEAST SQUARES FIT TO EQUATION (5.1).

```
   T         T1(OBS)        T1(CALC)        REL WT         DATE
  4.20     2.830+000      2.124+000      5.4593390386    03/21/66
  4.20     2.850+000      2.124+000      5.5367755047    03/21/66
  3.57     3.300+000      2.499+000      7.4232668817    03/21/66
  3.57     2.860+000      2.499+000      5.5756982355    03/21/66
  3.00     3.600+000      2.974+000      8.8343010822    03/21/66
  1.93     4.300+000      4.622+000     12.6038755414    03/21/66
  1.93     3.900+000      4.622+000     10.3680339092    03/21/66
  1.56     4.500+000      5.719+000     13.8035954414    03/21/66
  1.10     5.500+000      8.110+000     20.6201857827    03/21/66
  6.00     2.300+000      1.484+000      3.6059762906    03/21/66
  5.80     1.780+000      1.535+000      2.1597684838    03/21/66
  7.35     8.200-001      1.200+000      0.4583475346    03/21/66
  7.35     1.100+000      1.200+000      0.8248074313    03/21/66
  8.10     9.400-001      1.075+000      0.6023139226    03/21/66
  8.40     5.500-001      1.028+000      0.2062018578    03/21/66
  8.40     6.500-001      1.028+000      0.2880009419    03/21/66
  9.05     4.400-001      9.305-001      0.1319691890    03/21/66
  9.05     5.200-001      9.305-001      0.1843206028    03/21/66
 10.00     3.300-001      7.888-001      0.0742326688    03/21/66
 10.00     3.900-001      7.888-001      0.1036803391    03/21/66
 11.70     3.400-001      5.282-001      0.0787997843    03/21/66
 13.00     2.200-001      3.470-001      0.0329922973    03/21/66
 78.00     8.200-005      8.451-005      0.0000000046    02/08/66
 78.00     8.000-005      8.451-005      0.0000000044    02/08/66
 86.00     5.200-005      6.021-005      0.0000000018    02/08/66
 89.00     4.800-005      5.332-005      0.0000000016    02/08/66
 89.00     4.600-005      5.332-005      0.0000000014    02/08/66
 94.50     3.700-005      4.302-005      0.0000000009    02/08/66
 94.50     3.800-005      4.302-005      0.0000000010    02/08/66
 78.00     1.020-004      8.451-005      0.0000000071    12/08/65
 78.00     1.060-004      8.451-005      0.0000000077    12/08/65
 78.00     9.800-005      8.451-005      0.0000000065    12/08/65
 86.50     6.400-005      5.899-005      0.0000000028    12/08/65
 86.00     6.000-005      6.021-005      0.0000000025    12/08/65
 93.70     4.350-005      4.436-005      0.0000000013    12/08/65
 93.50     4.700-005      4.470-005      0.0000000015    12/08/65
 98.70     3.900-005      3.678-005      0.0000000010    12/08/65
  4.20     2.400+000      2.124+000      3.9263560366    11/05/65
  3.52     3.200+000      2.534+000      6.9801885096    11/05/65
  3.51     3.200+000      2.542+000      6.9801885096    11/05/65
  2.46     3.300+000      3.626+000      7.4232668817    11/05/65
  7.00     7.100-001      1.265+000      0.3436243191    11/05/65
  7.30     6.100-001      1.209+000      0.2536453266    11/05/65
  9.70     3.600-001      8.338-001      0.0883430108    11/05/65
 11.20     3.400-001      6.047-001      0.0787997843    11/05/65
  4.20     2.350+000      2.124+000      3.7644620160    11/03/65
  4.20     2.350+000      2.124+000      3.7644620160    11/03/65
```

```
  3.57     2.780+000     2.499+000     5.2681336795     11/03/65
  3.20     3.000+000     2.788+000     6.1349313073     11/03/65
 45.10     6.500-004     5.188-004     0.0000002880     10/15/65
 45.00     6.350-004     5.229-004     0.0000002749     10/15/65
 46.10     5.400-004     4.803-004     0.0000001988     10/15/65
 50.10     4.300-004     3.613-004     0.0000001260     10/15/65
 50.20     4.000-004     3.589-004     0.0000001091     10/15/65
 54.70     3.350-004     2.703-004     0.0000000765     10/15/65
 54.10     3.300-004     2.802-004     0.0000000742     10/15/65
 58.40     2.600-004     2.187-004     0.0000000461     10/15/65
 58.50     2.500-004     2.175-004     0.0000000426     10/15/65
 63.50     1.650-004     1.669-004     0.0000000186     10/15/65
 63.30     1.600-004     1.686-004     0.0000000175     10/15/65
 67.00     1.620-004     1.403-004     0.0000000179     10/15/65
 67.00     1.050-004     1.403-004     0.0000000075     10/15/65
 72.30     1.280-004     1.092-004     0.0000000112     10/15/65
 72.30     1.250-004     1.092-004     0.0000000107     10/15/65
 76.00     1.120-004     9.231-005     0.0000000086     10/15/65
 75.80     1.030-004     9.314-005     0.0000000072     10/15/65
 80.20     7.000-005     7.681-005     0.0000000033     10/15/65
 80.20     8.600-005     7.681-005     0.0000000050     10/15/65
 77.30     1.250-004     8.715-005     0.0000000107     10/15/65
 77.30     1.030-004     8.715-005     0.0000000072     10/15/65
 74.00     9.800-005     1.010-004     0.0000000065     10/15/65
 73.90     1.030-004     1.015-004     0.0000000072     10/15/65
 70.00     1.140-004     1.215-004     0.0000000089     10/15/65
 67.30     1.450-004     1.382-004     0.0000000143     10/15/65
 14.00     7.000-002     2.384-001     0.0033401293     10/14/65
 14.00     1.200-001     2.384-001     0.0098158901     10/14/65
 15.90     3.600-002     1.120-001     0.0008834301     10/14/65
 15.90     3.600-002     1.120-001     0.0008834301     10/14/65
 16.50     2.800-002     8.849-002     0.0005344207     10/14/65
 17.80     2.500-002     5.430-002     0.0004260369     10/14/65
 17.80     2.100-002     5.430-002     0.0003006116     10/14/65
 19.80     1.800-002     2.752-002     0.0002208575     10/14/65
 19.80     1.700-002     2.752-002     0.0001969995     10/14/65
 19.80     1.600-002     2.752-002     0.0001745047     10/14/65
 21.20     8.000-003     1.805-002     0.0000436262     10/14/65
 21.20     9.500-003     1.805-002     0.0000615197     10/14/65
 22.70     1.140-002     1.202-002     0.0000885884     10/14/65
 22.70     9.200-003     1.202-002     0.0000576956     10/14/65
 24.60     4.800-003     7.618-003     0.0000157054     10/14/65
 24.60     5.000-003     7.618-003     0.0000170415     10/14/65
 26.20     6.100-003     5.423-003     0.0000253645     10/14/65
 25.80     4.700-003     5.883-003     0.0000150578     10/14/65
 32.70     1.800-003     1.851-003     0.0000022086     10/14/65
 32.40     1.800-003     1.929-003     0.0000022086     10/14/65
 32.40     1.750-003     1.929-003     0.0000020876     10/14/65
 35.50     1.300-003     1.299-003     0.0000011520     10/14/65
 34.70     1.400-003     1.430-003     0.0000013361     10/14/65
 34.70     1.500-003     1.430-003     0.0000015337     10/14/65
 39.00     1.100-003     8.893-004     0.0000008248     10/14/65
 39.00     1.000-003     8.893-004     0.0000006817     10/14/65
 39.00     1.000-003     8.893-004     0.0000006817     10/14/65
```

46.40	5.300-004	4.696-004	0.0000001915	10/14/65
46.40	5.500-004	4.696-004	0.0000002062	10/14/65
50.80	4.200-004	3.449-004	0.0000001202	10/14/65
50.80	4.100-004	3.449-004	0.0000001146	10/14/65
55.50	2.550-004	2.579-004	0.0000000443	10/14/65
55.50	2.750-004	2.579-004	0.0000000516	10/14/65
79.00	6.100-005	8.090-005	0.0000000025	09/30/64
79.00	5.300-005	8.090-005	0.0000000019	09/30/64
79.00	5.000-005	8.090-005	0.0000000017	09/30/64
87.00	3.100-005	5.780-005	0.0000000007	09/30/64
87.00	3.500-005	5.780-005	0.0000000008	09/30/64
94.50	2.800-005	4.302-005	0.0000000005	09/30/64
99.50	2.350-005	3.572-005	0.0000000004	09/30/64
106.50	1.800-005	2.794-005	0.0000000002	09/30/64
106.50	2.000-005	2.794-005	0.0000000003	09/30/64
113.00	1.400-005	2.258-005	0.0000000001	09/30/64
113.00	1.600-005	2.258-005	0.0000000002	09/30/64
121.00	9.600-006	1.771-005	0.0000000001	09/30/64
70.00	1.100-004	1.215-004	0.0000000082	07/30/64
75.00	9.500-005	9.654-005	0.0000000062	07/30/64
75.00	7.000-005	9.654-005	0.0000000033	07/30/64
79.50	7.400-005	7.917-005	0.0000000037	07/27/64
79.50	8.000-005	7.917-005	0.0000000044	07/27/64
82.00	6.500-005	7.113-005	0.0000000029	07/27/64
82.00	7.400-005	7.113-005	0.0000000037	07/27/64
86.50	4.800-005	5.899-005	0.0000000016	07/27/64
86.50	5.400-005	5.899-005	0.0000000020	07/27/64
90.40	4.200-005	5.044-005	0.0000000012	07/27/64
96.00	3.300-005	4.065-005	0.0000000007	07/27/64
101.00	3.100-005	3.384-005	0.0000000007	07/27/64
101.00	3.200-005	3.384-005	0.0000000007	07/27/64
105.20	2.800-005	2.921-005	0.0000000005	07/27/64
111.00	2.500-005	2.407-005	0.0000000004	07/27/64
80.00	7.400-005	7.748-005	0.0000000037	07/24/64
94.00	4.200-005	4.385-005	0.0000000012	07/24/64
105.00	4.500-005	2.941-005	0.0000000014	07/24/64
78.00	6.100-005	8.451-005	0.0000000025	07/23/64
85.80	7.200-005	6.070-005	0.0000000035	07/23/64
94.60	5.000-005	4.286-005	0.0000000017	07/23/64
98.00	4.500-005	3.774-005	0.0000000014	07/23/64
100.00	3.300-005	3.508-005	0.0000000007	07/23/64
104.70	3.700-005	2.971-005	0.0000000009	07/23/64
110.20	3.550-005	2.471-005	0.0000000009	07/23/64

APPENDIX II.

DATA FOR KCl

GPERPENDICULAR LINE IN KCL

EXPERIMENTAL VALUES OF T1 VS T, ALONG WITH T1 VALUES CALCULATED FROM LEAST SQUARES FIT TO EQUATION (5.9).

```
     T          T1(OBS)        T1(CALC)        REL WT          DATE
   73.90       7.000-005      6.035-005    0.0000003104     04/12/67
   73.90       7.500-005      6.035-005    0.0000003563     04/12/67
   77.20       5.500-005      4.899-005    0.0000001916     04/12/67
   68.90       9.500-005      8.364-005    0.0000005717     04/12/67
   68.70       9.200-005      8.476-005    0.0000005362     04/12/67
    1.77       5.300-001      4.051-001   17.7940941970     04/20/66
    3.57       1.000-001      2.009-001    0.6334672196     04/20/66
    3.38       1.080-001      2.122-001    0.7388761649     04/20/66
    2.83       1.500-001      2.534-001    1.4253012440     04/20/66
    2.38       2.650-001      3.013-001    4.4485235492     04/20/66
    2.04       3.000-001      3.515-001    5.7012049760     04/20/66
    1.67       6.500-001      4.294-001   26.7639900255     04/20/66
    1.30       8.200-001      5.516-001   42.5943358438     04/20/66
    1.10       7.800-001      6.519-001   38.5401456375     04/20/66
    3.83       1.500-001      1.872-001    1.4253012440     04/06/67
    3.53       1.900-001      2.031-001    2.2868166625     04/06/67
    2.98       1.300-001      2.406-001    1.0705596011     04/06/67
    2.49       1.350-001      2.880-001    1.1544940076     04/06/67
    2.04       3.600-001      3.515-001    8.2097351654     04/06/67
    1.64       3.600-001      4.373-001    8.2097351654     04/06/67
   25.20       4.900-003      9.500-003    0.0015209548     04/07/67
   30.00       1.900-003      3.855-003    0.0002286817     04/07/67
   30.00       2.300-003      3.855-003    0.0003351042     04/07/67
   35.00       1.250-003      1.736-003    0.0000989793     04/07/67
   35.00       1.420-003      1.736-003    0.0001277323     04/07/67
   40.30       6.600-004      8.750-004    0.0000275938     04/07/67
   40.30       6.500-004      8.750-004    0.0000267640     04/07/67
   45.00       4.650-004      5.299-004    0.0000136971     04/07/67
   45.00       4.000-004      5.299-004    0.0000101355     04/07/67
   47.70       3.800-004      4.108-004    0.0000091473     04/07/67
   47.60       4.050-004      4.145-004    0.0000103904     04/07/67
   27.20       2.330-003      6.447-003    0.0003439030     04/10/67
   27.30       2.730-003      6.325-003    0.0004721168     04/10/67
   37.00       1.010-003      1.317-003    0.0000646200     04/10/67
   37.20       1.010-003      1.283-003    0.0000646200     04/10/67
   45.10       4.200-004      5.248-004    0.0000111744     04/10/67
   45.10       4.340-004      5.248-004    0.0000119317     04/10/67
   50.30       3.400-004      3.272-004    0.0000073229     04/10/67
   50.30       3.600-004      3.272-004    0.0000082097     04/10/67
   54.70       3.000-004      2.293-004    0.0000057012     04/10/67
   54.70       3.350-004      2.293-004    0.0000071091     04/10/67
   59.90       2.050-004      1.556-004    0.0000026621     04/10/67
   59.80       1.940-004      1.568-004    0.0000023841     04/10/67
   64.60       1.350-004      1.119-004    0.0000011545     04/10/67
   64.60       1.430-004      1.119-004    0.0000012954     04/10/67
   69.10       8.100-005      8.253-005    0.0000004156     04/10/67
   69.00       8.600-005      8.308-005    0.0000004685     04/10/67
```

```
    72,50      7,500=005      6.604-005      0.0000003563      04/10/67
    72,40      8.000=005      6.647-005      0.0000004054      04/10/67
    79,70      4.400-005      4.199-005      0,0000001226      03/25/67
    78,80      4.700=005      4.437-005      0.0000001399      03/25/67
    78,30      4.900=005      4.576-005      0,0000001521      03/25/67
    78,00      4.600=005      4.662-005      0.0000001340      03/25/67
    77,50      5.300=005      4,809-005      0,0000001779      03/25/67
    79,80      4.000=005      4.174-005      0.0000001014      03/25/67
    82,30      3.600=005      3.591-005      0.0000000821      03/25/67
    88,50      2.300=005      2.513-005      0.0000000335      03/25/67
    95,20      1.500=005      1.756-005      0.0000000143      03/25/67
    98,80      1.700=005      1.466-005      0.0000000183      03/25/67
    77.20      4.300=005      4.899-005      0.0000001171      03/27/67
    77,20      4.800=005      4,899-005      0,0000001460      03/27/67
    87,50      2.500=005      2.658=005      0,0000000396      03/27/67
    87,30      2.350-005      2.688-005      0,0000000350      03/27/67
    87,40      2.400-005      2.673-005      0.0000000365      03/27/67
    86.00      2.600-005      2.894-005      0.0000000428      03/27/67
    85,90      2.800=005      2,910-005      0.0000000497      03/27/67
    84.10      2,850=005      3.230-005      0.0000000515      03/27/67
    84.00      2,700=005      3.249-005      0,0000000462      03/27/67
    91,00      2.000-005      2.191-005      0.0000000253      03/27/67
    91.00      1.900=005      2.191-005      0,0000000229      03/27/67
    92,50      1.900=005      2.022-005      0,0000000229      03/27/67
    92.50      1.850=005      2.022-005      0.0000000217      03/27/67
    94.00      1.770-005      1.868-005      0,0000000198      03/27/67
    94.10      1.700=005      1.859-005      0.0000000183      03/27/67
    94,50      1.750=005      1.820-005      0.0000000194      03/27/67
    94.50      1.900=005      1.820-005      0,0000000229      03/27/67
    96.50      1.550=005      1.643-005      0.0000000152      03/27/67
    96.20      1.550=005      1.668-005      0.0000000152      03/27/67
    99,90      1.600-005      1.389-005      0.0000000162      03/27/67
   102,70      1.350=005      1.216-005      0,0000000115      03/27/67
   103,00      1,200=005      1.199-005      0.0000000091      03/27/67
   103,80      1.220=005      1.156-005      0.0000000094      03/27/67
   104,90      1.160-005      1.099-005      0.0000000085      03/27/67
    94,50      1.600=005      1,820-005      0.0000000162      03/27/67
    97,90      1,500=005      1,532-005      0,0000000143      03/27/67
    98,00      1.500-005      1,525-005      0.0000000143      03/27/67
   101.20      1.280=005      1.305-005      0.0000000104      03/27/67
   101,20      1.230=005      1.305-005      0.0000000096      03/27/67
   105,80      1.140=005      1.056-005      0,0000000082      03/27/67
   105,80      1.140=005      1.056-005      0.0000000082      03/27/67
   107,50      9.200=006      9.793-006      0.0000000054      03/27/67
   107,50      9.900=006      9.793-006      0.0000000062      03/27/67
   109.10      9.300=006      9.139-006      0,0000000055      03/27/67
   110,00      8,000=006      8.796-006      0.0000000041      03/27/67
   110.10      7,700=006      8.759-006      0.0000000038      03/27/67
   112,40      6,500=006      7.961-006      0,0000000027      03/27/67
   112,20      6,800=006      8.026-006      0,0000000029      03/27/67
   112,40      7.700=006      7.961-006      0.0000000038      03/27/67
   112,40      8,500=006      7.961-006      0.0000000046      03/27/67
   114,20      7,700=006      7,402-006      0.0000000038      03/27/67
   114,30      7,100=006      7.373-006      0.0000000032      03/27/67
```

```
114.30     7.600-006     7.373-006     0.0000000037     03/27/67
116.10     7.200-006     6.868-006     0.0000000033     03/27/67
116.10     7.200-006     6.868-006     0.0000000033     03/27/67
117.80     6.000-006     6.434-006     0.0000000023     03/27/67
117.80     6.600-006     6.434-006     0.0000000028     03/27/67
114.50     7.400-006     7.314-006     0.0000000035     03/29/67
114.50     7.500-006     7.314-006     0.0000000036     03/29/67
118.80     5.700-006     6.196-006     0.0000000021     03/29/67
118.70     5.200-006     6.219-006     0.0000000017     03/29/67
120.40     5.800-006     5.838-006     0.0000000021     03/29/67
120.40     5.700-006     5.838-006     0.0000000021     03/29/67
122.90     5.200-006     5.335-006     0.0000000017     03/29/67
123.00     4.900-006     5.316-006     0.0000000015     03/29/67
124.10     4.900-006     5.114-006     0.0000000015     03/29/67
124.10     4.830-006     5.114-006     0.0000000015     03/29/67
125.30     4.500-006     4.906-006     0.0000000013     03/29/67
125.30     4.380-006     4.906-006     0.0000000012     03/29/67
125.30     4.260-006     4.906-006     0.0000000011     03/29/67
127.50     4.500-006     4.554-006     0.0000000013     03/29/67
127.50     4.350-006     4.554-006     0.0000000012     03/29/67
128.30     4.600-006     4.434-006     0.0000000013     03/29/67
128.30     4.500-006     4.434-006     0.0000000013     03/29/67
129.70     4.000-006     4.236-006     0.0000000010     03/29/67
129.70     3.800-006     4.236-006     0.0000000009     03/29/67
131.50     3.700-006     3.998-006     0.0000000009     03/29/67
131.40     3.600-006     4.011-006     0.0000000008     03/29/67
131.30     4.000-006     4.024-006     0.0000000010     03/29/67
131.30     3.800-006     4.024-006     0.0000000009     03/29/67
127.90     4.340-006     4.493-006     0.0000000012     03/30/67
127.90     4.200-006     4.493-006     0.0000000011     03/30/67
131.50     3.700-006     3.998-006     0.0000000009     03/30/67
131.40     4.000-006     4.011-006     0.0000000010     03/30/67
133.00     4.000-006     3.814-006     0.0000000010     03/30/67
133.00     3.600-006     3.814-006     0.0000000008     03/30/67
134.00     3.900-006     3.698-006     0.0000000010     03/30/67
134.00     4.000-006     3.698-006     0.0000000010     03/30/67
135.90     3.800-006     3.492-006     0.0000000009     03/30/67
135.90     3.400-006     3.492-006     0.0000000007     03/30/67
136.80     3.920-006     3.399-006     0.0000000010     03/30/67
137.60     3.600-006     3.320-006     0.0000000008     03/30/67
137.40     3.700-006     3.340-006     0.0000000009     03/30/67
140.20     3.350-006     3.081-006     0.0000000007     03/30/67
140.00     3.350-006     3.098-006     0.0000000007     03/30/67
142.80     2.950-006     2.865-006     0.0000000006     03/30/67
142.60     2.720-006     2.881-006     0.0000000005     03/30/67
144.50     2.860-006     2.736-006     0.0000000005     03/30/67
144.60     2.740-006     2.729-006     0.0000000005     03/30/67
147.60     2.520-006     2.521-006     0.0000000004     03/30/67
147.60     2.480-006     2.521-006     0.0000000004     03/30/67
149.60     2.400-006     2.396-006     0.0000000004     03/30/67
152.80     2.240-006     2.213-006     0.0000000003     03/30/67
152.90     2.200-006     2.208-006     0.0000000003     03/30/67
154.10     2.240-006     2.145-006     0.0000000003     03/30/67
154.20     2.240-006     2.140-006     0.0000000003     03/30/67
```

```
    GPARALLEL LINE IN KCL

EXPERIMENTAL VALUES OF T1 VS T, ALONG WITH T1 VALUES CALCULATED FROM
LEAST SQUARES FIT TO EQUATION (5,9).


      T         T1(OBS)        T1(CALC)         REL WT          DATE
    73.90      1.090-004      9.114-005      0.0000001934     04/12/67
    77.20      8.100-005      7.707-005      0.0000001068     04/12/67
    73.90      9.100-005      9.114-005      0.0000001348     04/12/67
    69.20      1.180-004      1.171-004      0.0000002267     04/12/67
    69.00      1.200-004      1.184-004      0.0000002344     04/12/67
    79.40      7.700-005      6.914-005      0.0000000965     03/25/67
    78.90      6.700-005      7.085-005      0.0000000731     03/25/67
    78.60      7.600-005      7.190-005      0.0000000940     03/25/67
    78.50      8.000-005      7.226-005      0.0000001042     03/25/67
    77.90      6.700-005      7.443-005      0.0000000731     03/25/67
    77.80      7.400-005      7.480-005      0.0000000891     03/25/67
    77.50      7.400-005      7.592-005      0.0000000891     03/25/67
    77.50      7.200-005      7.592-005      0.0000000844     03/25/67
    79.50      7.000-005      6.881-005      0.0000000798     03/25/67
    79.90      6.800-005      6.748-005      0.0000000753     03/25/67
    79.70      7.000-005      6.814-005      0.0000000798     03/25/67
    82.20      6.200-005      6.044-005      0.0000000626     03/25/67
    81.80      6.000-005      6.160-005      0.0000000586     03/25/67
    82.30      5.900-005      6.015-005      0.0000000567     03/25/67
    82.30      6.300-005      6.015-005      0.0000000646     03/25/67
    88.50      4.600-005      4.525-005      0.0000000344     03/25/67
    88.00      4.400-005      4.628-005      0.0000000315     03/25/67
    97.10      3.000-005      3.137-005      0.0000000147     03/25/67
    97.00      3.220-005      3.149-005      0.0000000169     03/25/67
   101.70      2.150-005      2.612-005      0.0000000075     03/25/67
   100.90      2.700-005      2.694-005      0.0000000119     03/25/67
   100.20      2.900-005      2.770-005      0.0000000137     03/25/67
   103.80      2.000-005      2.409-005      0.0000000065     03/25/67
   103.80      2.500-005      2.409-005      0.0000000102     03/25/67
   119.90      1.350-005      1.374-005      0.0000000030     03/25/67
   118.20      1.500-005      1.451-005      0.0000000037     03/27/67
    77.20      7.500-005      7.707-005      0.0000000916     03/27/67
    77.20      7.400-005      7.707-005      0.0000000891     03/27/67
    87.40      4.300-005      4.754-005      0.0000000301     03/27/67
    87.50      4.250-005      4.732-005      0.0000000294     03/27/67
    85.80      5.000-005      5.111-005      0.0000000407     03/27/67
    85.90      4.600-005      5.088-005      0.0000000344     03/27/67
    84.60      5.300-005      5.401-005      0.0000000457     03/27/67
    84.50      5.300-005      5.426-005      0.0000000457     03/27/67
    90.90      3.450-005      4.072-005      0.0000000194     03/27/67
    90.80      3.800-005      4.090-005      0.0000000235     03/27/67
    92.50      3.100-005      3.801-005      0.0000000156     03/27/67
    92.50      3.400-005      3.801-005      0.0000000188     03/27/67
    94.20      2.700-005      3.537-005      0.0000000119     03/27/67
    94.30      3.400-005      3.522-005      0.0000000188     03/27/67
    94.30      3.500-005      3.522-005      0.0000000199     03/27/67
    96.50      2.700-005      3.215-005      0.0000000119     03/27/67
```

96.50	2.850-005	3.215-005	0.0000000132	03/27/67
99.90	2.350-005	2.803-005	0.0000000090	03/27/67
99.90	2.400-005	2.803-005	0.0000000094	03/27/67
104.90	2.000-005	2.311-005	0.0000000065	03/27/67
94.50	3.300-005	3.492-005	0.0000000177	03/28/67
94.50	3.300-005	3.492-005	0.0000000177	03/28/67
97.80	2.720-005	3.049-005	0.0000000120	03/28/67
97.80	2.770-005	3.049-005	0.0000000125	03/28/67
101.20	2.420-005	2.663-005	0.0000000095	03/28/67
101.20	2.510-005	2.663-005	0.0000000103	03/28/67
105.80	2.000-005	2.234-005	0.0000000065	03/28/67
105.80	2.070-005	2.234-005	0.0000000070	03/28/67
105.80	2.150-005	2.234-005	0.0000000075	03/28/67
107.60	2.140-005	2.091-005	0.0000000075	03/28/67
107.60	2.150-005	2.091-005	0.0000000075	03/28/67
109.00	2.100-005	1.988-005	0.0000000072	03/28/67
109.00	1.990-005	1.988-005	0.0000000064	03/28/67
110.00	1.700-005	1.916-005	0.0000000047	03/28/67
110.00	1.830-005	1.916-005	0.0000000055	03/28/67
112.30	1.750-005	1.769-005	0.0000000050	03/28/67
112.40	1.760-005	1.763-005	0.0000000050	03/28/67
112.40	1.630-005	1.763-005	0.0000000043	03/28/67
114.10	1.850-005	1.663-005	0.0000000056	03/28/67
114.20	1.730-005	1.658-005	0.0000000049	03/28/67
116.00	1.700-005	1.560-005	0.0000000047	03/28/67
116.10	1.740-005	1.555-005	0.0000000049	03/28/67
117.90	1.600-005	1.466-005	0.0000000042	03/28/67
117.90	1.570-005	1.466-005	0.0000000040	03/28/67
114.40	1.500-005	1.646-005	0.0000000037	03/29/67
114.50	1.480-005	1.641-005	0.0000000036	03/29/67
118.60	1.350-005	1.433-005	0.0000000030	03/29/67
118.60	1.300-005	1.433-005	0.0000000028	03/29/67
120.50	1.300-005	1.348-005	0.0000000028	03/29/67
120.30	1.380-005	1.357-005	0.0000000031	03/29/67
120.50	1.400-005	1.348-005	0.0000000032	03/29/67
120.40	1.260-005	1.353-005	0.0000000026	03/29/67
123.00	1.210-005	1.247-005	0.0000000024	03/29/67
123.00	1.220-005	1.247-005	0.0000000024	03/29/67
124.00	1.160-005	1.210-005	0.0000000022	03/29/67
124.00	1.230-005	1.210-005	0.0000000025	03/29/67
125.30	1.130-005	1.163-005	0.0000000021	03/29/67
127.50	9.800-006	1.090-005	0.0000000016	03/29/67
127.50	1.100-005	1.090-005	0.0000000020	03/29/67
128.60	1.080-005	1.055-005	0.0000000019	03/29/67
128.80	1.030-005	1.049-005	0.0000000017	03/29/67
129.70	9.400-006	1.023-005	0.0000000014	03/29/67
129.70	9.500-006	1.023-005	0.0000000015	03/29/67
131.20	1.000-005	9.801-006	0.0000000016	03/29/67
131.10	8.700-006	9.829-006	0.0000000012	03/29/67
128.00	1.060-005	1.074-005	0.0000000018	03/30/67
128.00	1.000-005	1.074-005	0.0000000016	03/30/67
131.30	9.900-006	9.774-006	0.0000000016	03/30/67
131.30	1.030-005	9.774-006	0.0000000017	03/30/67
133.30	9.700-006	9.247-006	0.0000000015	03/30/67

133.10	8.700-006	9.298-006	0.0000000012	03/30/67
134.00	9.500-006	9.072-006	0.0000000015	03/30/67
134.00	8.800-006	9.072-006	0.0000000013	03/30/67
136.00	8.500-006	8.597-006	0.0000000012	03/30/67
136.00	9.400-006	8.597-006	0.0000000014	03/30/67
136.70	8.550-006	8.439-006	0.0000000012	03/30/67
136.60	8.800-006	8.461-006	0.0000000013	03/30/67
136.60	8.900-006	8.461-006	0.0000000013	03/30/67
138.00	7.900-006	8.156-006	0.0000000010	03/30/67
137.80	7.700-006	8.199-006	0.0000000010	03/30/67
139.90	8.400-006	7.767-006	0.0000000011	03/30/67
139.90	8.250-006	7.767-006	0.0000000011	03/30/67
143.20	7.400-006	7.151-006	0.0000000009	03/30/67
143.10	7.800-006	7.169-006	0.0000000010	03/30/67
144.80	7.400-006	6.878-006	0.0000000009	03/30/67
147.60	7.000-006	6.435-006	0.0000000008	03/30/67
147.60	7.200-006	6.435-006	0.0000000008	03/30/67
150.00	6.600-006	6.087-006	0.0000000007	03/30/67
150.20	7.000-006	6.059-006	0.0000000008	03/30/67
152.70	6.200-006	5.728-006	0.0000000006	03/30/67
152.80	6.300-006	5.716-006	0.0000000006	03/30/67
24.40	5.700-003	1.603-002	0.0005289146	04/07/67
24.60	4.000-003	1.532-002	0.0002604689	04/07/67
30.20	2.650-003	4.787-003	0.0001143214	04/07/67
30.20	2.200-003	4.787-003	0.0000787918	04/07/67
35.00	1.500-003	2.157-003	0.0000366284	04/07/67
35.00	1.850-003	2.157-003	0.0000557159	04/07/67
40.30	1.100-003	1.072-003	0.0000196980	04/07/67
40.30	1.020-003	1.072-003	0.0000169370	04/07/67
45.00	6.700-004	6.485-004	0.0000073078	04/07/67
45.00	7.700-004	6.485-004	0.0000096520	04/07/67
47.50	2.950-004	5.135-004	0.0000014167	04/07/67
47.50	3.950-004	5.135-004	0.0000025400	04/07/67
28.75	2.580-003	6.317-003	0.0001083616	04/10/67
29.10	2.650-003	5.899-003	0.0001143214	04/10/67
36.20	1.290-003	1.815-003	0.0000270904	04/10/67
36.50	1.220-003	1.740-003	0.0000242301	04/10/67
45.10	4.840-004	6.422-004	0.0000038135	04/10/67
45.10	4.560-004	6.422-004	0.0000033851	04/10/67
50.20	5.100-004	4.076-004	0.0000042342	04/10/67
54.80	3.350-004	2.865-004	0.0000018269	04/10/67
54.90	3.500-004	2.844-004	0.0000019942	04/10/67
60.00	2.700-004	2.014-004	0.0000011868	04/10/67
60.00	2.700-004	2.014-004	0.0000011868	04/10/67
64.70	2.960-004	1.511-004	0.0000014263	04/10/67
64.80	1.500-004	1.502-004	0.0000003663	04/10/67
69.20	1.020-004	1.171-004	0.0000001694	04/10/67
72.30	1.070-004	9.908-005	0.0000001864	04/10/67
72.20	1.070-004	9.961-005	0.0000001864	04/10/67
4.18	2.950-001	3.765-001	1.4167064415	04/06/67
4.18	2.870-001	3.765-001	1.3409100015	04/06/67
3.88	3.400-001	4.056-001	1.8818875568	04/06/67
3.46	2.650-001	4.549-001	1.1432141322	04/06/67
3.04	4.000-001	5.177-001	2.6046686601	04/06/67

```
2,41     4.400-001     6.530-001     3,1516732787     04/06/67
1,79     1.250+000     8.792-001    25,4364126958     04/20/67
1,80     9.000-001     8.743-001    13,1862363413     04/20/67
3,57     3.000-001     4.408-001     1,4651373713     04/20/67
3,38     3,000-001     4.656-001     1.4651373713     04/20/67
2,83     9.800-001     5.561-001    15,6346436818     04/20/67
2,38     7.500-001     6.613-001     9,1571085704     04/20/67
2,38     6.400-001     6.613-001     6,6680029697     04/20/67
2,38     4.900-001     6.613-001     3,9086609205     04/20/67
2.38     4.400-001     6.613-001     3,1516732787     04/20/67
2.04     7.700-001     7.715-001     9,6519994158     04/20/67
2,04     9.500-001     7.715-001    14,6920719729     04/20/67
1,66     1.090+000     9.481-001    19,3414412308     04/20/67
1,30     9.600-001     1.211+000    15,0030066820     04/20/67
1,10     1.100+000     1.431+000    19,6979579921     04/20/67
```

APPENDIX III.

FORTRAN PROGRAM TOWPLOT USED IN CURVE FITTING

THE FOLLOWING LISTING OF PROGRAM TOWPLOT CONTAINS THE THEORETICAL RELAXATION RATES USED TO OBTAIN FIGURE 8 AND FIGURES 9 AND 10.

```
      PROGRAM TOWPLOT
C
C      THIS PROGRAM IS FOR LEAST SQUARES ANALYSIS OF SPIN-LATTICE
C      RELAXATION DATA AND INCLUDES FUNCTIONS FOR EVALUATING TRANSPORT
C      INTEGRALS.  ALSO INCLUDED ARE OPTIONS FOR PLOTTING THE OBSERVED
C      AND CALCULATED POINTS, AND FOR PRINTING THE RESULTS.
C
C
C      THE FUNCTIONAL FORM OF EACH FIT IS INSERTED INTO SUBROUTINE DEFN.
C      EACH FIT IS MADE TO ALL SETS OF DATA READ IN.
C
C      THE ORDER OF DATA TO BE READ IN IS AS FOLLOWS
C         (1) NUMBER OF SETS OF DATA TO BE FITTED (I2).
C         (2) NUMBER OF FITS PER DATA SET (I2).
C         (3) THEN FOR EACH SET OF EXPERIMENTAL POINTS THERE SHOULD BE...
C              (A) HEADER CARD IDENTIFYING THE EXPERIMENT (10A8).
C              (B) DECK OF EXPERIMENTAL DATA, EACH CARD HAVING
C                  TEMPERATURE, T1, AND DATE (F10.1, E15.1, 15X, A8).
C      ALL POINTS FROM THE SAME DATE SHOULD BE PLACED TOGETHER IN THE
C      DECK, SINCE ALL POINTS FROM A GIVEN DATE WILL BE PLOTTED
C      WITH A UNIQUE SYMBOL.
C
C      IF NOTPRINT = 1, EXPERIMENTAL AND CALCULATED T1 ARE NOT PRINTED.
C      IF NOTPLOT = 1, NO PLOT WILL BE MADE,
C          NOTPRINT AND NOTPLOT ARE DEFINED IN SUBROUTINE DEFINE.
C
C      THE SCALE FACTORS FOR PLOTTING ARE SY, SX, SYY, SXX, AND ARE
C      DEFINED IN SUBROUTINE DEFINE,
C      SY AND SX ARE SCALE FACTORS FOR PLOTS OF LOG(T) AND LOG(T1).
C      THEY ARE 100 TIMES THE NUMBER OF INCHES PER CYCLE ON THE LL PLOT.
C      SYY AND SXX ARE SCALE FACTORS FOR THE PLOTTING OF SYMBOLS
C      DENOTING THE EXPERIMENTAL POINTS, AND SHOULD BOTH HAVE THE SAME
C      VALUE.  THEIR VALUE IS 1000 TIMES THE DESIRED HEIGHT (IN INCHES)
C      OF THE SYMBOLS.
C
      COMMON T(500),TOW(500),TOWIN(500),WAT(500),WAIT(500),NLO,NHI,NEX
      COMMON LIN(500), NDATE(500), NDP, HIPLUS, LTH, NOVAR, NVLESS
      COMMON DATA(5), VECTOR(6,6), AVE(5), COEN(5), SIGMCO(5),SIGMA(5)
      COMMON NODATE, KDATE(500),SIGY, NOIN, NNWT, INDEX(5)
      COMMON SY, SX, SYY, SXX, NOTPRINT, NOTPLOT
      DIMENSION LHEAD(10)
      TYPE DOUBLE COEN,SIGMA,SIGY,VECTOR,DATA,WAIT
      LTH = 0
C      READ IN NUMBER OF SETS OF DATA
         READ 1, NLINS
C      READ IN NUMBER OF FITS PER DATA SET
         READ 1, NFITS
         DO 500 K= 1, NLINS
C      READ IN HEADER CARD IDENTIFYING SET OF DATA
```

```
      READ 10, (LHEAD(L), L=1,10)
C      READ IN MEASURED T AND T1
         KDATE(1) = 1
           READ 5, T(1),TOW(1),NDATE(1)
           DO 110 I=2,500
           READ 5, T(I), TOW(I), NDATE(I)
         IF (NDATE(I) - NDATE(I-1)) 100, 105, 100
  100 KDATE(I) = KDATE(I-1) + 1
      GO TO 109
  105 KDATE(I) = KDATE(I-1)
  109 IF(T(I)) 115, 115, 110
  110      NDP = I
  115 CONTINUE
C      CALCULATE WEIGHTS FOR LEAST SQUARES FIT
         SUMWAT = 0.0
         DO 120 I= 1,NDP
         TOWIN(I) = 1.0 / TOW(I)
         WAT(I) = TOW(I) + TOW(I)
  120    SUMWAT = SUMWAT + WAT(I)
      AVGWT = SUMWAT / NDP
           DO 125 I = 1,NDP
  125      WAIT(I) = WAT(I) / AVGWT
      DO 500 NEX = 1, NFITS
      PRINT 10, (LHEAD(L), L=1,10)
      CALL STEPREG
      IF(NOTPRINT) 400, 400, 450
  400 CALL VARFIT
  450 IF(NOTPLOT) 460, 460, 500
  460 CALL GRFTOW
  500 CONTINUE
C       STOP PLOTTER
      CALL PLOT(HIPLUS, 2.5, -1, SY, SX)
    1 FORMAT(I2)
    5 FORMAT(F10.1, E15.1, 15X, A8)
   10 FORMAT (10A8)
      END
```

```
      SUBROUTINE DEFINE (X, Y)
      COMMON T(500),TOW(500),TOWIN(500),WAT(500),WAIT(500),NLO,NHI,NEX
      COMMON LIN(500), NDATE(500), NDP, HIPLUS, LTH, NOVAR, NVLESS
      COMMON DATA(5), VECTOR(6,6), AVE(5), COEN(5), SIGMCO(5),SIGMA(5)
      COMMON NODATE, KDATE(500),SIGY, NOIN, NNWT, INDEX(5)
      COMMON SY, SX, SYY, SXX, NOTPRINT, NOTPLOT
      TYPE DOUBLE COEN,SIGMA,SIGY,VECTOR,DATA,WAIT
      TYPE DOUBLE U, V, W, Z
      SY=115. $ SX=225.
         SXX = 66.  $  SYY = 66.
            NOTPRINT = 0  $  NOTPLOT = 0
C
C      AFTER STATEMENTS 10 THRU 50 THE NUMBER OF VARIABLES TO BE USED IN
C      IN EACH FIT IS DEFINED BY A STATEMENT OF THE FORM
C            NOVAR = N
C      WHERE N IS AN INTEGER CONSTANT EQUAL TO (1 + THE NUMBER OF
C      COEFFICIENTS TO BE DETERMINED IN THE LEAST SQUARES FIT).
C
      GO TO (10, 20, 30, 40,50), NEX
   10 CONTINUE
C
      NOVAR = 4
C
      GO TO 99
   20 CONTINUE
C
      NOVAR = 3
C
      GO TO 99
   30 CONTINUE
C
C
      GO TO 99
   40 CONTINUE
C
C
      GO TO 99
   50 CONTINUE
C
C
   99 NVLESS =  NOVAR - 1
      RETURN
C       *****  *****  *****  *****  *****  *****  *****  *****  *****
         ENTRY DEFN
C
      THE PARAMETERS INPUT TO THIS SUBROUTINE FROM STEPREG ARE X, THE
C      MEASURED TEMPERATURE AND Y, THE INVERSE OF THE MEASURED T1.
C
C      AFTER STATEMENTS 100 THRU 500 THE FUNCTIONS TO BE USED IN THE FIT
C      ARE DEFINED BY STATEMENTS OF THE FORM
C           DATA(1) = BLAH BLAH
C           DATA(2) = BLAH
C           DATA(3) = ETC
C      THE DEPENDENT VARIABLE IN THE LEAST SQUARES FIT MUST BE
```

```
C      EQUATED TO DATA(M), WHERE M = NOVAR.
C      NOTE THAT FOUR DUMMY DOUBLE PRECISION VARIABLES HAVE BEEN
C      PROVIDED FOR CONVENIENCE IN CONSTRUCTING FUNCTIONS.
C      THESE DUMMY VARIABLES ARE U, V, W, AND Z.
C
        GO TO (100, 200, 300, 400, 500), NEX
  100 CONTINUE
C
        V = TRNSPRT(8, 170., X)
        U = Y  $  Z = X  $  W = Z**9  $  DATA(1) = Z  $  DATA(2) = V *W
        DATA(4) = U  $  DATA(3) = DEXP(-575./ Z)
C
      GO TO 999
  200 CONTINUE
C
        V = TRNSPRT(8, 170., X)
        U = Y  $  Z = X  $  W = Z**9  $  DATA(1) = Z  $  DATA(2) = V *W
        DATA(3) = U
C
      GO TO 999
  300 CONTINUE
C
C
      GO TO 999
  400 CONTINUE
C
C
      GO TO 999
  500 CONTINUE
C

C
  999 RETURN
      END
```

```
      SUBROUTINE VARFIT
C
C       THIS SUBROUTINE CALCULATES THE STANDARD DEVIATION, CHECKS TO
C       SEE THAT THE SUM OF THE WEIGHTS IS EQUAL TO THE NUMBER OF DATA
C       POINTS, AND CALCULATES (FROM THE FIT) A T1 VALUE FOR EACH
C       EXPERIMENTAL TEMPERATURE.
C
      COMMON T(500),TOW(500),TOWIN(500),WAT(500),WAIT(500),NLO,NHI,NEX
      COMMON LIN(500), NDATE(500), NDP, HIPLUS, LTH, NOVAR, NVLESS
      COMMON DATA(5), VECTOR(6,6), AVE(5), COEN(5), SIGMCO(5),SIGMA(5)
      COMMON NODATE, KDATE(500),SIGY, NOIN, NNWT, INDEX(5)
      COMMON SY, SX, SYY, SXX, NOTPRINT, NOTPLOT
      TYPE DOUBLE COEN,SIGMA,SIGY,VECTOR,DATA,WAIT
      TYPE DOUBLE CALC
      PRINT 25
   25 FORMAT(1H0,6X1HT,9X7HT1(OBS),8X8HT1(CALC),4X12H1.0/T1 (OBS),
     1  4X13H1.0/T1 (CALC),6X3HDEV,9X6HREL WT,12X4HDATE)
      SUMSQ = 0.0
      SUMWAIT = 0.0
      DO 125 N = 1,NDP
         SUMWAIT = SUMWAIT + WAIT(N)
      CALL DEFN(T(N), 0.0)     $ CALC = 0.0
      DO 120 K = 1, NOIN
  120 CALC = CALC  + COEN (K) * DATA(INDEX(K))
      DEV = TOWIN(N) - CALC
      TIMCAL = 1.0/CALC
      PRINT 30,T(N),TOW(N),TIMCAL,TOWIN(N),CALC,DEV,WAIT(N),NDATE(N)
  125    SUMSQ = SUMSQ + DEV*DEV*WAIT(N)
   30 FORMAT(F10.2, 5F15.3, F15.10, 7XA8)
      XNDP = NDP + 1
      VARF = SQRTF (SUMSQ/XNDP)
      PRINT 35, VARF
   35 FORMAT(//, 17H VARIANCE OF FIT=  F15.9)
      PRINT 40, SUMWAIT
   40 FORMAT(//, *SUM OF WEIGHTS =* F15.9)
      END
```

```
      FUNCTION TRNSPRT(NN,D,T)
C
C      THIS FUNCTION CALCULATES THE TRANSPORT INTEGRAL OF ORDER NN
C      FOR DEBYE TEMPERATURE D AND TEMPERATURE T,
C      NOTE THAT FUNCTIONS TINTGRND AND SIMPSON ARE REQUIRED.
C
      COMMON /NM/N
         EXTERNAL TINTGRND
      N=NN
         O = 0.00001
         TRNSPRT = SIMPSON (0, D/T, 0.001, TINTGRND)
         RETURN
      END
```

```
      FUNCTION TINTGRND (Z)
C
C      THIS FUNCTION DEFINES THE INTEGRAND FOR FUNCTION TRNSPRT.
C
      COMMON /NM/N
         IF(Z-300) 2, 1, 1
    1       TINTGRND = 0
            RETURN
    2    EZ = EXPF (Z)
         EZ1 = EZ - 1.0
         EZ1SQ = EZ1 * EZ1
         TINTGRND = EZ * (Z**N) / EZ1SQ
         RETURN
      END
```

```
      FUNCTION SIMPSON(AA,B,ERR,FCT)
C
C       THIS FUNCTION EVALUATES THE TRANSPORT INTEGRAL BY SIMPSONS RULE.
C
        DIMENSION DX(30),EPSP(30),X2(30),X3(30),F2(30),F3(30),F4(30),
     1            FMP(30),FBP(30),PVAL(30,3),LVF(30),EST2(30),EST3(30)
C       THIS IS A TRANSLATION OF A STANFORD SUBALGOL PROCEDURE

        A=AA
        EPS=ERR
C       PSEUDO PARAMETER SETUP, ETC.
        LVL=0
        ABSAREA=1.0
        EST=1.0
        FA=FCT(A)
        AB2=(A+B)/2.0
        FM=4.0*FCT(AB2)
        FB=FCT(B)
        DA=B-A

 99     LVL=LVL+1
        DX(LVL)=DA/3.0
        SX=DX(LVL)/6.0
        ADX2=A+DX(LVL)/2.0
        F1=4.0*FCT(ADX2)
        X2(LVL)=A+DX(LVL)
        X2L=X2(LVL)
        F2(LVL)=FCT(X2L)
        X3(LVL)=X2(LVL)+DX(LVL)
        X3L=X3(LVL)
        F3(LVL)=FCT(X3L)
        EPSP(LVL)=EPS
        X3D=X3(LVL)+DX(LVL)/2.0
        F4(LVL)=4.0*FCT(X3D)
        FMP(LVL)=FM
        EST1=(FA+F1+F2(LVL))*SX
        FBP(LVL)=FB
        EST2(LVL)=(F2(LVL)+F3(LVL)+FM)*SX
        EST3(LVL)=(F3(LVL)+F4(LVL)+FB)*SX
        SUM=EST1+EST2(LVL)+EST3(LVL)
        ABSAREA=ABSAREA-ABSF(EST)+ABSF(EST1)+ABSF(EST2(LVL))
     1          +ABSF(EST3(LVL))

        IF(ABSF(EST-SUM)-EPSP(LVL)*ABSAREA)98,98,97
 98        IF(EST-1.0)96,97,96
 97     IF(LVL-30)92,95,96
C          DONE ON THIS LEVEL
 96        IF(LVL-30)93,95,93
 95           VAL1=EST-SUM
              VAL2=ABSAREA*EPSP(LVL)
              PRINT 94,VAL1,VAL2
 94           FORMAT (74HTHE RECURSION HAS DESCENDED TO LEVEL 30, WITHO
     1UT SATISFYING THE TOLERANCE./37HTHE ESTIMATE OF THE ABSOLUTE ERROR
     2 IS,E16.8/43HAND THE TOLERANCE REQUIRED AT THIS LEVEL IS,E16.8/)
```

```
93          LVL=LVL-1
            LEAVE=LVE(LVL)
            PVAL(LVL,LEAVE)=SUM
            GO TO (91,90,89),LEAVE


92        LVE(LVL)=1
          DA=DX(LVL)
          FM=F1
          FB=F2(LVL)
          EPS=EPSP(LVL)/1.7
          EST=EST1
          GO TO 99


91        LVE(LVL)=2
          DA=DX(LVL)
          FA=F2(LVL)
          FM=FMP(LVL)
          FB=F3(LVL)
          EPS=EPSP(LVL)/1.7
          EST=EST2(LVL)
          A=X2(LVL)
          GO TO 99


90        LVE(LVL)=3
          DA=DX(LVL)
          FA=F3(LVL)
          FM=F4(LVL)
          FB=FBP(LVL)
          EPS=EPSP(LVL)/1.7
          EST=EST3(LVL)
          A=X3(LVL)
          GO TO 99


89        SUM=PVAL(LVL,1)+PVAL(LVL,2)+PVAL(LVL,3)
          IF(LVL-1)88,88,93
88        SIMPSON=SUM
          RETURN
        END
```

```
      SUBROUTINE STEPREG
C     SIMPLE STEPWISE REGRESSION
C
C      THIS SUBROUTINE PERFORMS A LEAST SQUARES FIT TO OBTAIN
C      COEFFICIENTS IN AN EXPRESSION OF THE FORM
C          Y = A(1)*X(1) + A(2)*X(2) + ...........
C      THE VARIABLES X(I) AND Y ARE THE SUBSCRIPTED VARIABLE DATA(N)
C      DEFINED IN SUBROUTINE DEFN.
C
      COMMON T(500),TOW(500),TOWIN(500),WAT(500),WAIT(500),NLO,NHI,NEX
      COMMON LIN(500), NDATE(500), NDP, HIPLUS, LTH, NOVAR, NVLESS
      COMMON DATA(5), VECTOR(6,6), AVE(5), COEN(5), SIGMCO(5),SIGMA(5)
      COMMON NODATE, KDATE(500),SIGY, NOIN, NNWT, INDEX(5)
      COMMON SY, SX, SYY, SXX, NOTPRINT, NOTPLOT
      TYPE DOUBLE COEN,SIGMA,SIGY,VECTOR,DATA,WAIT
C     IFSTEP = 1, DO NOT PRINT EACH STEP
C     IFRAW  = 1   DO NOT PRINT RAW SUMS AND SQUARES
C     IFAVE  = 1   DO NOT PRINT AVERAGES
C     IFRESD = 1   DO NOT PRINT RESIDUAL SUMS SQUARES
C     IFCOEN = 1   DO NOT PRINT PARTIAL COEFFICIENTS
C     IFPRED = 1   DO NOT CALC PREDICTED VALUES
C     IFCNST = 1   DO NOT HAVE CONST TERM IN EQUATION
    8 FORMAT(/)
      EFIN=0.0000001
      EFOUT=0.0000001
           TOL  = .00001
      IFCNST=1
      IFSTEP = 1
      IFRAW = 1
      IFAVE = 1
      IFAVG = 1
      IFRESD = 1
      IFCOEN = 1
      CALL DEFINE (0.0, 0.0)
      INVAR = NOVAR
      NOIN = 0
      VAR  = 0
      K    = 0
      FLEVEL = 0
      NOENT = 0
      NOMIN = 0
      NOMAX = 0
      NVP1 = NOVAR + 1
  110 DO 120 I = 1, NVP1
  130 DO 120 J = 1, NVP1
  120 VECTOR(I,J) = 0.0
         DO 510 N= 1,NDP
         CALL DEFN(T(N), TOWIN(N))
  530 DO 540 I = 1, NOVAR
  550 VECTOR(I,NOVAR + 1) = VECTOR(I, NOVAR + 1) + DATA(I) * WAIT(N)
  560 DO 540  J = 1, NOVAR
  540 VECTOR(I, J) = VECTOR (I, J) + DATA (I) * DATA(J) * WAIT(N)
  510 VECTOR(NVP1, NVP1) = VECTOR(NVP1, NVP1) + WAIT(N)
  565 NOVMI = NOVAR - 1
```

```
  566 NOVPL = NOVAR + 1
C     CALCULATION OF RESIDUAL SUMS OF SQUARES AND CROSS PRODUCTS
  650 IF(IFCNST) 900,651,735
  735 GO TO 780
  651 IF(VECTOR(NOVPL,NOVPL)) 652,652,655
  652 PRINT 654
      GO TO 910
  655 DO 660 I = 1, NOVAR
  670 DO 660 J = I, NOVAR
  660 VECTOR (I,J) = VECTOR (I,J) - (VECTOR(I,NOVPL) * VECTOR (J,NOVPL)
     - / VECTOR (NOVPL, NOVPL))
  680 DO 690  I = 1, NOVAR
  690 AVE(I)  = VECTOR(I,NOVPL) / VECTOR(NOVPL,NOVPL)
  780 NOSTEP = -1
  781 ASSIGN  1320  TO NUMBER
  782 DEFR    = VECTOR(NOVPL,NOVPL) - 1.0
  790 DO 800  I = 1,NOVAR
  791 IF(VECTOR(I,I)) 792,794,810
  792 PRINT  793, I
      GO TO 910
  793 FORMAT (31H ERROR RESIDUAL SQUARE VARIABLE I4,31H IS NEGATIVE,PROB
     1LEM TERMINATED )
  794 PRINT 795, I
  796 SIGMA(I) =      1.0
  797 GO TO 800
  795 FORMAT (1H010H VARIABLE I5,13H IS CONSTANT )
  810 SIGMA(I) =DSQRT  (VECTOR (I,I))
  800 VECTOR(I,I) = 1.0
  820 DO 830  I = 1,NOVMI
  840 IP1 = I + 1
  841 DO 830 J = IP1, NOVAR
  850 VECTOR(I,J) = VECTOR(I,J) /( SIGMA(I)* SIGMA(J))
  830 VECTOR(J,I) = VECTOR(I,J)
 1000 NOSTEP = NOSTEP + 1
 1001 IF (VECTOR( NOVAR,NOVAR)) 1002,1002,1010
 1002 NSTPM1 = NOSTEP - 1
      PRINT 1004, NSTPM1
      GO TO 1381
 1010 SIGY =  SIGMA(NOVAR) *DSQRT  (VECTOR(NOVAR,NOVAR)/ DEFR)
 1015 DEFR =DEFR-1.0
 1016 IF (DEFR )  1017,1017, 1020
 1017 PRINT  1019 ,NOSTEP
 1018 PRINT                 1019, NOSTEP
      GO TO 1381
 1020 VMIN = 0.0
 1030 VMAX = 0.0
 1035 NOIN = 0
 1040 DO 1050  I = 1,NOVMI
 1041 IF (VECTOR (I,I)) 1042,1050,1060
 1042 PRINT 1044, I, NOSTEP
 1043 PRINT                 1044, I, NOSTEP
 1045 GO TO 1381
 1060 IF(VECTOR(I,I) - TOL)   1050,1080,1080
 1080 VAR = VECTOR(I,NOVAR) * VECTOR(NOVAR,I) / VECTOR(I,I)
```

```
1090 IF(VAR)1100,1050,1110
1100 NOIN = NOIN + 1
1120 INDEX(NOIN) = I
1130 COEN(NOIN)  = VECTOR(I,NOVAR) * SIGMA(NOVAR) / SIGMA (I)
1140 SIGMCO(NOIN) = (SIGY / SIGMA(I)) *DSQRT (VECTOR(I,I))
1150 IF (VMIN) 1160,1170,904
 904 PRINT                  906
     PRINT 906
     GO TO 910
1170 VMIN = VAR
1180 NOMIN = I
1190 GO TO 1050
1160 IF(VAR - VMIN)1050,1050,1170
1110 IF (VAR - VMAX)1050,1050,1210
1210 VMAX = VAR
1220 NOMAX = I
1050 CONTINUE
1230 IF (NOIN) 903,1240,1245
 903 PRINT                  907
     PRINT  907
     GO TO  910
1240 PRINT                65, SIGY
1260 GO TO 1350
1245 IF (IFCNST) 900,1250,1246
1246 CNST = 0.0
1247 GO TO 1300
1250 CNST = AVE(NOVAR)
1270 DO 1280 I = 1,NOIN
1290 J = INDEX(I)
1280 CNST = CNST - (COEN(I) * AVE(J))
1300 IF(IFSTEP) 900,1310,1320
1310 IF (NOENT) 1311,1311,1313
1311 PRINT                 91,NOSTEP, K
1312 GO TO 1314
1313 PRINT                 92,NOSTEP, K
1314 PRINT                70,FLEVEL, SIGY,CNST,
    1 (INDEX(J),COEN(J),SIGMCO(J), J = 1, NOIN )
1315 GO TO NUMBER, (1320,1580)
1320 FLEVEL = VMIN * DEFR / VECTOR (NOVAR,NOVAR)
1330 IF(EFOUT + FLEVEL) 1350, 1350, 1340
1340 K =  NOMIN
1345 NOENT = 0
     GO  TO  1391
1350 FLEVEL = VMAX * DEFR / (VECTOR(NOVAR,NOVAR)-  VMAX)
1360 IF (EFIN - FLEVEL) 1370,1361,1380
1361 IF (EFIN) 1380,1380,1370
1370 K = NOMAX
1390 NOENT =  K
1391 IF(K) 1392,1392,1400
1392 PRINT                1395, NOSTEP
1393 PRINT 1395, NOSTEP
1394 GO TO 910
1400 DO 1410   I = 1,NOVAR
1420 IF (I-K) 1430,1410,1430
```

```
1430 DO 1440    J = 1, NOVAR
1450 IF (J-K) 1460,1440,1460
1460 VECTOR(I,J) = VECTOR(I,J) - (VECTOR(I,K) * VECTOR (K,J) / VECTOR
    -(K,K))
1440 CONTINUE
1410 CONTINUE
1470 DO 1480   I = 1, NOVAR
1490 IF (I-K) 1500,1480,1500
1500 VECTOR (I,K)   =   -   VECTOR (I,K) / VECTOR (K,K)
1480 CONTINUE
1510 DO 1520 J = 1, NOVAR
1530 IF (J-K) 1540,1520,1540
1540 VECTOR(K,J) =    VECTOR (K,J) / VECTOR (K,K)
1520 CONTINUE
1550 VECTOR(K,K) =  1.0 / VECTOR(K,K)
1560 GO TO 1000
1380 PRINT 75, NOSTEP
1381 IF (IFSTEP) 900, 1580,1570
 900 PRINT  905
     GO TO 910
1570 ASSIGN  1580  TO NUMBER
1571 GO TO  1310
1580 PRINT                    1586,(L,VECTOR(L,L),L=1,NOVMI )
 910 CONTINUE
  65 FORMAT (25H0  STANDARD ERROR OF Y = F12.6 )
  70 FORMAT (11H   F LEVEL  F12.4/25H   STANDARD ERROR OF Y = F12.4/12H
    1   CONSTANT F13.5/56H                 VARIABLE   COEFFICIENT   STD ERR
    2OR OF COEF //  (16H                  X-I3,E15.5,E15.5))
  75 FORMAT (10H COMPLETED I5,20H STEPS OF REGRESSION)
  91 FORMAT (9H0STEP NO.I5 /19H   VARIABLE REMOVED I8)
  92 FORMAT (9H0STEP NO.I5 /20H   VARIABLE ENTERING I8)
 654 FORMAT (31H  ZERO NUMBER OF DATA. SO LONG.)
 905 FORMAT (42H ERROR IN CONTROL CARD, PROBLEM TERMINATED)
 906 FORMAT (25H ERROR, VMIN PLUS, SOLONG)
 907 FORMAT (26H  ERROR,NOIN MINUS, SOLONG )
1004 FORMAT (1H037HY SQUARE NON-POSITIVE,TERMINATE STEP  I 5)
1019 FORMAT (1H029H NO MORE DEGREES FREEDOM STEP I 5 )
1044 FORMAT (1H010H SQUARE X-I5,17H NEGATIVE, SOLONG I5,6H STEPS)
1395 FORMAT (12H  K=0. STEP I6, 7H SOLONG)
1586 FORMAT (24H0     DIAGONAL  ELEMENTS //20H   VAR.NO.     VALUE//
    1(1H  I 7, F16.6))
     RETURN
     END
```

```
      SUBROUTINE GRFTOW
C
C     TO PLOT EXPERIMENTAL AND CALCULATED T1 VERSUS TEMPERATURE
C     ON A LOG LOG SCALE,
C
      COMMON T(500),TOW(500),TOWIN(500),WAT(500),WAIT(500),NLO,NHI,NEX
      COMMON LIN(500), NDATE(500), NDP, HIPLUS, LTH, NOVAR, NVLESS
      COMMON DATA(5), VECTOR(6,6), AVE(5), COEN(5), SIGMCO(5),SIGMA(5)
      COMMON NODATE, KDATE(500),SIGY, NOIN, NNWT, INDEX(5)
      COMMON SY, SX, SYY, SXX, NOTPRINT, NOTPLOT
      DIMENSION TC(500), YKURV(500)
      TYPE DOUBLE COEN,SIGMA,SIGY,VECTOR,DATA,WAIT
      TYPE DOUBLE YKURV
      TYPE DOUBLE BSCHG
      BSCHG = 0.4342944819
C      PLOT T1(CALC) VS TEMP
         TC(1) = 1.0
         DO 600 K = 2,90
  600    TC(K) = TC(K-1) + 0.1
         TC(91) = 10.0
         DO 605 K = 92, 370
  605    TC(K) = TC(K-1) + 0.5
           DO 610 K = 1,370
           YKURV(K) = 0.0    $ CALL DEFN(TC(K), 0.0)
           DO 606 J = 1, NOIN
  606      YKURV(K) = YKURV(K) + COEN(J) * DATA(INDEX(J))
           YKURV(K) = -LOGF (YKURV(K))  *  BSCHG
  610      TC(K) = LOGF (TC(K))  *  BSCHG
C      ESTABLISH BOUNDS FOR PLOTTER
         LOBND = XFIXF( YKURV(370)) - 1     $ XLOBD = LOBND
         KIBND = XFIXF (YKURV(1)) + 1     $ XHIBD = KIBND
C      INITIALIZE PLOTTER
      CALL PLOT(0.0, 0.0, 0, 100., 100.)
      CALL PLOT(0.0, 30., 2, 100., 100.)
      CALL PLOT (XLOBD, 2.5, 0, SY, SX)
C      SET UPPER BOUND ON LENGTH OF PLOTTER PAPER
      LTH = 6 + 4 * XABSF(KIBND - LOBND)  + LTH
      CALL PLOT (LTH, 0.0, 3)
C      CALIBRATE PLOTTER PAPER AND PLOT CURVE
      CALL PLOT (XLOBD, 0.0, 1, SY, SX)
      CALL PLOT (XHIBD, 0.0, 1, SY, SX)
      CALL PLOT (YKURV(1), TC(1), 2)
      DO 620 K = 2,370
  620 CALL PLOT (YKURV(K) , TC(K), 1)
      CALL PLOT (XLOBD, 2.0, 2)
      CALL PLOT (XHIBD, 2.0, 1)
      CALL PLOT (XHIBD, 0.0, 1)
      LHIP = XABSF(KIBND - 1)    $ LLOM = XABSF(LOBND + 1)
         DO 630 L = LHIP, LLOM, 2
         YL = -L
         CALL PLOT(YL, 0.0, 2)
         CALL PLOT(YL, 2.5, 1)
         LM = -L-1
         IF (LM - LOBND) 635, 635, 625
```

```
  625    YL = LM   $ CALL PLOT (YL, 2.5, 2)
  630 CALL PLOT (YL, 0.0, 1)
  635 CALL PLOT(XLOBD, 1.0, 2)
      CALL PLOT(XHIBD, 1.0, 1)
C      PLOT EXPERIMENTAL POINTS
         DO 650 K = 1, NDP
         KAR = KDATE(K)
         EX = LOGF(T(K)) * BSCHG    $ WY = LOGF(TOW(K)) * BSCHG
         CALL PLOT(WY, EX, 2, SY, SX)
  650    CALL CHARAC (WY,EX, KAR,SY, SX, SYY, SXX)
      HIPLUS = XHIBD  +  1.0
      CALL PLOT (HIPLUS, 2.5, 2, SY, SX)
      END
```

```
      SUBROUTINE CHARAC(YP, XP, KT, SY, SX, SYY, SXX)
C      TO PLOT SYMBOLS AT THE EXPERIMENTAL POINTS.
      DIMENSION Y(6), X(6)
      GO TO (100,200,300,400,500,600,700,800,900,1000,1100,1200), KT
C     TO PLOT A DIAMOND ABOUT POINT (X,Y)
  100 ASSIGN 150 TO NUMBER
      GO TO 405
  150 CALL PLOT (YP, X(1), 2, SYY, SXX)
      CALL PLOT(Y(4), XP, 1)
      CALL PLOT(YP, X(2), 1)
      CALL PLOT(Y(3), XP, 1)
      CALL PLOT(YP, X(1), 1)
      CALL PLOT(YP, XP, 2)
      RETURN
C     TO PLOT A RIGHT POINTING TRIANGLE ABOUT POINT (X, Y)
  200 A = .1
  205 X(1)= XP  + A /1.732
      Y(1)= YP
      X(2)= XP - A /3.464
  207 Y(2)= YP - A /2.0
      X(3)= X(2)
      Y(3)= YP + A /2.0
      Y(4)= Y(1)
      X(4)=X(1)
  208 CALL PLOT(Y(1), X(1), 2, SYY, SXX)
      DO 210 J=1,4
  210 CALL PLOT(Y(J), X(J), 1, SYY, SXX)
      CALL PLOT(YP, XP, 2, SYY, SXX)
      RETURN
C     TO PLOT AN X AT POUNT (X,Y)
  300 ASSIGN 350 TO NUMBER
  305 A= .1
      X(1)= XP + .354 * A
      Y(1)=YP - .354 * A
      X(3)= XP - .354 *A
      Y(3)= YP + .354 * A
      X(4)= X(3)
      Y(4)= Y(1)
      X(2)= X(1)
      Y(2)= Y(3)
      GO TO  NUMBER, (350,550)
  350 CALL PLOT(Y(1), X(1), 2, SYY, SXX)
      CALL PLOT(Y(3), X(3), 1, SYY, SXX)
      CALL PLOT(Y(2), X(2), 2, SYY, SXX)
      CALL PLOT(Y(4), X(4), 1, SYY, SXX)
      CALL PLOT(YP, XP, 2, SYY, SXX)
      RETURN
C     TO PLOT A CROSS AT POINT (X,Y)
  400 ASSIGN 450 TO NUMBER
  405 A = .1
      X(1)= XP + .5 * A
      X(2)= XP - .5 * A
      Y(3)= YP - .5 * A
      Y(4)= YP + .5 * A
```

```
      GO TO NUMBER, (450, 150)
  450 CALL PLOT(YP, X(1), 1, SYY, SXX)
      CALL PLOT(YP, X(2), 1, SYY, SXX)
      CALL PLOT(Y(3), XP, 2, SYY, SXX)
      CALL PLOT(Y(4), XP, 1, SYY, SXX)
      CALL PLOT(YP, XP, 2, SYY, SXX)
      RETURN
C     TO PLOT A SQUARE AT POINT (X,Y)
  500 ASSIGN 550 TO NUMBER
      GO TO 305
  550 CALL PLOT(Y(1), X(1), 2, SYY, SXX)
      X(5)= X(1)
      Y(5)= Y(1)
      DO 560 J=1,5
  560 CALL PLOT(Y(J), X(J), 1, SYY, SXX)
      CALL PLOT(YP, XP, 2, SYY, SXX)
      RETURN
C     TO PLOT A LEFT POINTING TRIANGLE ABOUT POINT (X, Y)
  600 A = .1
      X(1) = XP - A/1.732
      Y(1) = YP
      X(2) = XP + A/3.464
      GO TO 207
C     TO PLOT AN UPWARD POINTING TRIANGLE ABOUT POINT (X, Y)
  700 A = .1
      X(1) = XP
      Y(1) = YP + A/1.732
      Y(2) = YP - A/3.464
  707 X(2) =XP    + A/2.0
      X(3) = XP - A/2.0
      Y(3) = Y(2)
      X(4) = X(1)
      Y(4) = Y(1)
      GO TO 208
C     TO PLOT A DOWNWARD POINTING TRIANGLE ABOUT POINT (X, Y)
  800 A = .1
      X(1) = XP
      Y(1) = YP - A/1.732
      Y(2) = YP + A/3.464
      GO TO 707
C      TO PLOT A DOWNWARD POINTING Y ABOUT POINT (X,Y)
  900 A = .1    $  AQ = .354 * A
      X(1) = XP + AQ  $  X(3) = XP - AQ  $  X(4) = XP
      Y(1) = Y(3) = YP + AQ  $  Y(4) = YP - AQ
  905 X(2) = X(5) = XP  $  Y(2) = Y(5) = YP
      CALL PLOT(Y(1), X(1), 2, SYY, SXX)
      DO 910 J = 1,3
  910 CALL PLOT (Y(J), X(J), 1)
      CALL PLOT (Y(4), X(4), 2)
      DO 915 J = 4,5
  915 CALL PLOT(Y(J), X(J), 1)
      CALL PLOT (YP, XP, 2)
      RETURN
C      TO PLOT AN UPWARD POINTING Y ABOUT POINT (X,Y)
```

```
 1000 A = .1    $  AQ = .354 * A
      X(1) = XP - AQ  $  X(3) = XP + AQ  $  X(4) = XP
      Y(1) = Y(3) = YP - AQ  $  Y(4) = YP + AQ
      GO TO 905
C      TO PLOT A LEFT POINTING Y ABOUT POINT (X,Y)
 1100 A = .1    $  AQ = .354 * A
      X(1) = X(3) = XP + AQ  $  X(4) = XP - AQ
      Y(1) = YP + AQ  $  Y(3) = YP - AQ  $  Y(4) = YP
      GO TO 905
C      TO PLOT A RIGHT POINTING Y ABOUT POINT (X,Y)
 1200 A = .1    $  AQ = .354 * A
      X(1) = X(3) = XP - AQ  $  X(4) = XP + AQ
      Y(1) = YP - AQ  $  Y(3) = YP + AQ  $  Y(4) = YP
      GO TO 905
      END
```

APPENDIX IV.

ASSIGNMENT OF WEIGHTS IN CURVE FITTING

Use of the least squares analysis for fitting theoretical functions to the experimental data requires minimizing the weighted sum

$$\sum_{i=1}^{N}\left(\frac{1}{\tau_{1\,\mathrm{obs}_i}} - \frac{1}{\tau_{1\,\mathrm{calc}_i}}\right)^2 w_i\ , \tag{A4.1}$$

where N is the number of data points. The method of assigning values to the weights w_i will now be discussed.

Let Y_i and y_i be the ith observed and calculated values, respectively, of a dependent variable. For the set of such values, the least squares condition is that

$$\sum_{i=1}^{N}(Y_i - y_i)^2 w_i \tag{A4.2}$$

be minimum. Let ΔY_i be the error in the measured value Y_i. Then from the theory of statistics,[30]

$$w_i\ (\Delta Y_i)^2 = \eta\ , \tag{A4.3}$$

where η is a constant. Hence

$$w_i = \frac{\eta}{(\Delta Y_i)^2}\ . \tag{A4.4}$$

In our experiments, we estimate that the percentage error in the measured τ_1 values is constant over the entire range of values, i.e.,

$$\frac{\Delta Y_i}{Y_i} = \zeta, \tag{A4.5}$$

where ζ is constant. Combining (A4.4) and (A4.5) results in

$$w_i = \frac{\eta}{\zeta^2} \frac{1}{Y_i^2} . \qquad (A4.6)$$

The implication of (A4.6) is that the weights used in (A4.1) should be of the form

$$w_i \propto (\tau_{1_{obs_i}})^2 . \qquad (A4.7)$$

Least squares curve fitting was performed by the regression analysis subroutine STEPREG in the computer program TOWPLOT (Appendix III). This subroutine requires that the sum of the weights for a set of data points be equal to the number of points, i.e.,

$$\sum_{i=1}^{N} w_i = N. \qquad (A4.8)$$

Combining (A4.8) with (A4.7) defines uniquely the weights as

$$w_i = \frac{\left(\tau_{1_{obs_i}}\right)^2}{\sum_{i=1}^{N} \left(\tau_{1_{obs_i}}\right)^2} . \qquad (A4.9)$$

In our measurements, the fractional error in measured temperatures was much less than that for τ_1. Therefore, the error in measured T values was not considered in deriving (A4.9).